XN-NF-84-18

PLANT TRANSIENT ANALYSIS FOR PALISADES NUCLEAR POWER PLANT WITH 50% STEAM GENERATOR PLUGGING

MARCH 1984

RICHLAND, WA 99352

EXXON NUCLEAR COMPANY, INC.

XN-NF-84-18

Issue Date: 3/9/84

PLANT TRANSIENT ANALYSIS FOR PALISADES NUCLEAR POWER PLANT WITH 50% STEAM GENERATOR PLUGGING

Prepared by: T R Lindquist 3/7/84
T. R. Lindquist
PWR Safety Analysis

Prepared by: William Nutt 3/7/84
W. T. Nutt
PWR Safety Analysis

Concur: W V Kayser 3/8/84
W. V. Kayser, Manager
PWR Safety Analysis

Concur: J.C. Chandler 3/8/84
J. C. Chandler, Lead Engineer
Reload Fuel Licensing

Concur: 3/8/84
J. N. Morgan, Manager
Proposals & Customer Services Engineering

Approve: R. B. Stout 8 MAR 84
R. B. Stout, Manager
Licensing & Safety Engineering

Approve: H G Wilkinson for 3/8/84
G. A. Sofer, Manager
Fuel Engineering & Technical Services

gf

EXXON NUCLEAR COMPANY, Inc.

NUCLEAR REGULATORY COMMISSION DISCLAIMER

IMPORTANT NOTICE REGARDING CONTENTS AND USE OF THIS DOCUMENT

PLEASE READ CAREFULLY

This technical report was derived through research and development programs sponsored by Exxon Nuclear Company, Inc. It is being submitted by Exxon Nuclear to the USNRC as part of a technical contribution to facilitate safety analyses by licensees of the USNRC which utilize Exxon Nuclear-fabricated reload fuel or other technical services provided by Exxon Nuclear for light water power reactors and it is true and correct to the best of Exxon Nuclear's knowledge, information, and belief. The information contained herein may be used by the USNRC in its review of this report, and by licensees or applicants before the USNRC which are customers of Exxon Nuclear in their demonstration of compliance with the USNRC's regulations.

Without derogating from the foregoing, neither Exxon Nuclear nor any person acting on its behalf:

A. Makes any warranty, express or implied, with respect to the accuracy, completeness, or usefulness of the information contained in this document, or that the use of any information, apparatus, method, or process disclosed in this document will not infringe privately owned rights; or

B. Assumes any liabilities with respect to the use of, or for damages resulting from the use of, any information, apparatus, method, or process disclosed in this document.

TABLE OF CONTENTS

LIST OF TABLES

LIST OF TABLES (Cont.)

LIST OF FIGURES

LIST OF FIGURES (Cont.)

LIST OF FIGURES (Cont.)

LIST OF FIGURES (Cont.)

LIST OF FIGURES (Cont.)

1.0 INTRODUCTION AND SUMMARY

Recent analyses[1,2] have addressed the limiting DNBR and pressure transients for Palisades at 2530 MWt with plugging levels up to 21%. The plant transient analysis reported here was performed to support operation of the Palisades Nuclear Power Plant for Cycle 6 at a power of 2125 MWt with 50% of the steam tubes plugged. The purpose of the analysis is to demonstrate that the plant protection system (PPS) protects the specified acceptable fuel design limits (SAFDLs) and vessel pressure design limits given in Table 1.1 for anticipated operational occurrences (AOOs) and that the postulated accidents (PAs) do not violate the criteria on fuel damage or vessel pressure given in Table 1.1. Further, it is demonstrated that the reactor meets the appropriate criteria for a loss of feedwater due to rupture of a feedwater line with loss of offsite power.

The present analysis provides a verification of the thermal margin using PTSPWR2[3] to simulate the plant response and XCOBRA-IIIC[4] to calculate the local coolant conditions in the core based on the plant response. The MDNBR is obtained from the local core conditions and the Exxon Nuclear DNB correlation, XNB[5]. The fuel failure criterion is verified by calculating the number of fuel rods expected to experience DNB. Asymmetric plugging levels are accounted for by including a 5^{o}F inlet temperature penalty in the DNBR calculation. The calculations support up to a 20% difference in plugging between the two steam generators.

The Loss of Normal Feedwater transient, coincident with a station blackout and the loss of auxiliary feedwater to the least plugged steam generator, was simulated with SLOTRAX.[6] The intent of this simulation is to assure adequate decay heat removal and to prevent the loss of primary coolant inventory through the pressurizer relief valves.

A description of the transient calculational methods is provided in Section 2.0. The transient events analyzed for operation at 2125 MWt are the most limiting events in terms of DNBR and pressure and comprise an adequate set of simulations to assure operation within the criteria of Table 1.1 for Cycle 6. The simulations of the limiting transients are discussed in Section 3.0. Section 4.0 provides a rationale for not analyzing the entire spectrum of transients in the Standard Review Plan (SRP) since they are bounded by prior analyses or by transients discussed in Section 3.0.

The key results of the analysis are summarized in Table 1.2 and confirm the criteria of Table 1.1 are met. The lowest value of MDNBR for any AOO is 1.372 for the control element assembly (CEA) drop event. The loss of feedwater transient resulted in a more severe pressurizer transient. However, the pressurizer did not fill with water and long term decay heat removal was established.

The analysis of the limiting transients has shown that the PPS settings provide the level of protection required by Table 1.1, that the transient allowances[7] in the thermal margin/low pressure (TM/LP) trip are appropriate, and that the limiting conditions for operation (LCOs) are sufficient to provide protection for those transients requiring them. Thus, the analysis supports operation of Palisades at 2125 MWt in Cycle 6 with 50% of the steam generator tubes plugged.

Table 1.1 Fuel and Vessel Design Limits

Event Class	Criteria
Anticipated Operational Occurrences (AOOs)	• Specified acceptable fuel design limits (SAFDLs) • MDNBR, based on XNB, > 1.17 • Local power density 21 kW/ft • Pressure < 2750 psia
Postulated Accident (PA)	• Fuel damage is limited to a small fraction of the fuel in the core • Pressure < 2750 psia

Table 1.2 Summary of Results

Transient	Maximum Power Level (MWt)	Maximum Core Average Flux (Btu/hr-ft^2)	Maximum Pressurizer Pressure (psia)	Maximum Primary to Secondary ΔP (psi)	MDNBR
CEA Drop	2199	144,344	1950	1383	1.372
Four Pump Coastdown	2160	139,666	2008	1347	1.579
PORV Failure	2218	144,452	1950	1347	1.636
Excess Load	2504	148,709	1950	1534	1.782
Loss of Electric Load	2260	142,443	2500	1527	1.828
Uncontrolled Rod Withdrawal					
Rod Withdrawal @ 6×10^{-4} $\Delta\rho$/sec from 2125 MWt	2671	150,096	2008	1350	1.679
Rod Withdrawal @ 2.5×10^{-5} $\Delta\rho$/sec from 2125 MWt	2388	152,907	2105	1436	1.674
Rod Withdrawal @ 6×10^{-4} $\Delta\rho$/sec from 1062.5 MWt	1631	83,844	1997	1208	2.007
Rod Withdrawal @ 5×10^{-5} $\Delta\rho$/sec from 1062.5 MWt	1286	82,584	2312	1308	1.664
Locked Rotor	2198	139.667	2053	1347	1.523

2.0 CALCULATIONAL METHODS AND INPUT PARAMETERS

2.1 CODE DESCRIPTION

The transient analysis for Palisades was performed using PTS-PWR2[3], the Exxon Nuclear Company plant transient simulation model for pressurized water reactors. The simulation code models the behavior of pressurized water reactors under both normal and abnormal conditions by solving the transient conservation equations for the primary and secondary systems numerically. Core neutronics behavior is modeled using point kinetics, and the transient conduction equation is solved for fuel temperatures and heat fluxes. State variables such as flow, pressure, temperature, mass inventory, steam quality, heat flux, reactor power and reactivity are calculated during the transient. Where appropriate the reactor protection system (RPS) and control system are modeled to describe the transients.

The system model used by PTSPWR2, shown in Figure 2.1, models the reactor, both primary coolant loops, both steam generators and both steam lines. All major components (pressurized, coolant pumps, and all major valves) are also modeled.

The present calculations were performed using the NOV76A version of the PTSPWR2 code, along with appropriate updates. These updates include:

(1) A correction to the mass balance on the secondary side of the steam generator.

(2) An improved pressurizer model.

(3) A modified set of trip functions to describe a Combustion Engineering plant.

(4) A dynamic flow coastdown model.

(5) Appropriate changes to the primary loop hydraulic behavior to describe the 2 hot leg - 4 cold leg configuration of Palisades.

Updates 1 and 2 were documented in Reference 3. Updates 3-5 were prepared specifically for this analysis.

For Palisades the calculated Thermal Margin/Low Pressure (TM/LP) trip is used in conjunction with the limiting conditions of operation (LCOs) to protect the specified acceptable fuel design limits (SAFDLs) based on departure from nucleate boiling (DNB). The DNB SAFDL limit is further protected by several trips based on single state variables. These latter trip setpoints are listed in Table 2.1 along with the uncertainties and the trip time delays appropriate for each of the RPS trips. The TM/LP trip depends on the hot leg temperature, T_H and the cold leg, T_C. The form of the trip function is:

$$P_{VAR} = \begin{array}{ll} 18.8269\,T_H - 1.2944T_C - 8587.479 & \text{Power} < 100\% \\ 23.9615\,T_H - 6.1932T_C - 8970.464 & \text{Power} > 100\% \end{array}$$

Pressurizer pressure is the system variable which is compared to the trip setpoint, P_{VAR}. The TM/LP trip protects the core from the onset of DNB with at least a 95% probability as long as the plant is operated within the limiting conditions of operation (LCOs), including the LCO on peak linear heat generation rate (LHGR) shown in Figure 2.2.

The scram curve shown in Figure 2.3 was used in the plant transient simulations. The time in the figure is measured from the holding coil release.

The pump response to a loss of power was modeled by setting the shaft rotation speed derivative equal to the pumping torque, divided by the effective inertia. The flow in each of the four cold legs was calculated based on the pump head and the required pressure drop. The effective inertia was then adjusted to provide a good fit to plant data for operation in prior cycles at lower plugging levels(1). The loop pressure drop was then adjusted to provide 99 Mlb/hr vessel flow for 50% tube plugging. This caused the plant to balance at full pump speed with reduced flow. The pump coastdown transient behavior was then determined by the effective inertia previously determined.

DNBR calculations were performed using XCOBRA-IIIC and Exxon Nuclear's critical heat flux correlation, XNB. The boundary conditions, core flow, inlet temperature, heat flux, and pressure were taken from the PTSPWR2 simulation at the time of MDNBR, as predicted by the hot channel model in PTSPWR2, and used as input to XCOBRA-IIIC runs. Figures 2.4 and 2.5 are axial shapes which satisfy the LCO on LHGR, Figure 2.1, with maximum radial peaking for 100% power and 50% power, respectively. Part power transients were assumed to retain the peaking shown in Figure 2.5. The parameter uncertainties described in Section 2.2 were applied to the boundary conditions for MDNBR calculation except in the case in which the trip occurred on the parameter. As an example, for transients terminated by the high flux trip, the value of heat flux calculated by PTSPWR2 at the time of MDNBR was used directly since the power errors, 2% calorimetric +3.5% transient allowance, were already included in the heat flux value via the trip function.

2.2 MODELING UNCERTAINTIES

The present plant transient analysis is a deterministic analysis. Thus, steady state measurement and instrumentation errors were taken into account in an additive fashion to ensure conservative calculations of MDNBR. The plant uncertainties related to initial conditions in the MDNBR calculations are:

Power	+ 2% for calorimetric error
Inlet coolant temperature	+ 7°F for deadband and measurement error and asymmetric steam generator plugging
RCS pressure	- 22 psi for steady-state measurement errors.

Combined with minimum design flow and peaking uncertainties, these parameter uncertainties conservatively bound the MDNBR. Uncertainties are accounted for in the trip functions and in the XCOBRA-IIIC analyses. Table 2.2 is a list of operating parameters used in this analysis.

The trip setpoints are summarized in Table 2.1. A verification of the TM/LP is presented in Reference 7. The TM/LP setpoint was modeled conservatively in the transient analysis to provide bounding simulations of the RPS response. This was done by including the effects of hot leg and cold leg temperature errors, thermal power calibration, asymmetric inlet temperature allowance and trip pressure bias.

The pressurizer control system was modeled in such a fashion that it could not mitigate the effects of transients. The spray system was operable during DNBR transients while the heaters were off, thus tending to minimize DNBR. For pressurization transients, e.g., loss-of-electric load, the spray system and pressurizer relief valves were removed from the simulation.

2.3 DESIGN PARAMETERS

The ENC fuel design parameters for Palisades are summarized in Table 2.3. Table 2.4 lists the bounding values for neutronics parameters, for beginning of cycle (BOC) and end of cycle (EOC).

Table 2.1 Trip Setpoints For Operation of Palisades Reactor at 2125 MWt.

	Setpoint	Uncertainty	Used in Analysis	Delay Time
High Neutron Flux	106.5%	± 5.5%	112.0%	0.4 sec
Low Reactor Coolant Flow	95%	± 2.0%	93.0%	0.6 sec
High Pressurizer Pressure	2255 psia	± 22 psi	2277 psia	0.6 sec
Low Pressurizer Pressure	1750 psia	± 22 psi	1728 psia	0.6 sec
Low Steam Generator Pressure	400 psia	± 22 psi	78 psia	0.6 sec
Low Steam Generator Level*	6 feet	± 10 in	6 feet 10 in.	0.6 sec

* Below operating level.

Table 2.2 Nominal Operating Parameters Used In the Transient Analysis of Palisades at 2125 MWt

Core	
Total Core Heat Output, MWt	2125
Total Core Heat Output, MBtu/hr	7252.7
Heat Generated in Fuel, %	97.5
System Pressure, psia	1950
Total Coolant Flow Rate, Mlbs/hr	99
Effective Core Flow Rate, Mlbs/hr	95.1
Core Inlet Coolant Temperature, ^{o}F	535
Average Core Coolant Temperature, ^{o}F	564
Hot Channel Factors	
Total Peaking Factor, F_Q^T	$F_A \times F_r \times F_L \times F_E$ = 2.607
Radial Peaking Factor, F_r^A	1.500
Axial Peaking Factor, F_Z	1.544
Local Interior Peaking Factor, F_L	1.093
Engineering Factor, F_E	1.030
Heat Transfer	
Core Average Heat Flux, Btu/hr-ft^2	139,671
Steam Generators	
Total Steam Flow, Mlbs/hr	8.97
Secondary Steam Pressure, psia	600
Feedwater Temperature, ^{o}F	395
Number of active Steam Generator Tubes,	
S.G.#1 (40% Plugging)	5111
S.G.#2 (60% Plugging)	3408

Table 2.3 Palisades Fuel Design Parameters for Exxon Nuclear Fuel

Fuel Radius	0.175 inches
Inner Clad Diameter	0.357 inches
Outer Clad Diameter	0.417 inches
Active Length	131.8 inches
Active Fuel Rods Per Bundle	208

Table 2.4 Kinetics Parameters.

Symbol	Parameter	Value: Beginning of Cycle	Value: End of Cycle
α_M	Moderator Coefficient ($\Delta\rho/^oF$) x 10^4	+ 0.50	- 3.50
α_D	Doppler Coefficient ($\Delta\rho/^oF$) x 10^5	- 0.87	- 2.11
α_P	Pressure Coefficient ($\Delta\rho$/psia) x 10^6	- 1.00	+ 7.00
α_B	Boron Worth Coefficient ($\Delta\rho$/ppm) x 10^4	- 0.80	- 1.00
β_{eff}	Delayed Neutron Fraction, %	.75	.45
α_{CRC}	Net* Rod Worth (% $\Delta\rho$)	- 2.90	- 2.90

* Total rod worth minus stuck rod worth

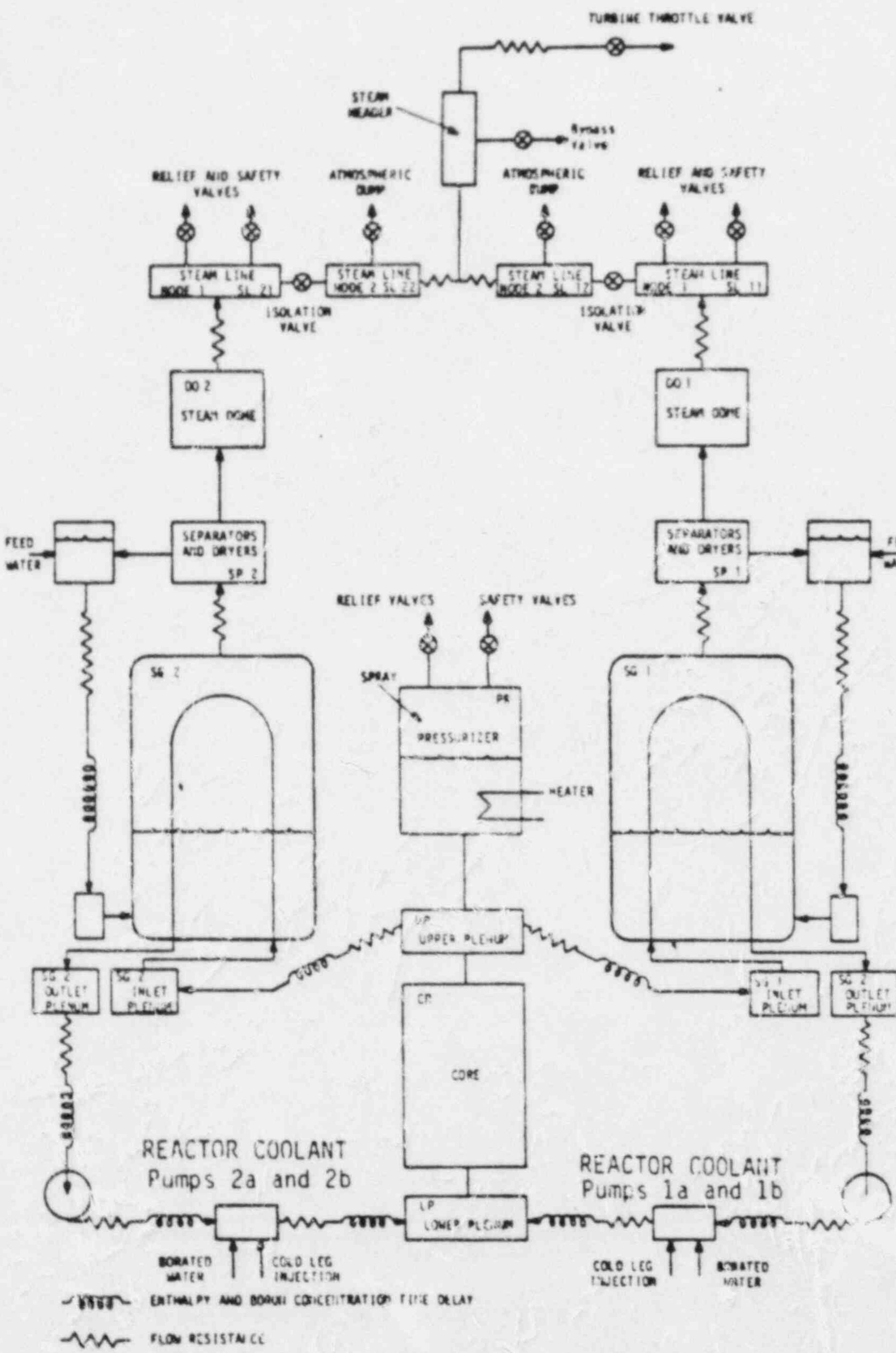

Figure 2.1 PTSPWR2 System Model

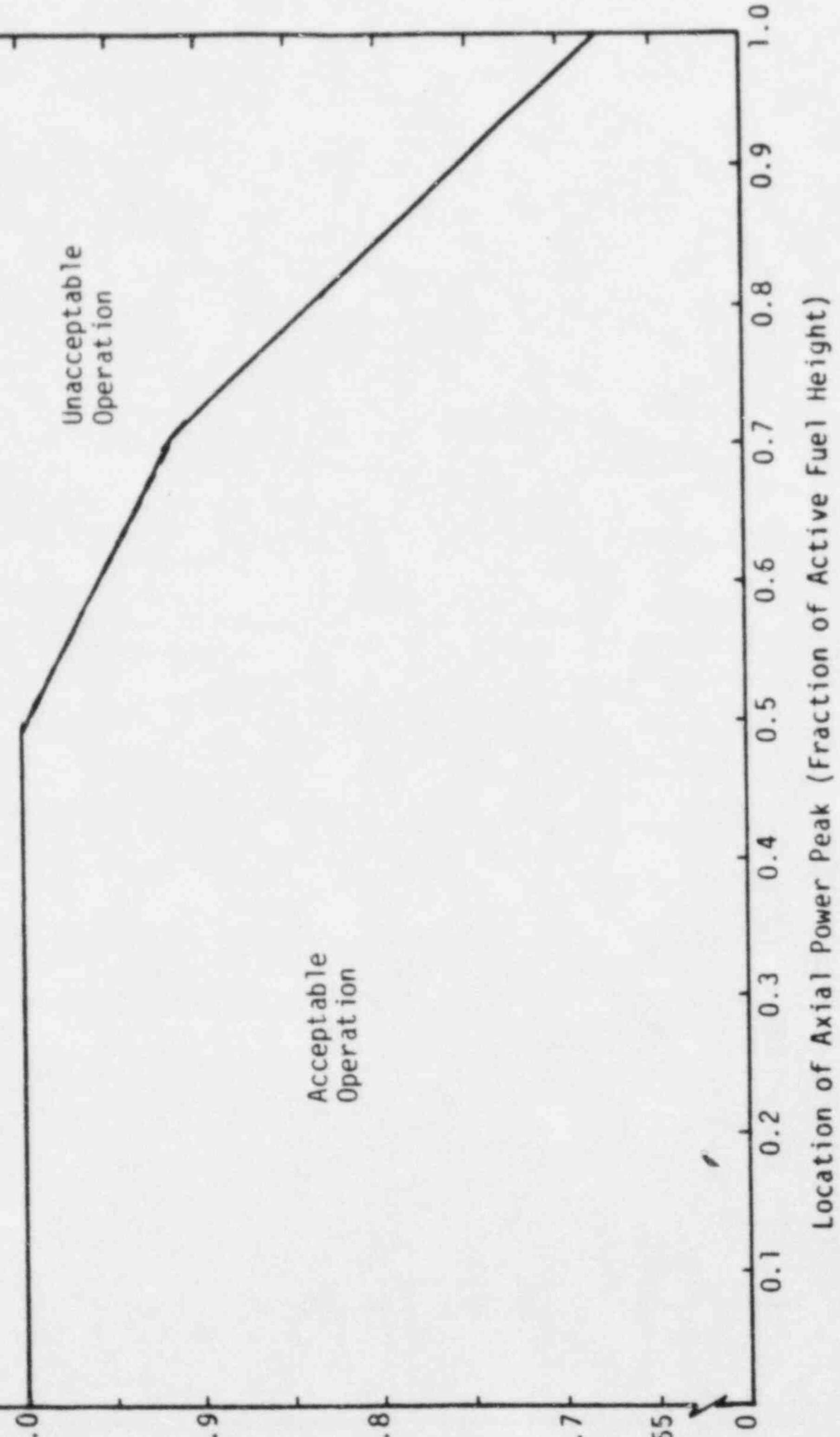

Figure 2.2 Limiting Condition for Operation Based on Linear Heat Generation Rate

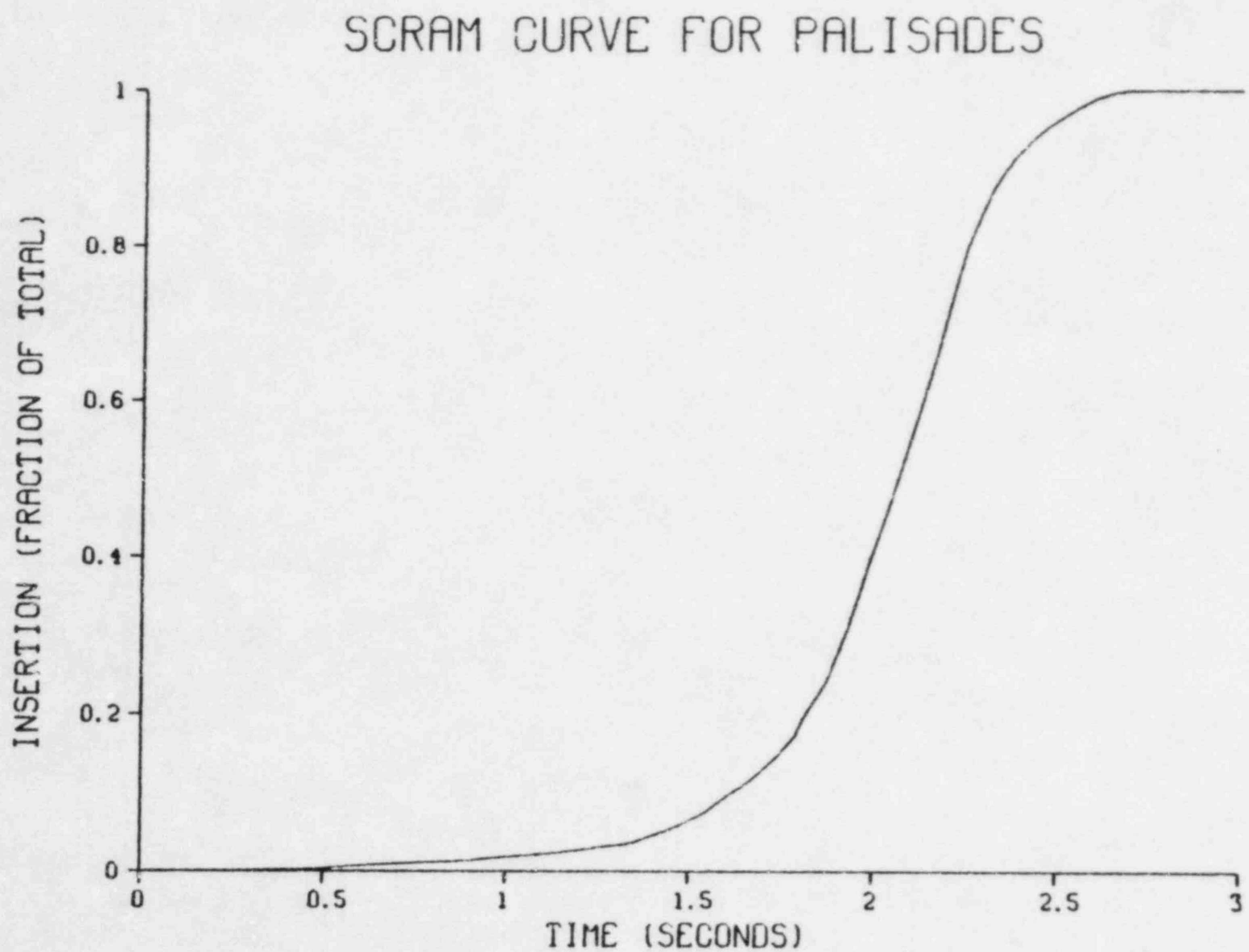

Figure 2.3 Scram Curve for Palisades

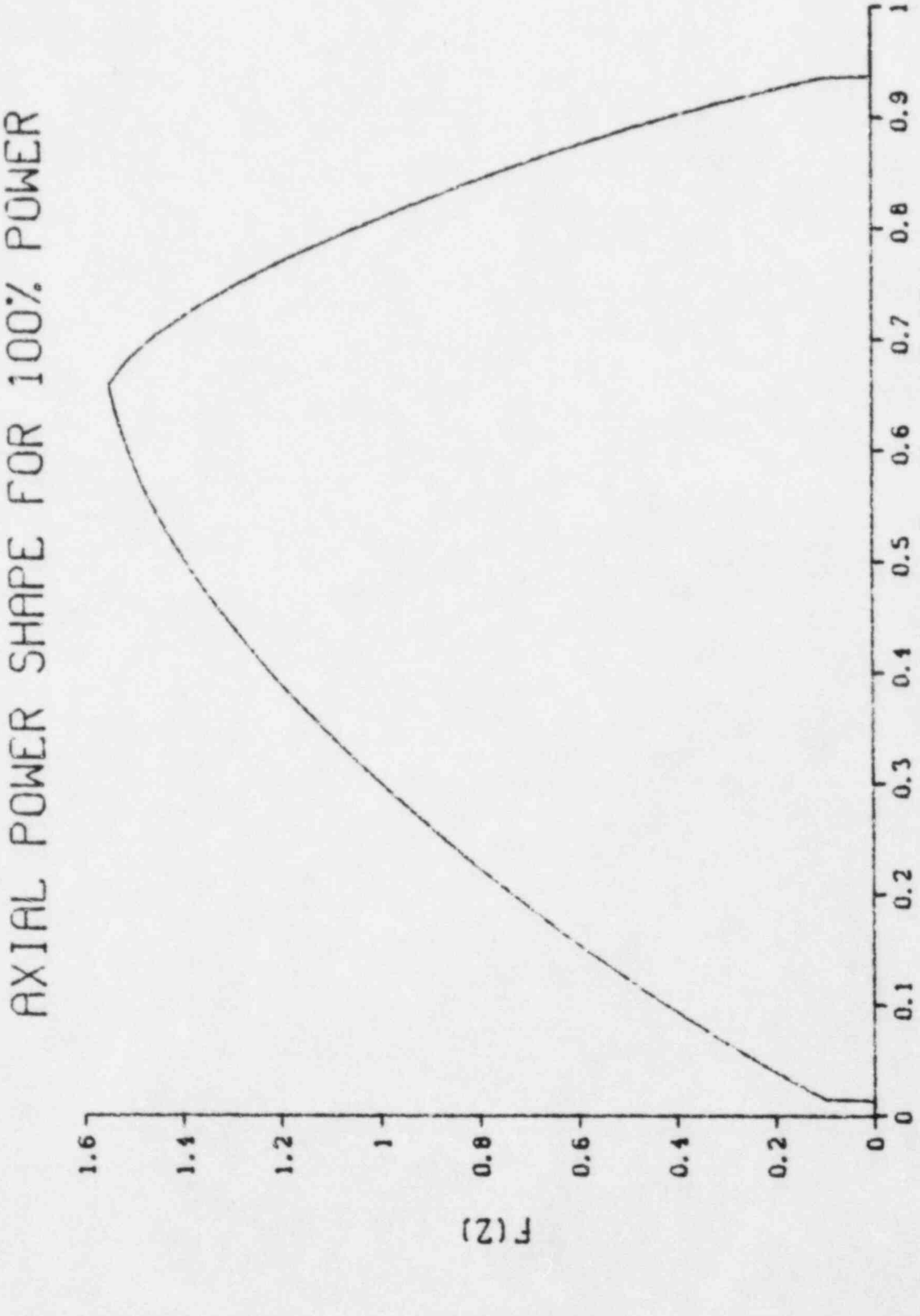

Figure 2.4 Limiting Axial Shape for MDnBR Calculations at 100% Power

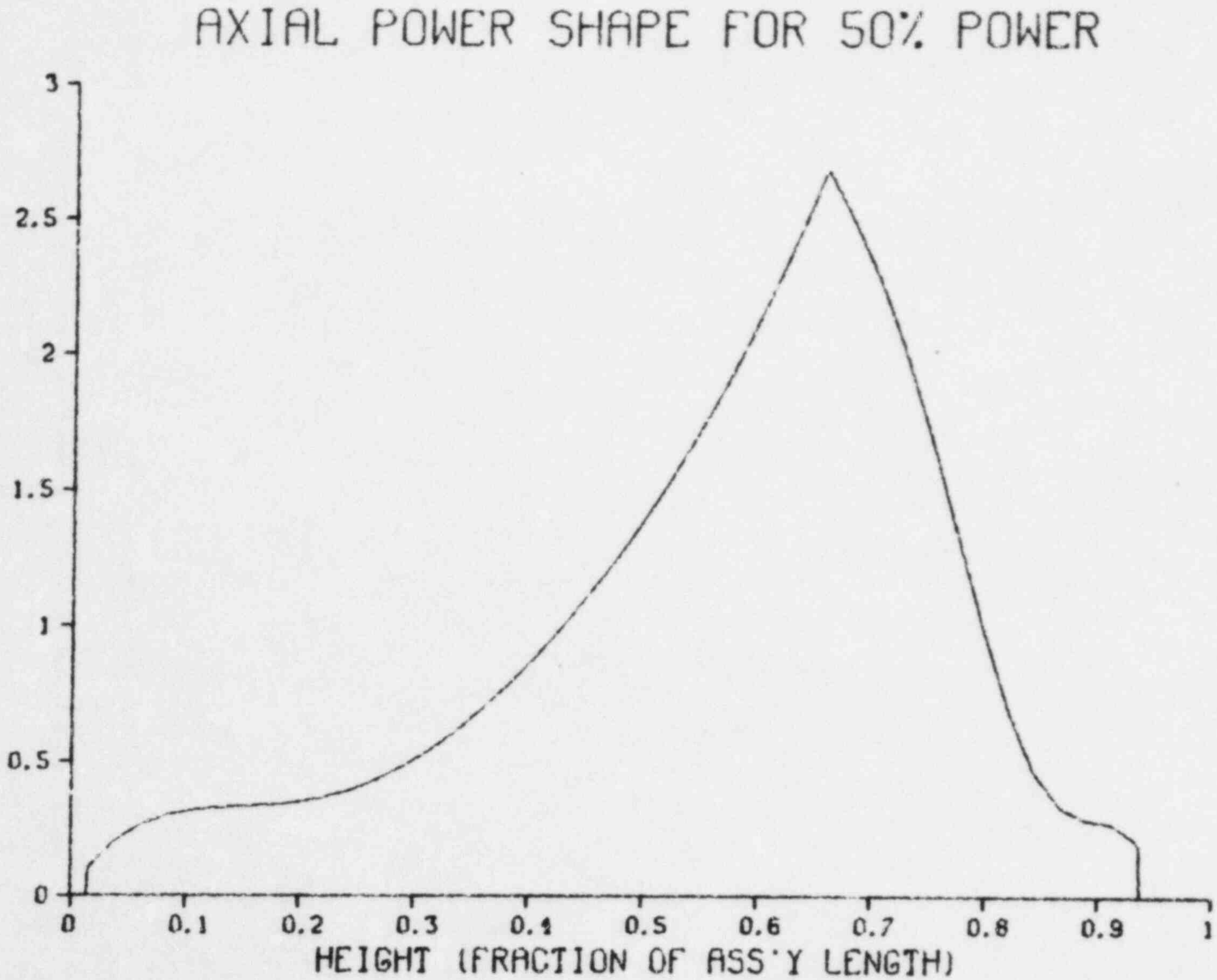

Figure 2.5 Limiting Axial Shape for MDNBR Calculations at 50% Power

3.0 TRANSIENT ANALYSIS

The transients analyzed for Palisades are categorized as either Anticipated Operation Occurrences (AOOs) or Postulated Accidents (PAs). The AOOs are further categorized as either requiring only the action of the reactor protection system (RPS) to meet the Specified Acceptable Fuel Design Limits (SAFDLs) or those requiring RPS action and/or observance of the Limiting Conditions of Operation (LCO).

Table 3.1 lists the transient events considered and summarizes the disposition of each transient. The boron dilution event was not analyzed since, as a reactivity insertion transient at power, it is bounded by the CEA withdrawal transient. The other transient not reanalyzed was the excess-feedwater flow transient since it produced a cooldown rate less severe than that produced by the excess-load transient. The loss of-A.C.-power event was not simulated as a DNBR transient since it is bounded by the four pump coastdown. The steam tube rupture was not reanalyzed since the TM/LP still protects against fuel damage and the radiation release is determined by the operating limits on primary and secondary activity levels.

The steam line rupture was not treated in this analysis since it is a secondary side-induced transient and would be no worse, from the point of view of a return to power, than the prior analysis. The two factors which would mitigate the event are: 1) reduced heat transfer area from primary to secondary which slows the cooldown, and 2) decreased primary loop flow which slows the transient and increases the core inlet boron concentration.

3.1 ANTICIPATED OPERATIONAL OCCURRENCES REQUIRING ONLY RPS ACTION

The transients analyzed which fall into this category are: the loss-of-load transient, the excess-load transient, and the RCS-depressurization transient.

3.1.1 Loss of Load Event

This event was analyzed to simulate plant performance upon a turbine trip without a direct reactor trip. The abrupt loss-of-heat sink results in a rapid rise in the reactor coolant system (RCS) temperature and an expansion of the coolant which produces an insurge of water into the pressurizer and, ultimately, an increase in pressurizer pressure. The criterion employed is that the peak transient pressure must not exceed the ASME code limit of 110% of design pressure (i.e., 2750 psia). The SAFDLs were not approached in this transient since power was appreciably less than that required to reach 21 kW/ft and the MDNBR occurred at the start of the event. The transient was simulated with bounding EOC kinetics. The pressurizer spray was turned off and the effects of the relief valves (PORVs) were also ignored in order to produce as high a pressure as possible during the simulated transient. The steam dump and bypass were also removed from the model for the same reason.

Figures 3.1 to 3.8 show the simulated plant response of the loss-of-load event. As the event was initiated, steam line flow dropped dramatically within the first few seconds (Figure 3.1). Shortly thereafter, primary temperatures began to rise rapidly due to the loss of the heat sink. The rapid expansion of the primary loop inventory caused an insurge into the pressurizer (Figure 3.3) and the subcooled water volume in the pressurizer rose (Figure 3.4), causing a dramatic rise in RCS pressure (Figure 3.5). The pressure rise produced a reactor trip on high pressurizer pressure. The safety relief valves opened (Figure 3.3) at about 10 seconds and controlled the pressure nearly at the setpoint. The maximum pressure reached was 2500.6 psia.

Figures 3.6 to 3.8 show the reactivity traces, the power and heat flux, respectively. Table 3.3 summarizes the events during the transient.

3.1.2 Excess Load Event

Inadvertent opening of the turbine control valve, steam dump valves and/or the steam bypass valve would result in increased steam flow and increased heat extraction. The resultant cooldown of the RCS would produce a positive reactivity insertion at EOC conditions when a large, negative moderator feedback coefficient exists. Protection against core damage is provided by the high neutron flux trip (VHPT), the low steam generator pressure trip, and the TM/LP trip.

The pressurizer heaters were assumed to be inoperable to provide a conservative MDNBR calculation. Bounding EOC kinetics parameters were used in the simulation.

The limiting excess-load transient is the simultaneous opening of steam dump and bypass valves. The plant response to this event was simulated by rapidly ramping in 2 seconds the steam flow to 179% of rated flow. Figures 3.9 to 3.17 show the simulated plant response. As the steamline flow increased, the heat extraction from the primary loop increased and the steam generator exit temperatures began to decrease (Figures 3.9 and 3.10). This cooldown transient propagated to the core and simultaneously caused a contraction of the coolant inventory. The net result is a reduction in the liquid volume in the pressurizer and the RCS pressure (Figures 3.11 and 3.12). The positive feedback from the moderator cooldown, Figure 3.15, produced a slight power ramp, Figure 3.16, which resulted in an increase in core heat flux, Figure 3.17, and a small reversal of the inventory shrinkage (Figure 3.11) before the reactor tripped on the high neutron flux trip.

Table 3.4 is an event summary for this transient and Table 3.5 summarizes the input for the XCOBRA-IIIC calculation of MDNBR.

3.1.3 RCS Depressurization Event

The event simulated was a failure of both pressurizer relief valves fully open. The kinetics parameters used in the simulation were bounding BOC values. The pressurizer heater capacity was set to zero to allow a more rapid depressurization.

Figure 3.18 to 3.23 summarize the transient results for this event. Table 3.6 is an event table for the transient, and Table 3.7 is a listing of the boundary conditions input to the XCOBRA-IIIC calculation. Figure 3.18 shows the steam flow through the relief valve following the inadvertent opening of the PORV. The RCS begins to depressurize (Figure 3.19) and power increases slightly (Figure 3.20). Core flow drops slightly due to the slight increase in core inlet temperature (Figure 3.22). The reactor trips on the TM/LP with ample margin to DNB. It is concluded that the bias in the TM/LP is sufficient to protect the core during this event.

3.2 ANTICIPATED OPERATIONAL OCCURRENCES REQUIRING RPS ACTION AND/OR OBSERVANCE OF THE LCOs

The transients discussed in this subsection require observance of the LCOs for DNB and for linear heat rates in order to protect the SAFDLs, and consist of: the loss-of-coolant flow event, the CEA withdrawal event, and the CEA drop event.

3.2.1 Loss-of-Coolant-Flow Event

Flow reductions result in an increase in enthalpy rise across the core and a subsequent increase in coolant temperature in the hot leg of the RCS. The increased local enthalpy and decreased flow result in a reduction of margin to DNB in the core. The most severe transient, a loss of power to all four RCS pumps simultaneously, was evaluated by simulating a coastdown of all four RCS pumps in the PTSPWR2 model and observing the MDNBR for the transient.

Bounding BOC kinetics were used. The pump coastdown curve, Figure 3.24, is a best estimate curve. The flow trip setpoint is set 3% low to provide a conservative MDNBR.

The event sequence for the transient is summarized in Table 3.8. Table 3.9 lists the input to XCOBRA-IIIC. Figures 3.24 to 3.30 show the simulated plant responses to the four-pump coastdown. The reactor thermal power increases slightly preceding the scram (Figure 3.25), although core heat flux falls due to the decreased heat transfer to the coolant (Figure 3.26). The core average temperature (TCA in Figure 3.27) shows the rise in average temperature which accompanies the reduced coolant flow in the core. This increase in core average temperature causes an increase in RCS inventory volume and an insurge to the pressurizer accompanied by a pressure increase

(Figures 3.28 and 3.29). The core inlet temperature remains fairly constant, falling only after the cold leg temperature decrease, resulting from the flow decrease in the steam generator, reaches the core (Figure 3.30).

3.2.2 CEA-Withdrawal Event

An inadvertent withdrawal of a bank of CEAs introduces positive reactivity which increases both core power and heat flux. Two potential initiators of this event are: 1) operator error; and 2) a malfunction of either the CEA drive mechanism or of the drive control system which results in an uncontrolled, continuous withdrawal of a CEA bank. Heat extraction through the steam generator lags behind the power increase and the increased power is converted to heat in the RCS. Protection against violation of some of the SAFDLs is provided by the VHPT, the TM/LP trip, or the high pressure trip.

A spectrum of uncontrolled rod withdrawls was simulated with PTSPWR2 by increasing the reactivity linearly at rates which could be achieved in the reactor.

Initial power for the transient was either 1062.6 MWt or 2125.2 MWt since the most limiting part-power transient was found to occur from 50% power.(2) The purpose of the simulations was to demonstrate that the fast rod withdrawals could not produce enough overshoot from scram delays to endanger either of the SAFDLs. Further, the simulation was to demonstrate that the heat-up rates used in setting the transient bias in the TM/LP were chosen such that the reactor would be tripped by a trip other than the TM/LP and such that the SAFDLs are not endangered during slow rod withdrawal transients.(8)

3.2.2.1 Rod Withdrawals From Full Power

The fastest reactivity insertion modeled was a linear ramp at $5x10^{-4}\Delta\rho$/sec. This value conservatively bounds the achievable rates. BOC kinetics were used to produce the greatest overshoot. The results of the simulation are displayed in Figures 3.31 to 3.37. The fast reactivity insertion (Figure 3.31) produced a rapid rise in reactor power (Figure 3.32) which was terminated by the high neutron flux trip. The peak heat flux in the core occurred between 3 and 4 seconds (Figure 3.33). The increased heat flux resulted in an increase in the loop temperatures (Figure 3.34), a rise in pressurizer pressure (Figure 3.35), and a decrease in coolant mass flow (Figure 3.36). Because of transport delays, the rapid increase in core inlet temperature, shown in Figure 3.37, occurred after the minimum DNBR.

Table 3.10 is an event table summarizing the transient. The overshoot to 2670.5 MWt corresponds to a transient 16.1 kW/ft. The transient results are benign in terms of either DNB or linear heat generation limits. Table 3.11 consists of the boundary conditions used in the XCOBRA-IIIC calculation.

A slow rod withdrawal transient was also run from 100% power. This transient does not serve as part of the basis for the TM/LP[7] and no verification of transient allowance is required. The transient was simulated using bounding BOC kinetics and a reactivity insertion rate of $2.5x10^{-5}$ $\Delta\rho$/second. Figures 3.38 to 3.45 show the transient behavior of several key system variables during the transient. As reactivity is inserted (Figure 3.38), the reactor power undergoes a nearly linear power ramp up to the high neutron flux trip (Figure 3.39). The core heat flux lags just slightly (Figure 3.40), and increasing primary loop temperatures (Figure 3.41) force more water into the pressurizer (Figure 3.42), causing an increase in pressurizer pressure (Figure 3.43). The core flow decreases as the density of the water in the cold leg decreases (Figure 3.44) and the core inlet temperature rises (Figure 3.45).

The transient is summarized as an event table in Table 3.12. The input for the DNBR calculation is described in Table 3.13.

As reported in Reference 2, the MDNBR for BOC kinetics was found to be nearly invariable with reactivity insertion rate. It was further found to rise witn decreasing reactivity insertion rates only as the high pressure trip became active in terminating the transient.

3.2.2.2 Rod Withdrawals From Part-Power

Rod withdrawal transients from part-power have been performed for operation at 2530 MWt[1,2]. Two observations were made: First, the most limiting transients start from 50% power; and second, the worst DNBR results occur at the highest average heatup and power increase rates at which the TM/LP has to function. Since the TM/LP, the VHPT and the high pressurizer pressure trip serve to protect against DNB in this transient and, since the basis for the TM/LP is protecting slow power transients from part-power, it is only necessary to show that the VHPT or the high pressure trip intervene at the required heatup and power increase rates.

The fast rod withdrawal from part power is not expected to be a DNBR limiting transient since the VHPT will allow only an increase of 15% of rated power before the trip setpoint is reached. A reactivity insertion rate of 5x10-4 $\Delta\rho$/second coupled with bounding BOC kinetics gives the fastest power ramp.

Figures 3.46 to 3.49 summarize the transient results for reactivities (Figure 3.46), power (Figure 3.47), core heat flux resulting from the power increase (Figure 3.48), and the primary loop temperatures (Figure 3.49) which increase in response to the increase core heat flux. Figures 3.50 to 3.52 show the time traces for pressurizer pressure, core flow and core inlet temperature. Table 3.14 is the event table for this transient, and Table 3.15 gives the XCOBRA-IIIC input for the MDNBR calculation.

Reference 2 reports a study of the spectrum of withdrawal rates from part power. While the BOC conditions were found to be more DNBR limiting for reactivity insertion rates greater than 2×10^{-4} $\Delta\rho$/second, the action of the TM/LP was required in the mid-cycle transients and, had enough reactivity been available, at EOC conditions. Thus, it is necessary to verify that the average primary temperature heatup rate and power rates used in creating the TM/LP will cause the VHPT or high pressure trip function to scram the reactor with an acceptable MDNBR resulting.

A reactivity insertion rate of 5×10^{-5} $\Delta\rho$/second using bounding EOC kinetics results in a transient which has a power ramp rate and average temperature ramp rate less than or equal to the values used in creating the TM/LP biases. Figures 3.53 to 3.61 summarize the transient results. Tables 3.16 and 3.17 are event tables and XCOBRA-IIIC input tables, respectively.

The rate of net reactivity insertion is quite low for this transient because of the large negative moderator feedback (Figure 3.53). The resulting power and heat flux rises (Figure 3.54 and 3.55) show a distinctly nonlinear behavior because of this effect. While the actual power does not ramp upward significantly in this transient, the steam generator pressure (Figure 3.56) and the primary loop temperatures (Figure 3.57) are increasing nearly linearly throughout the transient. This produces a nearly constant insurge of liquid into the pressurizer (Figure 3.58) but, because of the pressurizer sprays, the pressure does not ramp up very rapidly until the gas volume becomes quite small and the power begins to rise because of the pressure effect on the moderator density. Core flow (Figure 3.60) falls throughout the transient as the cold leg heats up and core inlet temperature rises nearly linearly.

This transient trips on the high pressurizer pressure trip with temperature and power ramp rates which do not exceed those used to calculate the TM/LP trip and this simulation has the effect of validating the TM/LP trip basis.

3.2.3 CEA Drop Event

A failure in the CEA drive mechanism can result in an inadvertent full-length insertion of a CEA during power operation. Fixed demand from the turbine would cause a cool-off transient in the RCS and, for negative moderator feedback, a return to the original power with a significantly greater radial peaking in the core. Since the power initially decreases following the dropping of the CEA, no reactor trip occurs and protection of the SAFDLs is provided solely by the LCOs.

This event was simulated by introducing a step decrease in total reactivity at steady-state and full power. Bounding EOC kinetics parameters were used and the reactivity insertion was selected to conservatively bound that due to the most reactive CEA being inserted. A radial peaking factor of 116% was included during the return to power. During the cooldown transient, inlet temperature fell, mass flow rose and pressure, which was not controlled in this transient, fell. The increased radial peaking and reduced pressure tended to decrease the DNBR while the decreased inlet temperature and increased flow tended to increase the DNBR.

Table 3.18 summarizes the event sequence of the transient. Table 3.19 is the XCOBRA-IIIC input used to calculate the MDNBR. This transient does not produce an MDNBR below the target value of 1.17 as would be expected since it was used to establish the LCO on inlet temperature in Reference 7. In the basis, no credit was taken for the cooldown of the core inlet flow, hence significant margin to DNB can be expected for this transient.

The initial decrease in reactivity due to the dropped CEA is offset by the doppler feedback initially as the fuel cools off (Figure 3.62). As the reactor power and heat flux fall off (Figures 3.63 and 3.64), the turbine flow begins to increase (Figure 3.65) to maintain a constant heat extraction from the plant. As the turbine flow increases, the primary loop cools off (Figure 3.66) and the RCS coolant inventory becomes more dense. This results in an increase moderator feedback and a reduction of the liquid in the pressurizer (Figure 3.67). The pressrizer pressure decreases (Figure 3.68) and the core mass flow increases in response to the cooldown of the primary loop. After 90 seconds, the reactor power has nearly stabilized and the minimum DNBR has already occurred.

3.3 POSTULATED ACCIDENTS

The events which fall in this category are assumed to occur infrequently and are not required to meet the SAFDLs. The ultimate criterion applied to these transients is a radiation exposure limit 10 CFR 100. In assessing the safety of operation in Cycle 6, a comparison of expected pin failure with prior cycles is used to judge the acceptability of the fuel performance. Fuel failure is conservatively assumed coincident with the occurrence of DNB. Hence, for the DNBR limiting accident analyzed in this subsection, the seized pump rotor, the expected number of fuel pins undergoing DNB was used as the evaluation criterion. In addition, the loss of normal feedwater transient was analyzed for long-term decay heat removal assuming the coincident failure of the automatic feedwater valve to the least plugged steam generator. Because of the decreased heat transfer area, decay heat removal at natural circulation flows can lead to the pressurizer filling due to RCS heatup.

3.3.1 Primary-Pump-Seizure Event

The instantaneous loss of pumping power caused by disintegration of the pump impeller or a complete seizure of the pump shaft would result in a rapid flow decrease through the affected cold leg, and would cause a reactor trip due to low flow in that loop. The flow reduction rate would be more drastic than in a total loss of pumping power and would create a more rapid approach to DNB. Bounding BOC kinetics parameters were used to maximize the power excursion and delay the shutdown of the power following the trip.

The transient was simulated by stopping one of the four pumps at full-power operation. Pressurizer pressure control was retained so that the spray would decrease the pressure transient. The results of the simulation are shown in Figures 3.70 to 3.77. The event sequence is summarized in Table 3.20. XCOBRA-IIIC input is in Table 3.21.

The instantaneous loss of pumping power to a single cold leg caused an immediate flow reversal in that cold leg. As the flow rose in the intact cold legs, due to the reduction in core flow for the intact loop and to the flow reversal in the seized loop for the intact leg in the seized loop, a near steady-state flow was achieved within 1 second. The new flow was 78.2% of the original flow and resulted from an 8% increase in flow in the intact loop, a reverse flow of about 30% in the seized locp, and an increased flow of about 153% in the intact leg of the seized loop. Figure 3.70 shows the core inlet flow transient.

Power rises slightly before the reactor trip (Figure 3.71); however, heat flux never rises as high as the initial value (Figure 3.72). The core inlet temperature is nearly constant for the first three seconds (Figure 3.73) before rising rapidly. Over the first 2-3 seconds, the only significant temperature changes are in the clad temperature and the core average temperature (Figure 3.74). The rise in core average temperature is reflected by the pressurizer surge flow (Figure 3.75). The pressurizer water volume continues to increase after the scram (Figure 3.76) as does the pressurizer pressure.

3.3.2 Loss of Feedwater with a Loss of Offsite Power

Operation of Palisades with 50% of the steam generator tubes plugged reduces the heat transfer area available to reject decay heat to the steam generators. Should the primary coolant become sufficiently hot, volumetric swell of the RCS inventory can potentially fill the pressurizer and force coolant out the safety and relief valves. A significant amount of inventory loss in the RCS or an inability to protect the core and achieve a cooldown without pumping power remains a possibility for a reactor with reduced heat transfer mechanisms. The reduced initial power tends to offset this effect by lowering the decay heat load on the system.

The analysis was performed for a limiting case, a loss of normal feedwater with loss of offsite power. This transient causes a loss of normal feedwater to both steam generators, a turbine trip, and a loss of offsite power. In addition, it was assumed that a valve failure results in auxiliary feedwater not being available for cooling to the least plugged steam generator. The simulation of the transient was performed using SLOTRAX with an asymmetric loop model which had 60/40 plugging in its steam generators.

The event was initiated from full power by ramping the normal feedwater to both steam generators to zero in one second. Table 3.22 is an event table for the transient. Simultaneous with the loss of normal feedwater, the reactor was tripped and the primary coolant pumps were allowed to coast down. Auxiliary feedwater was not introduced until 1 minute after main feedwater pumps stopped to allow for time necessary to start the motor on the auxiliary feedwater pump. Upon initiation of auxiliary feedwater, a valve failure results in the total output from the motor-driven auxiliary feedwater pump being introduced into the 60% plugged steam generator. The plant was then allowed to recover passively without the benefit of letdown flows in the RCS.

Figures 3.78 to 3.82 summarize the transient results. The reactor thermal power (Figure 3.78) is predominantly decay heat after the first few seconds. The loop flow rates (Figure 3.79) show the asymmetric flow behavior of the two loops with their different plugging levels. The steam generator liquid level for the intact steam generator reflects the fact that it is isolated and floods up to a level at which it is controlled by dumping steam either to the atmosphere or to the condenser, automatically. The affected steam generator dries out in 2975 seconds (Figure 3.80).

A key system variable is the average temperature of the RCS. It should reach an early peak and decrease with time which provides decay heat removal via natural circulation. The peak value determines the amount of expansion of the primary loop coolant inventory and thus the change in liquid level of the pressurizer. Figure 3.81 shows the RCS temperature as a function of time. Figure 3.82 shows the liquid level in the pressurizer.

The results of the simulation (Figures 3.81 and 3.82) demonstrate that the pressurizer does not fill and that decay heat removal via natural circulation is established.

Table 3.1 Transient Events

Transient	Disposition
AOOs Requiring Only RPS Action	
Boron Dilution	Not Analyzed
Loss of Load	Analyzed
Loss of Feedwater	Not Analyzed
Excess Load	Analyzed
Excess Feedwater	Not Analyzed
RCS Depressurization	Analyzed
AOOs Requiring RPS Action and/or LCO	
Loss of Coolant Flow	Analyzed
Loss of A.C. Power	Not Analyzed
CEA Withdrawal	Analyzed
CEA Drop	Analyzed
PAs	
Seized Rotor	Analyzed
Steam Line Rupture	Not Analyzed
Steam Generator Tube Rupture	Not Analyzed
Loss of Feedwater with a Loss of Offsite Power	Analyzed

Table 3.2 Index of Symbols

Symbol	Description	Units
CFWPR	Volume of water in the pressurizer	ft^3
DK	Net reactivity	$
DKDOP	Doppler feedback	$
DKMAN	Manual reactivity inserted	$
DKMOD	Moderater pressure feedback	$
LEVPR	Pressurizer liquid level	ft
LEVSG1	Downcomer liquid level in steam generator #1	ft
LNB1	Subcooled level in steam generator #1	ft
PL	Reactor power	MWt
PPR	Pressurizer pressure	PSIA
PSG1	Pressure in steam generator #1	PSIA
GDA	Core heat flux	$Btu/hr\text{-}ft^2$
GPR	Pressurizer heater power	kWt
GT	Total power extracted from the steam generators	Btu/sec
TAVG1	Average temperature in Loop 1	^{o}F
TCA	Core average temperature	^{o}F
TCIO	Core inlet temperature	^{o}F
TCLAD	Average clad temperature	^{o}F
TCL1	Cold leg temperature in Loop 1	^{o}F
THL1	Hot leg temperature in Loop 1	^{o}F
TLPI	Reactor vessel lower plenum inlet temperature	^{o}F
TSG1PI	Inlet temperature to steam generator #1	^{o}F

Table 3.2 Index of Symbols (Cont.)

Symbol	Description	Units
TSG1PO	Outlet temperature from steam generator #1	°F
WDOSLT	Flow from dome to steamline	lb/sec
WFWT	Total feedwater flow	lb/sec
WPRRV	Pressruizer relief valve flow	lb/sec
WPRSU	Pressurizer safety valve flow	lb/sec
WRV1	Flow from the relief valve in steamline #1	lb/sec
WSV1	Flow from the safety valve in steamline #1	lb/sec
WTB	Flow through turbine	lb/sec
WUPPR	Surge flow to pressurizer	lb/sec

Table 3.3 Event Table For The Loss of Electric Load

Time	Event	Value or Setpoint
0	Turbine flow reduce to zero	
4.62	Peak power	2259.8 MWt
5.87	Peak core heat flux	142443 BTU/hr ft^3
8.76	Reactor trip on high pressurizer pressure	2277 psia
10.34	Pressurizer safety valve opened	2500 psia
10.77	Peak core average temperature	573.3 ^oF
10.90	Peak pressurizer pressure	2500.6 psia

Table 3.4 Event Table For Excess Load

Time	EVENT	Value or Setpoint
0	Begin ramping turbine flow	
2.0	Maximum turbine flow	179% of rated
8.49	High neutron flux trip	2380.2 MWt
9.05	Peak power level	2504 MWt
9.66	MDNBR	1.782
9.77	Peak core heat flux	148,709 Btu/hr-ft^2

Table 3.5 XCOBRA-IIIC Input For Excess Load

VARIABLE	VALUE	UNITS
Pressure	1918.4	psia
Inlet temperature	536.38	°F
Core flow	25,805	lb/sec
Power	2259.3	MWt

Table 3.6 Event Table For The PORV Failure

TIME (Seconds)	EVENT	VALUE OR SETPOINT
0	Pressurizer relief valve opens	
31.63	Reactor trip on TM/LP	1722.6 psia
	Peak power level	2218 MWt
32.01	Peak core heat flux	144,451 Btu/hr-ft^2
32.31	Peak core average temperature	565 ^{o}F
32.32	Minimum DNBR	1.636

Table 3.7 XCOBRA-IIIC Input for PORV Failure

VARIABLE	VALUE	UNITS
Pressure	1733.6	psia
Inlet temperature	541.7	°F
Core flow	25.413	lbs/sec
Power	2238.6	MWt

Table 3.8 Event Table For The Four Pump Coastdown

TIME (Seconds)	EVENT	VALUE OR SETPOINT
0	Pump trip	
	Peak core heat flux	139,666 Btu/hr-ft^2
1.28	Reactor trip on low flow	93%
1.56	Peak Reactor Power	2160.3 MWt
2.81	Minimum DNBR	1.579
3.32	Peak core average temperature	569^{o}F
5.07	Peak pressurizer pressure	2008 psia

Table 3.9 XCOBRA-IIIC Input For Four Pump Coastdown

VARIABLE	VALUE	UNITS
Pressure	19956.5	psia
Inlet temperature	542.7	^{o}F
Core flow	20,547	lb/sec
Power	2108	MWt

Table 3.10 Event Table For Fast Rod Withdrawal From 100% Power

TIME (Seconds)	EVENT	VALUE OR SETPOINT
0	Maximum rod withdrawal rate initiated	5×10^{-4} $\Delta \rho$/second
1.89	Reactor trip in high neutron flux	2380 MWt
2.50	Peak power level	2670.5 MWt
3.36	Minimum DNBR	1.679
3.42	Peak core heat flux	150,095 Btu/hr-ft^2
3.58	Peak core average temperature	565^{o}F
5.32	Peak pressurizer pressure	2008 psia

Table 3.11 XCOBRA-IIIC Input for Fast Rod Withdrawal From 100% Power

VARIABLE	VALUE	UNITS
Pressure	1960	psia
TINLET	542.5	°F
Core flow	25,390	lb/sec
power	2280	MWt

Table 3.12 Event Table For The Slow Rod Withdrawal At 100% Power

TIME (Second)	EVENT	VALUE OR SETPOINT
0	Reactivity insertion begins	2.5×10^{-5} ΔP/sec.
30.00	Reactor trip on high neutron flux	2380 MWt
30.53	Minimum DNBR	1.674
30.61	Peak core heat flux	152,906 BTU/hr-ft^2
31.27	Peak core average temperature	568 ^{o}F
33.27	Peak pressurizer pressure	2105 PSIA

Table 3.13 XCOBRA-IIIC Input For Slow Rod Withdrawal From 100% Power

VARIABLE	VALUE	UNITS
Pressure	2062	PSIA
Inlet temperature	545.2	^oF
Core flow	25,329	lb/sec
Power	2320	MWT

Table 3.14 Event Table For Fast Rod Withdrawal From 50% Power

TIME (Seconds)	EVENT	VALUE OR SETPOINT
0	Reactivity insertion begins	5×10^{-4} Δp/sec
3.16	Variable high power trip	1392 MWt
3.79	Peak power level	1630.9 MWt
4.79	Minimum DNBR	2.007
4.80	Peak core heat flux	83,843 Btu/hr-ft^2
4.97	Peak core average temperature	556 °F
5.83	Peak pressurizer pressure	1997 PSIA

Table 3.15 XCOBRA-IIIC Input For Fast Rod Withdrawal From 50% Power

VARIABLE	VALUE	UNITS
Pressure	1965.3	PSIA
Inlet temperature	545.8	^oF
Core flow	25,387	lb/sec
Power	1276	MWt

Table 3.16 Event Table for Slow Rod Withdrawal from 50% Power

Time (seconds)	Event	Value or Setpoint
0	Reactivity insertion begins	5×10^{-5} $\Delta\rho$/sec.
216.27	Minimum DNBR	1.664
234.11	Reactor trip on high pressurizer pressure	2277 psia
	Peak power level	1285.6 MWt
234.68	Peak core heat flux	82,584 Btu/hr-ft^2
235.31	Peak core average temperature	587°F
235.52	Steam line safety valves opened	1000 psia
235.55	Peak steam dome pressure	1002 psia
236.32	Peak pressurizer pressure	2312 psia

Table 3.17 XCOBRA-IIIC Input for Slow Rod Withdrawal from 50% Power

Variable	Value	Units
Pressure	2165.6	PSIA
Inlet Temperature	580	^oF
Core Flow	25,354	lb/second
Power	1395	MWt

Table 3.18 Event Table for CEA Drop

Time (Seconds)	Event	Value or Setpoint
0	CEA Drop	$-2x10^{-3}$ $\Delta\rho$/sec.
2.13	Minimum Power	1796 MWt
56.19	Peak power level	2199 MWt
63.52	Peak core heat flux	144,344 Btu/hr-ft^2
71.44	Minimum DNBR	1.372

Table 3.19 XCOBRA-IIIC Input for CEA Drop

Variable	Value	Units
Pressure	1929.7	PSIA
Inlet temperature	534.5	^{o}F
Core flow	25,504	lb/sec.
Power	2,237	MWt
Radial peaking*	1.9595	

*This peaking represents 116% of the Technical Specification limiting on radial peaking for an interior channel.

Table 3.20 Event Table for the Locked Rotor

Time (Seconds)	Event	Value or Setpoint
0	Pump seizure	-
0.48	Reactor trip on low flow	93%
0.80	Peak power level	2198 MWt
1.38	Minimum DNBR	1.523
1.77	Peak core temperature	570^{o}F
5.02	Peak pressurizer pressure	2053 psia

Table 3.21 XCOBRA-IIIC Input for the Locked Rotor

Variable	Value	Units
Pressure	1964.5	PSIA
Inlet temperature	542.5	°F
Core flow	20,263	lb/sec.
Power	2133	MWt

Table 3.22 Event Table for Loss of Feedwater with Loss of Offsite Power

Time (Seconds)	Event	Value or Setpoint
0	Reactor trip; primary and main feedwater pumps coastdown	-
25.0	Maximum steam generator pressure	1009.0 psia (intact) 1012.9 psia (isolated)
60.0	Auxiliary feedwater initiated to intact steam generator	70.8 lbm/sec.
2800.0	Maximum pressurizer pressure	1983.3 psia
2875.0	Maximum pressurizer water volume	1332.8 ft^3
2975.0	Isolated steam generator dries out	-

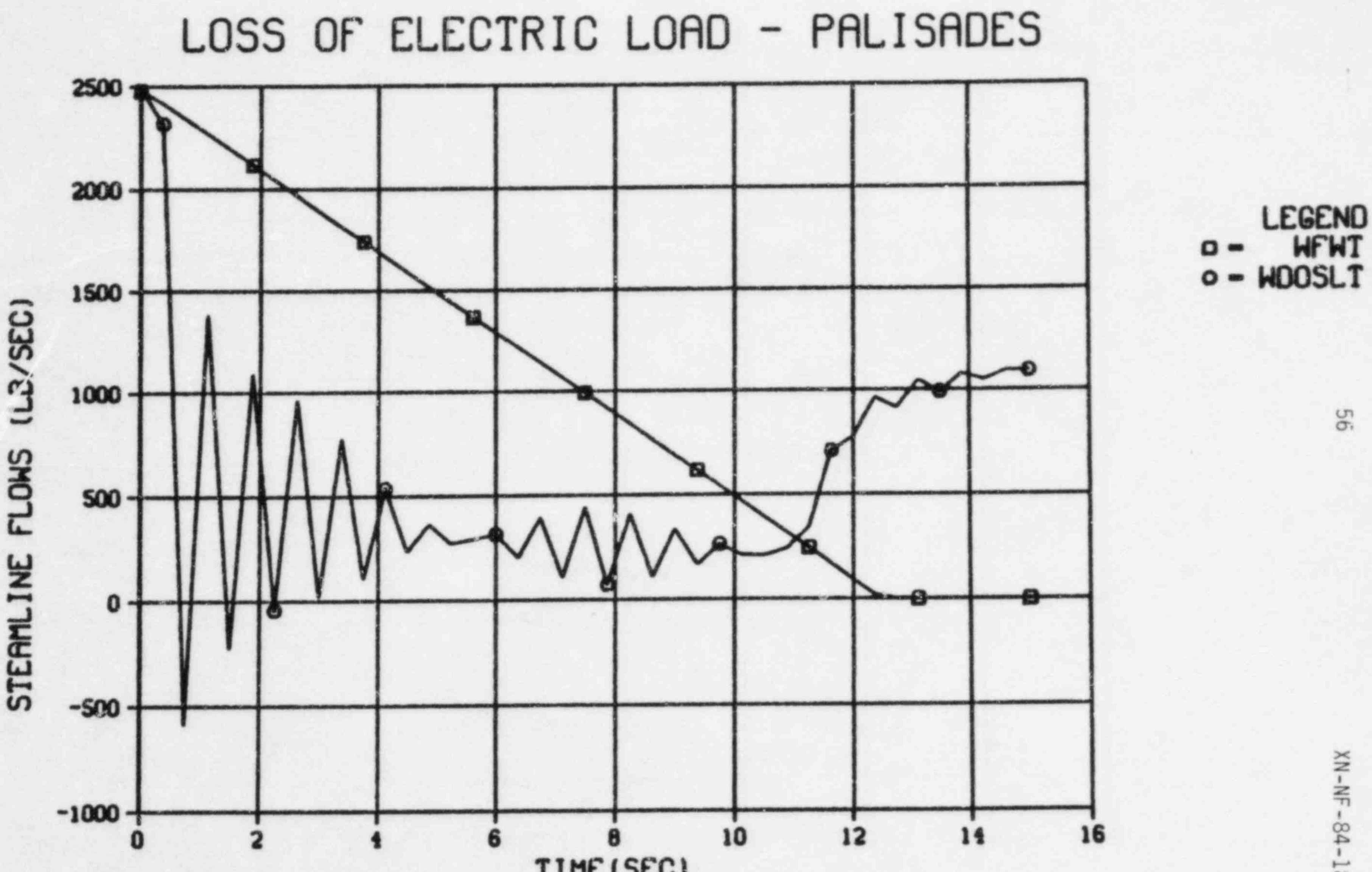

Figure 3.1 Steam Generator Flows for Loss of Electric Load

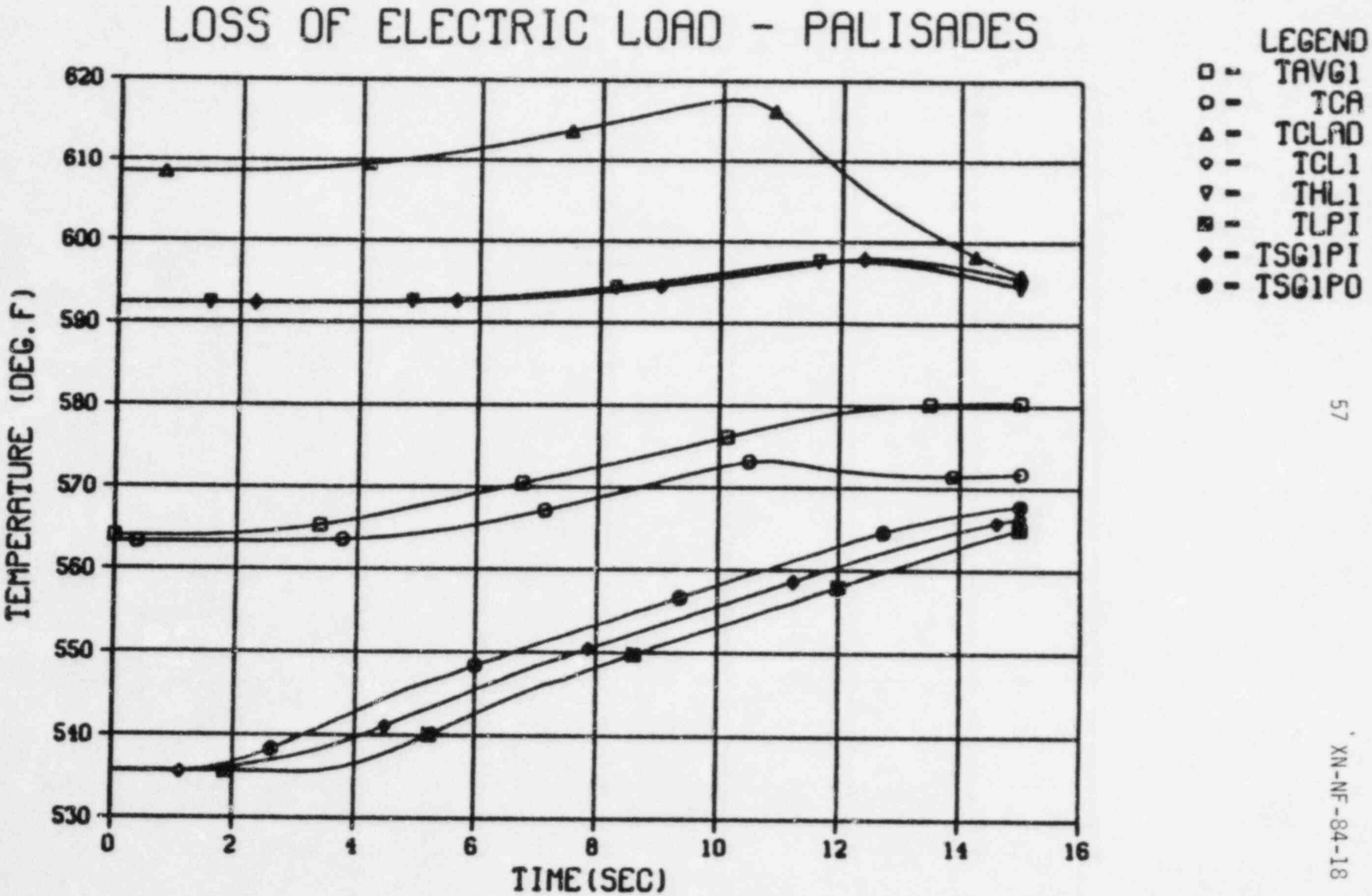

Figure 3.2 Primary Loop Temperatures for Loss of Electric Load

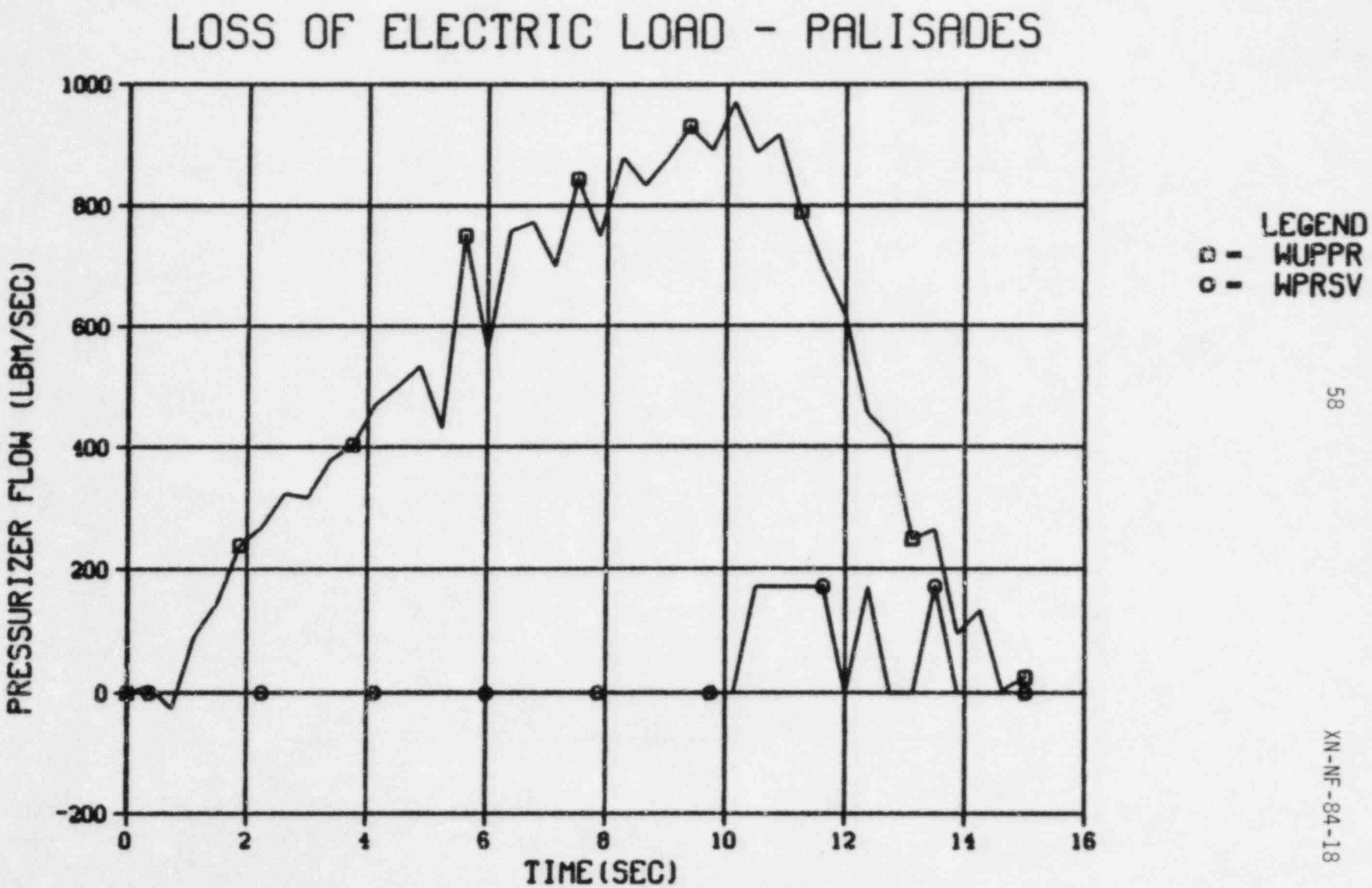

Figure 3.3 Pressurizer Flows for Loss of Electric Load

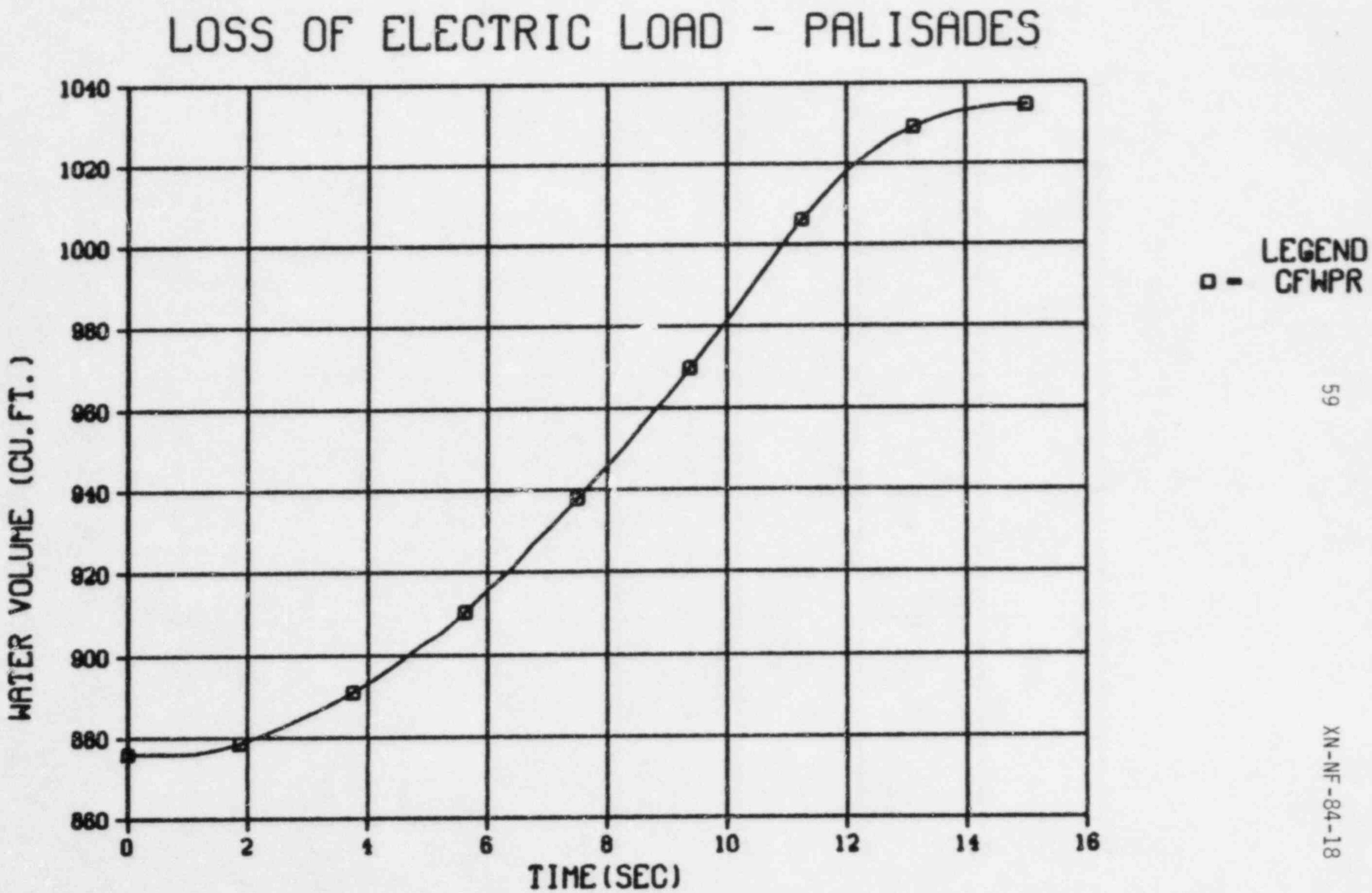

Figure 3.4 Liquid Volume in Pressurizer for Loss of Electric Load

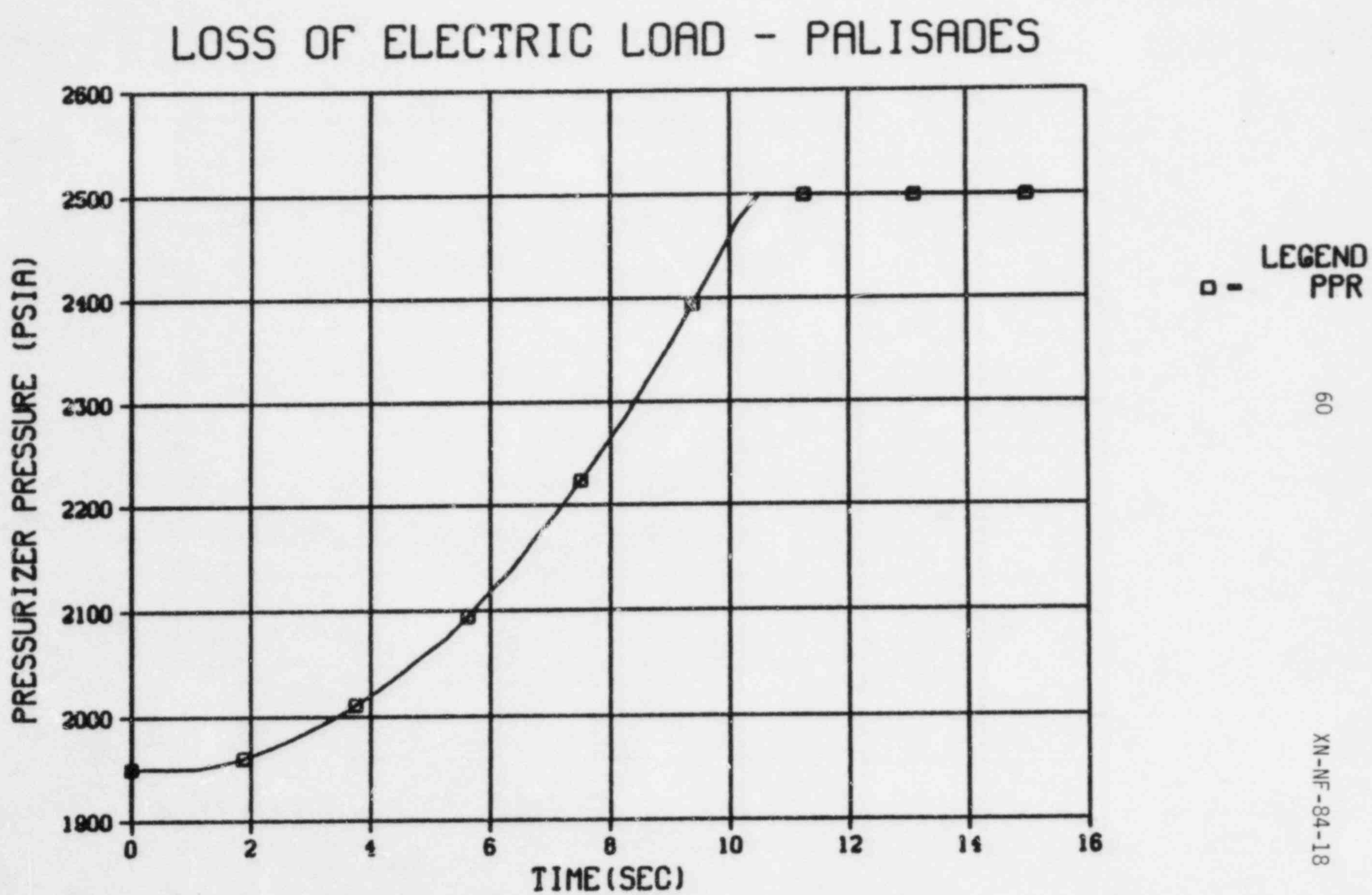

Figure 3.5 Pressurizer Pressure for Loss of Electric Load

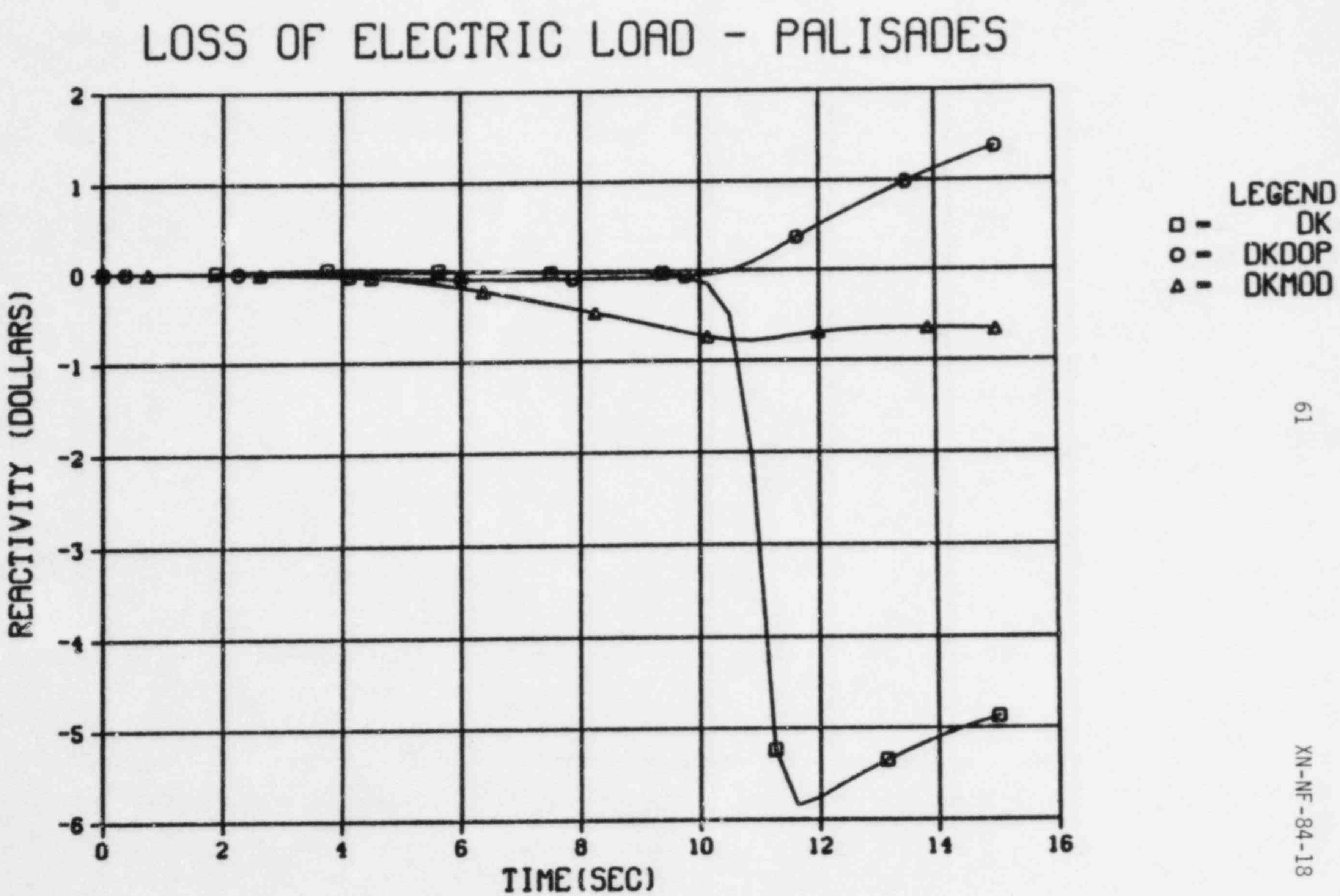

Figure 3.6 Reactivities for Loss of Electric Load

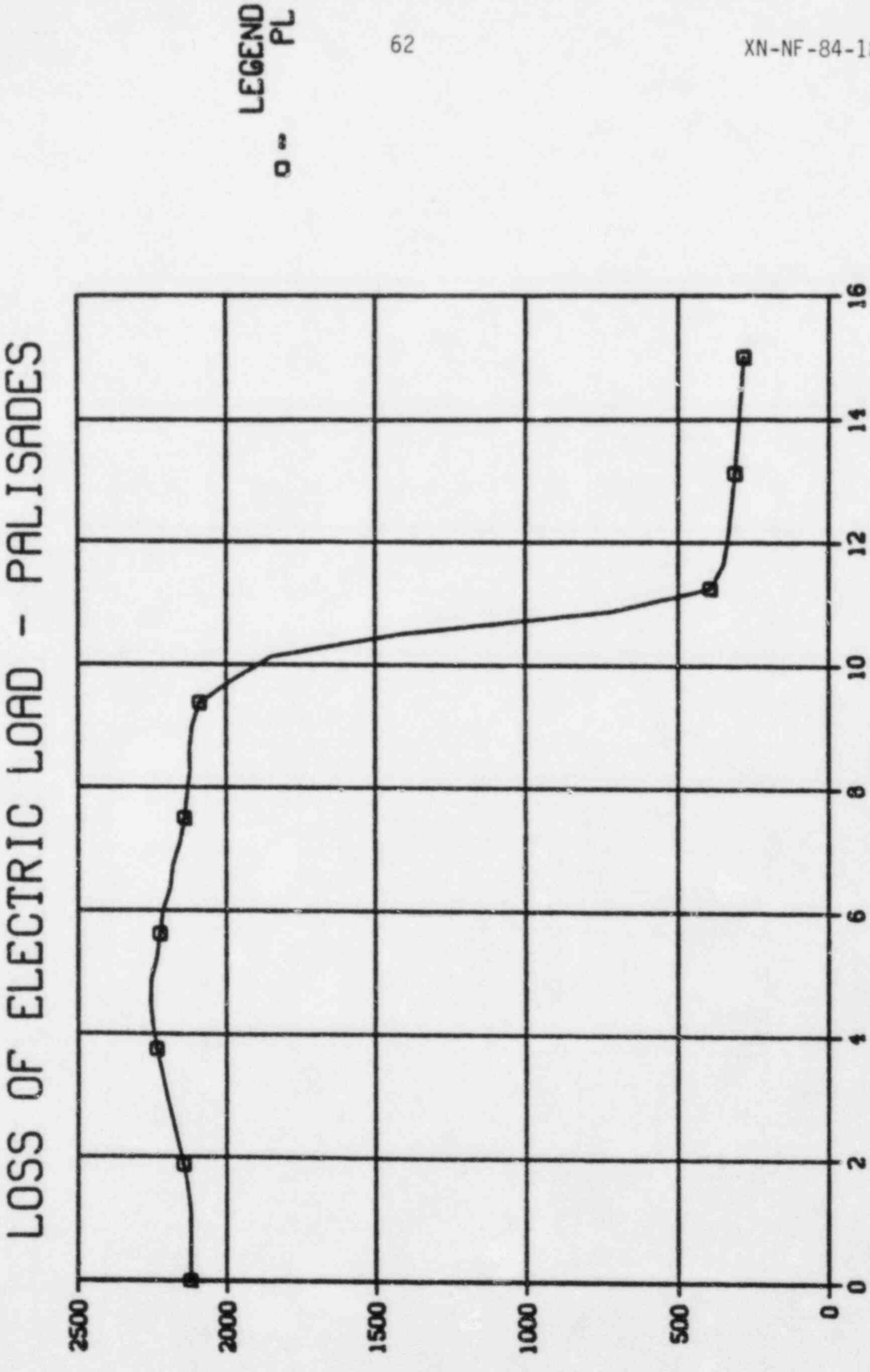

Figure 3.7 Reactor Power for Loss of Electric Load

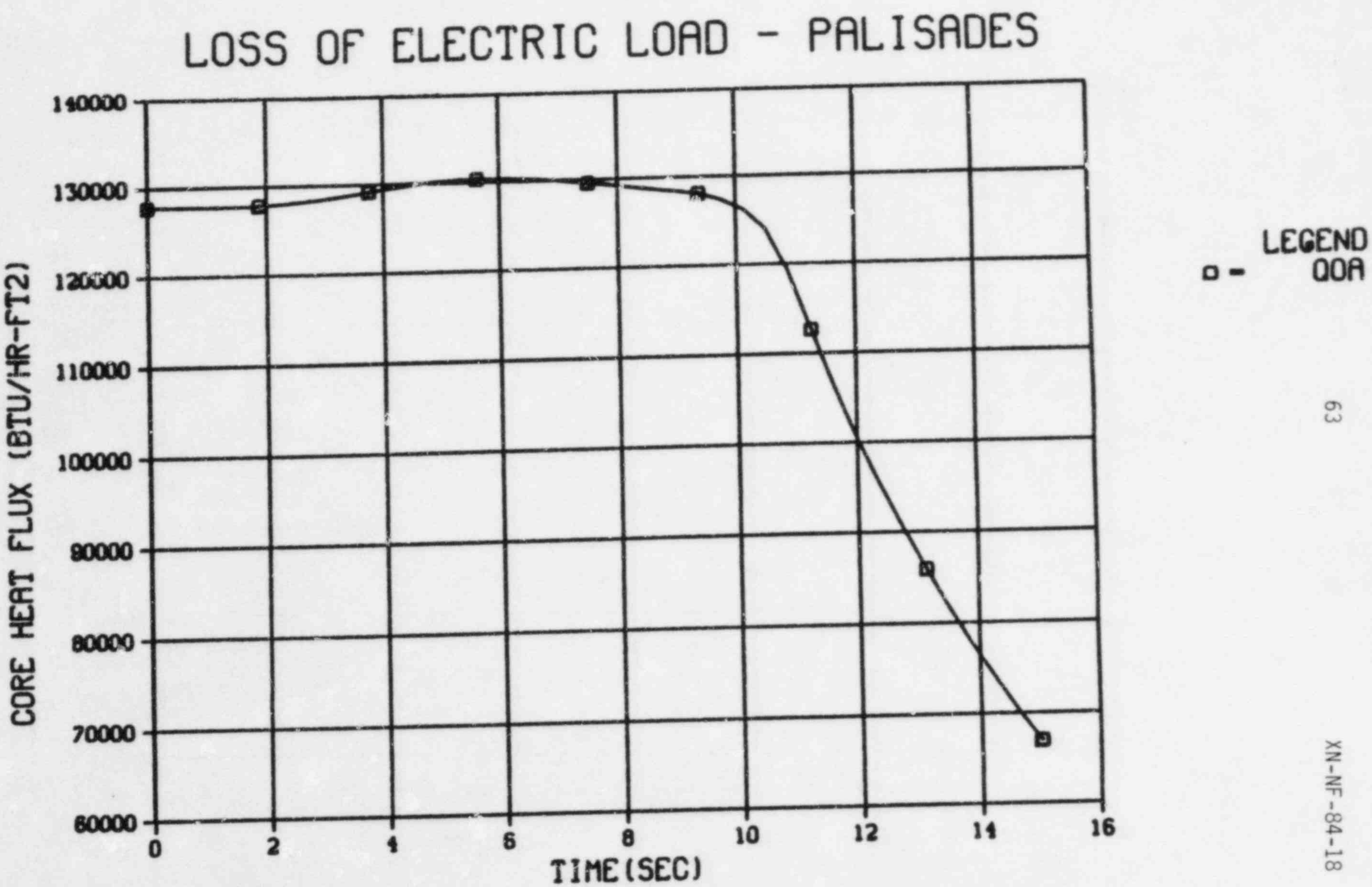

Figure 3.8 Core Heat Flux for Loss of Electric Load

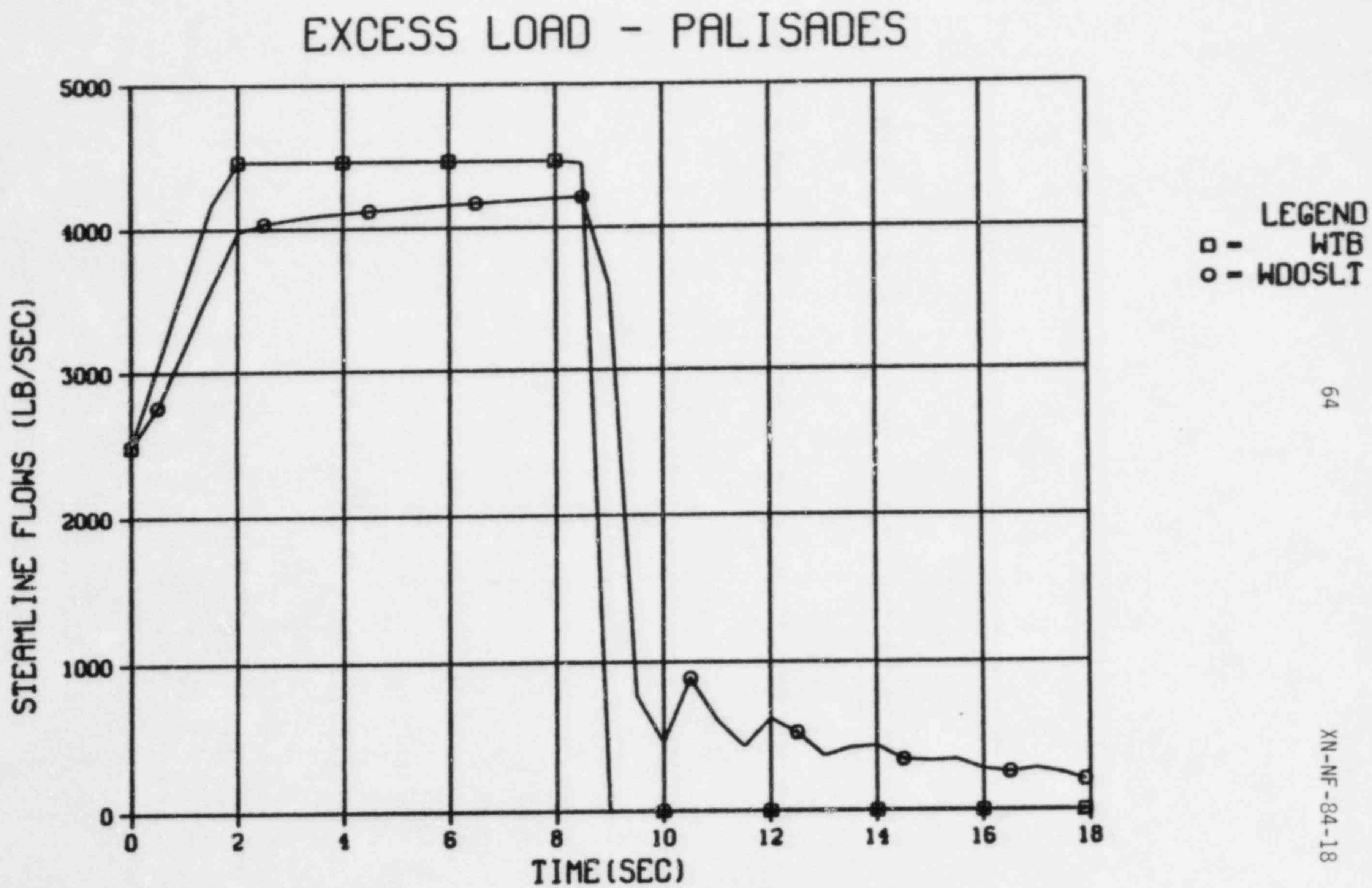

Figure 3.9 Steam Line Flows for Excess Load

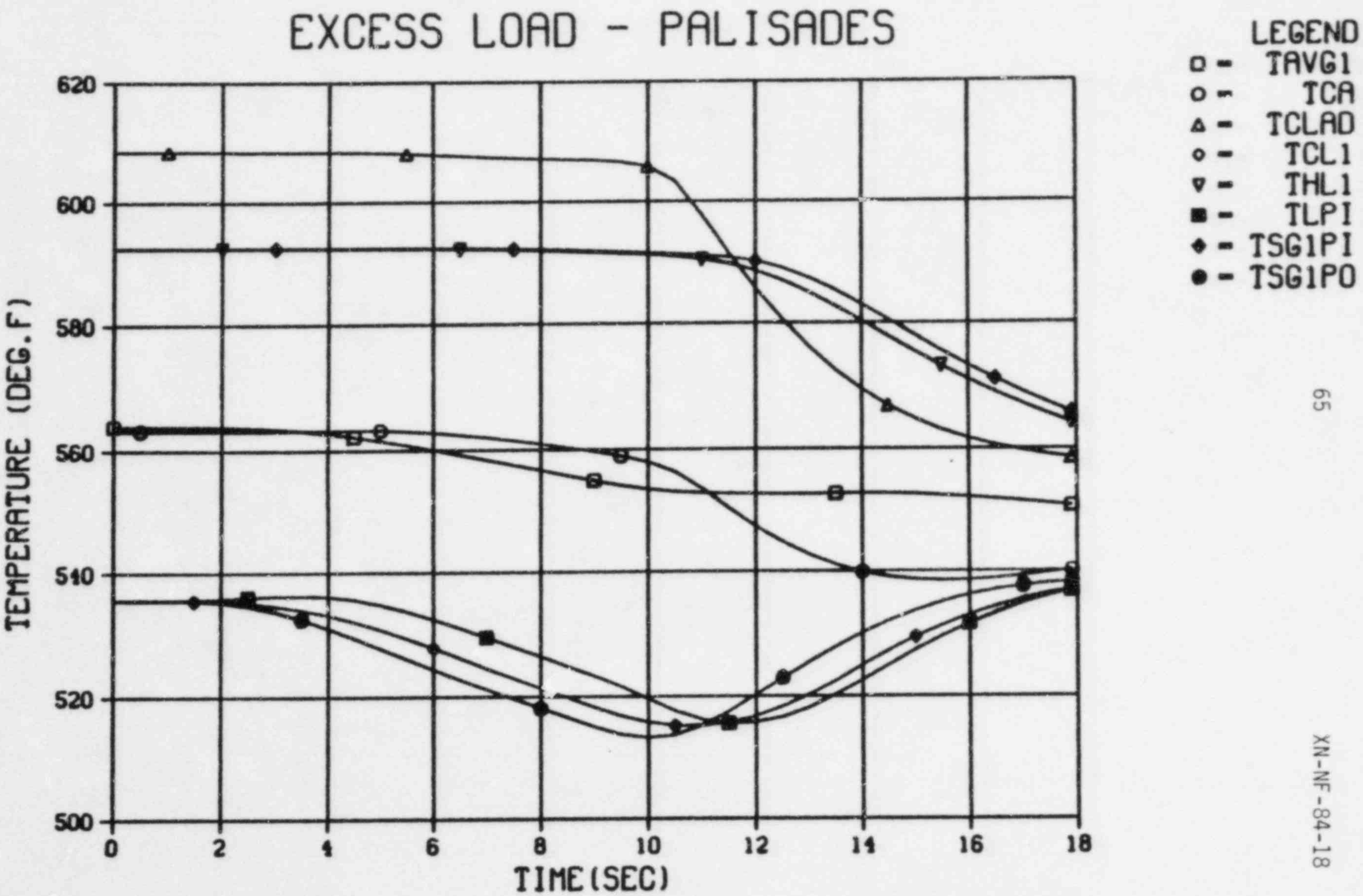

Figure 3.10 Primary Loop Temperatures for Excess Load

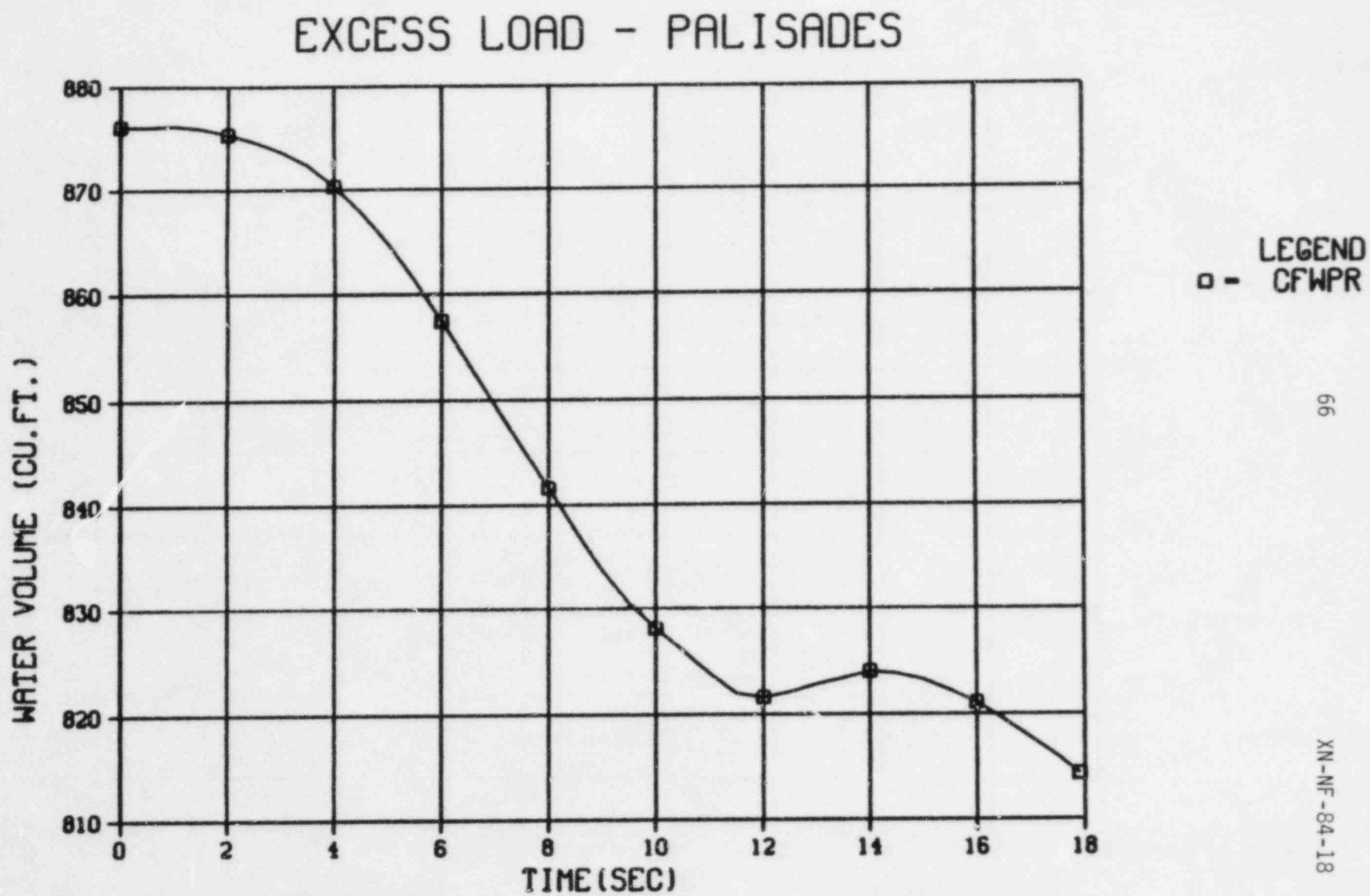

Figure 3.11 Liquid Volume in Pressurizer for Excess Load

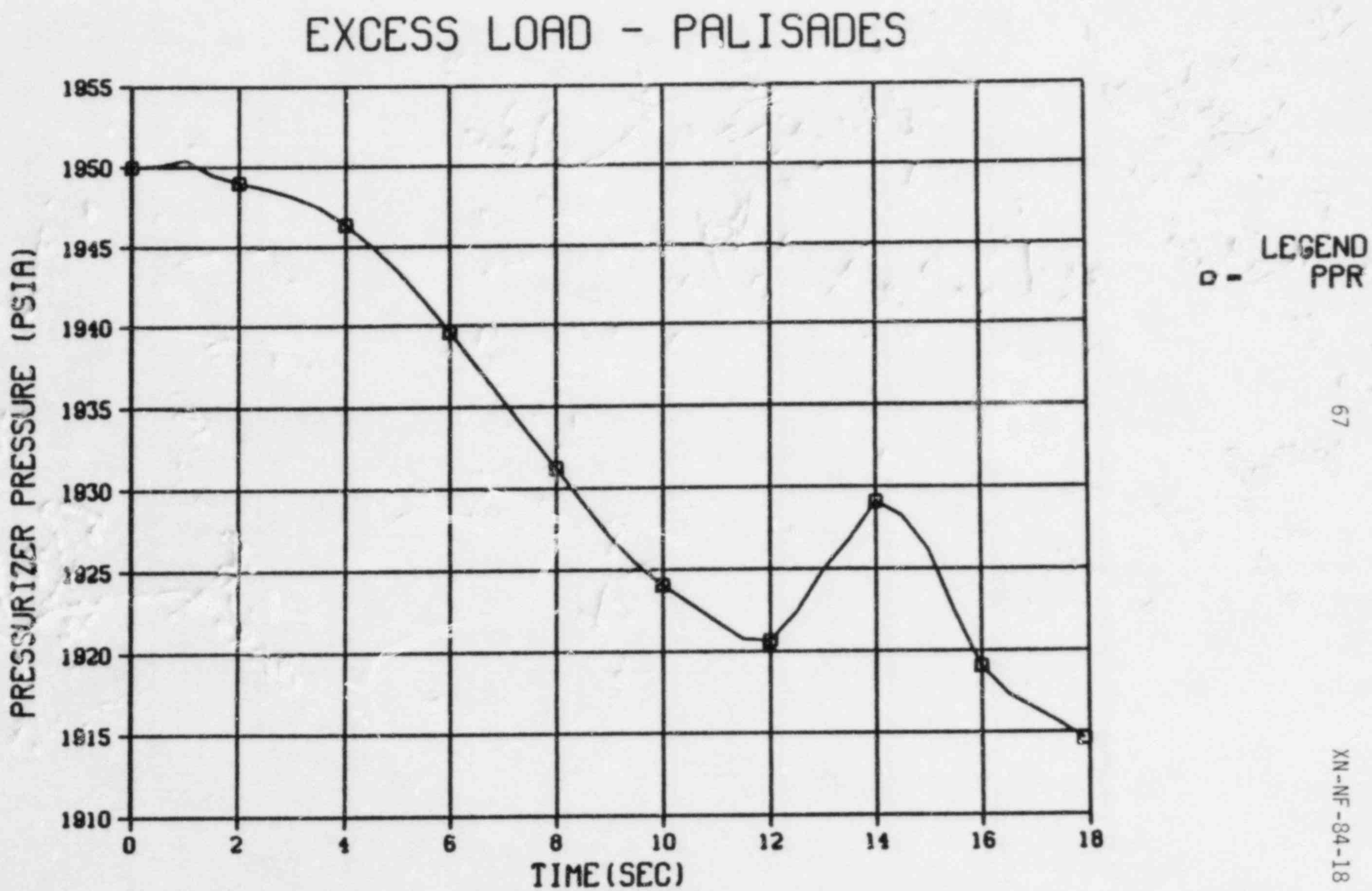

Figure 3.12 Pressurizer Pressure for Excess Load

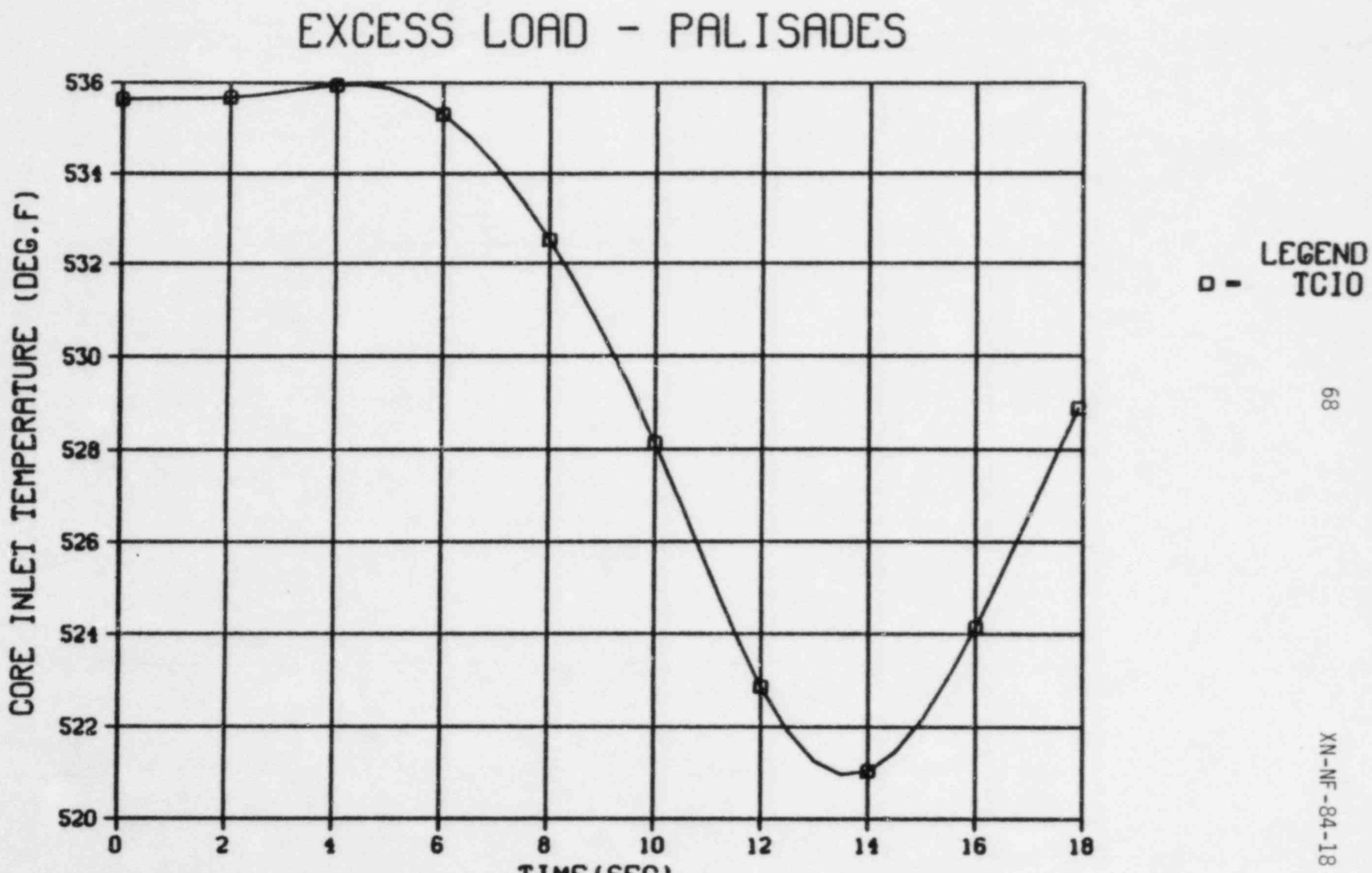

Figure 3.13 Core Inlet Temperature for Excess Load

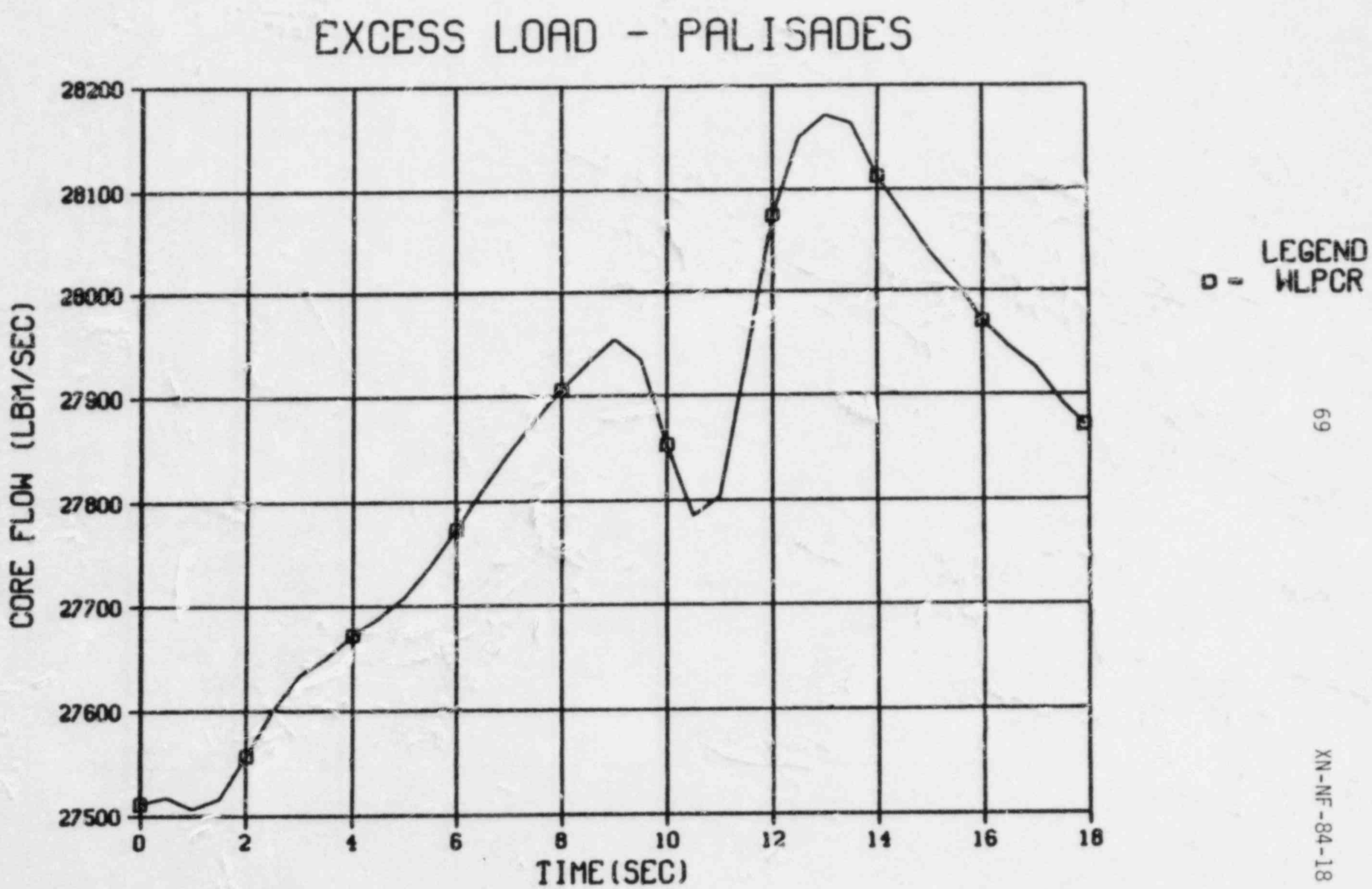

Figure 3.14 Core Flow for Excess Load

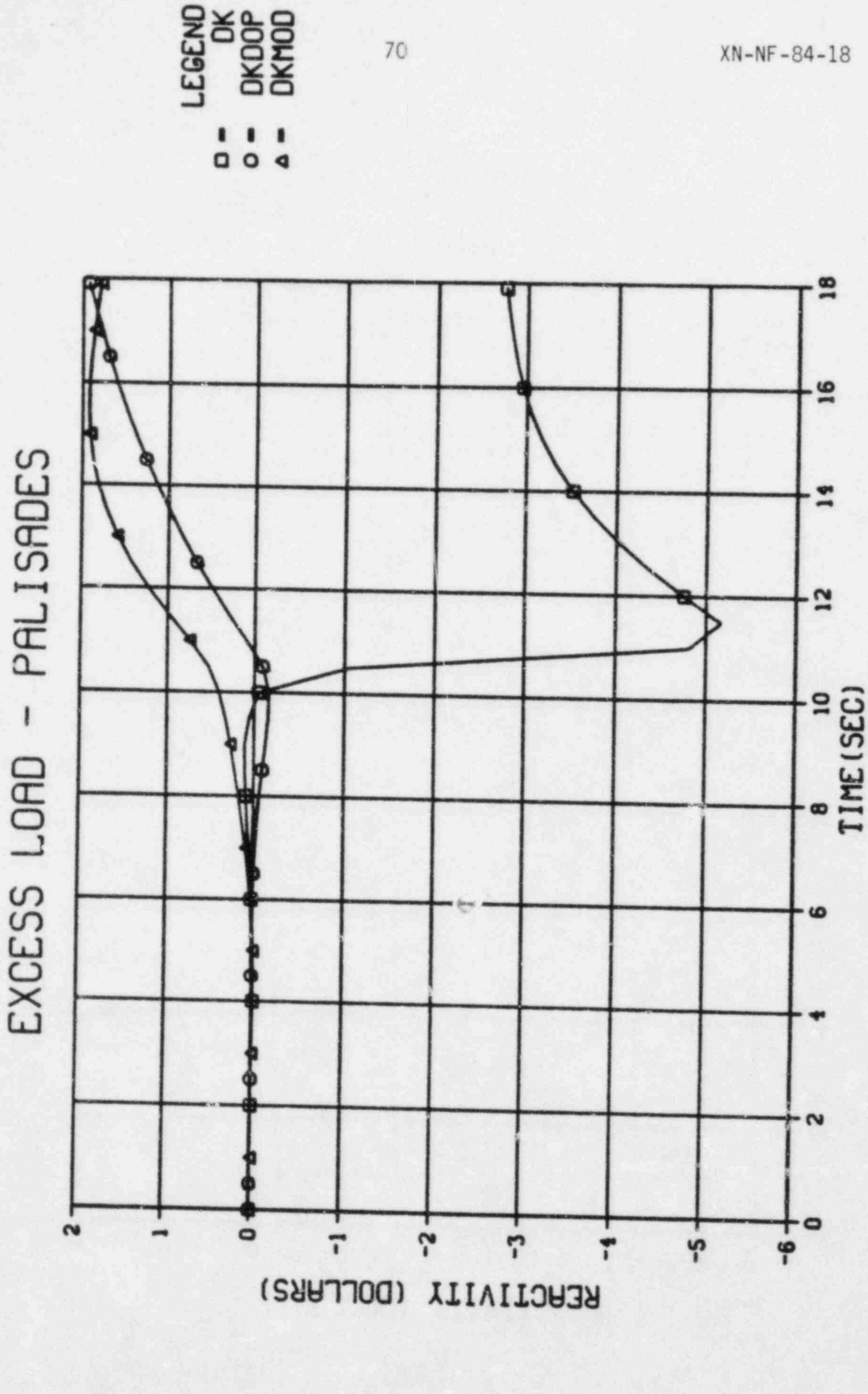

Figure 3.15 Reactivities for Excess Load

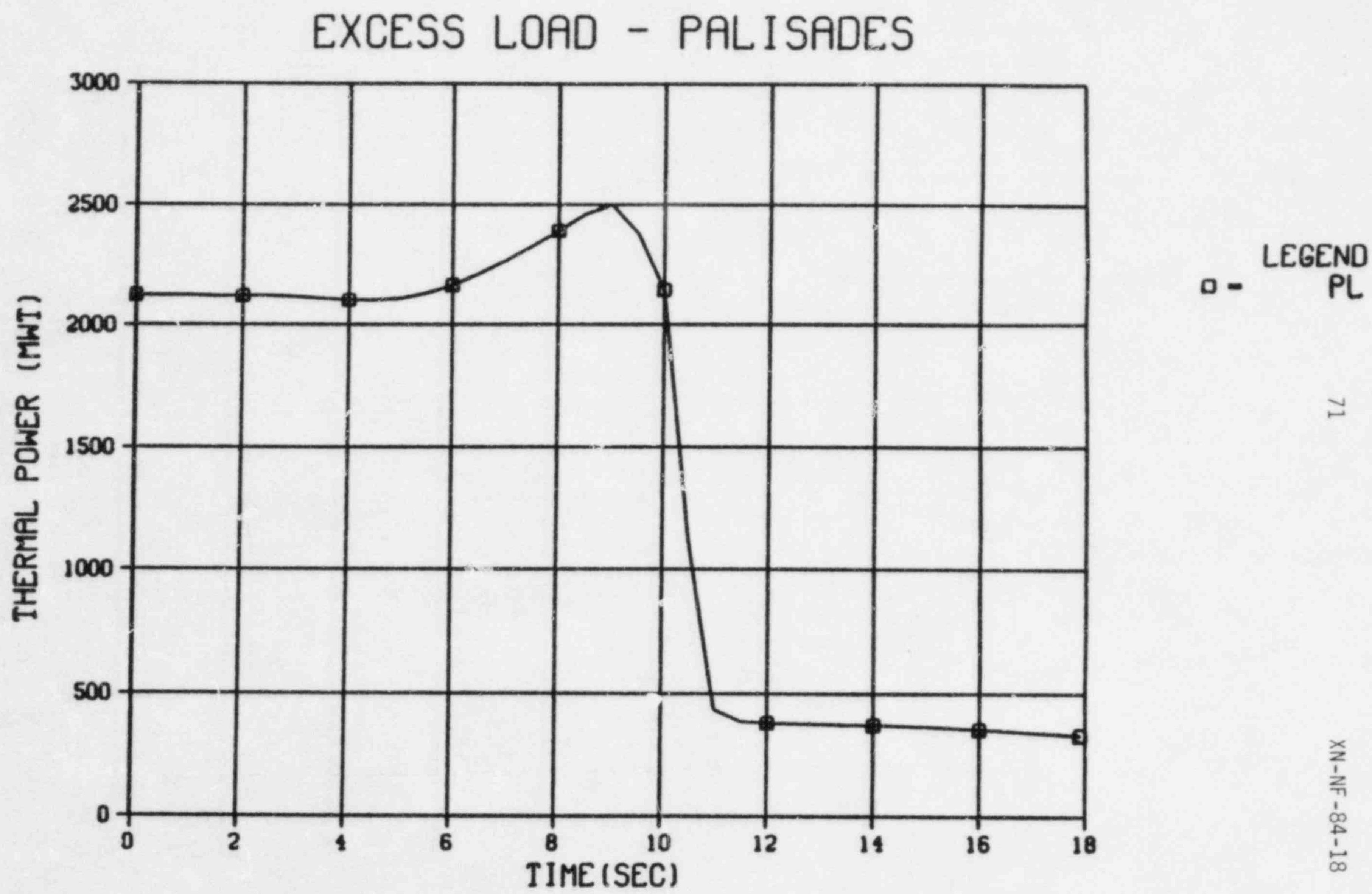

Figure 3.16 Reactor Power for Excess Load

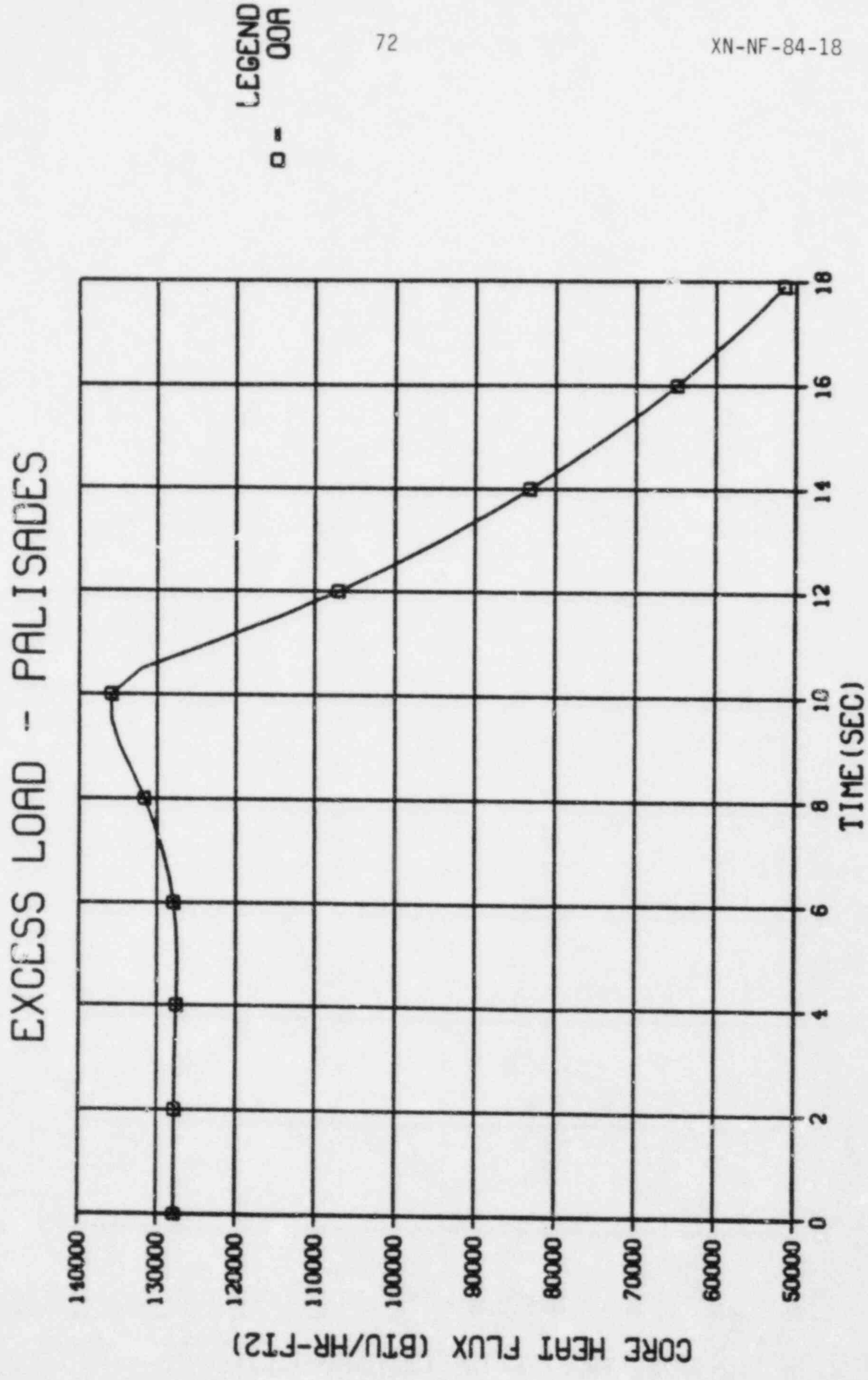

Figure 3.17 Core Heat Flux for Excess Load

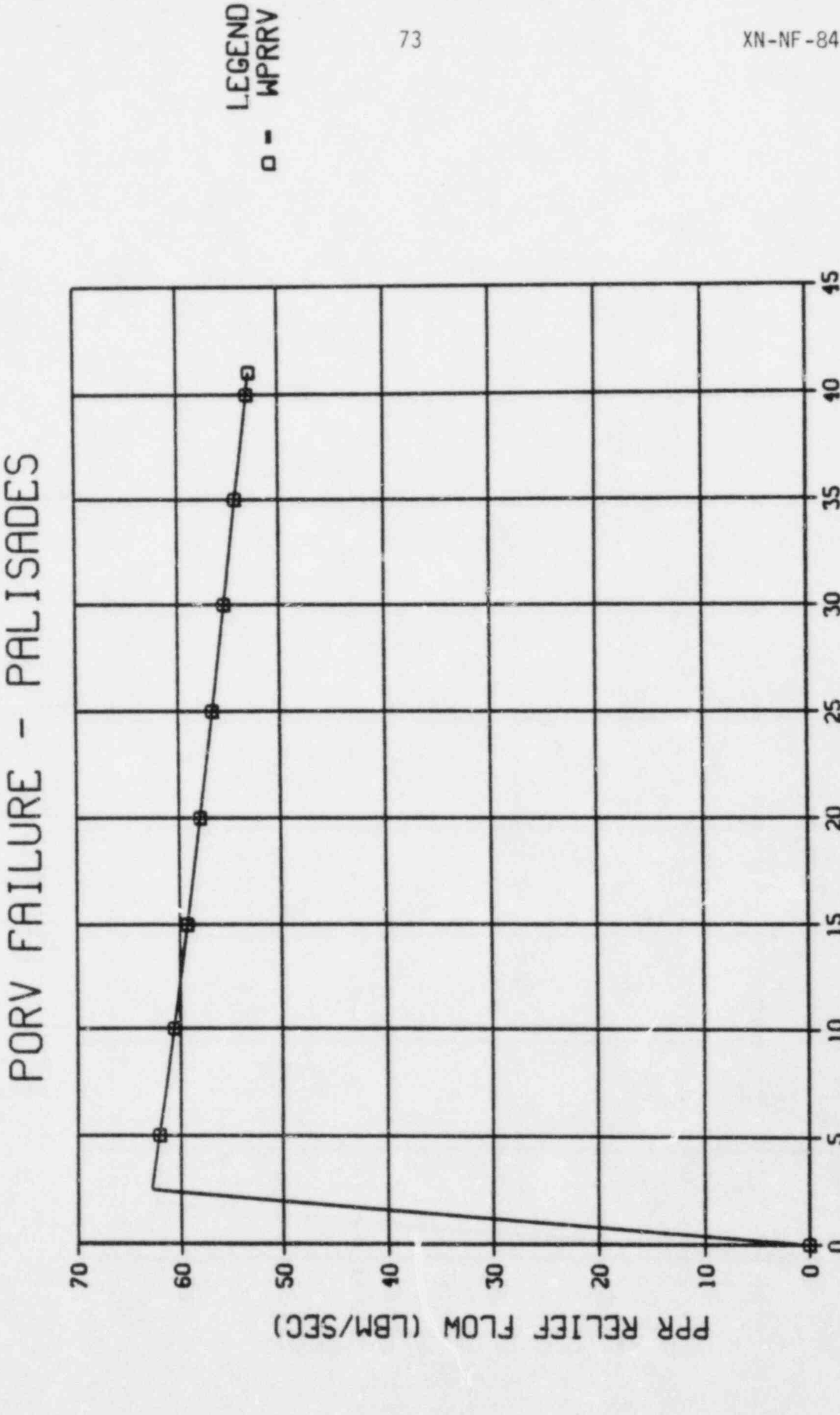

Figure 3.18 Pressurizer Relief Valve Flow for the PORV Failure

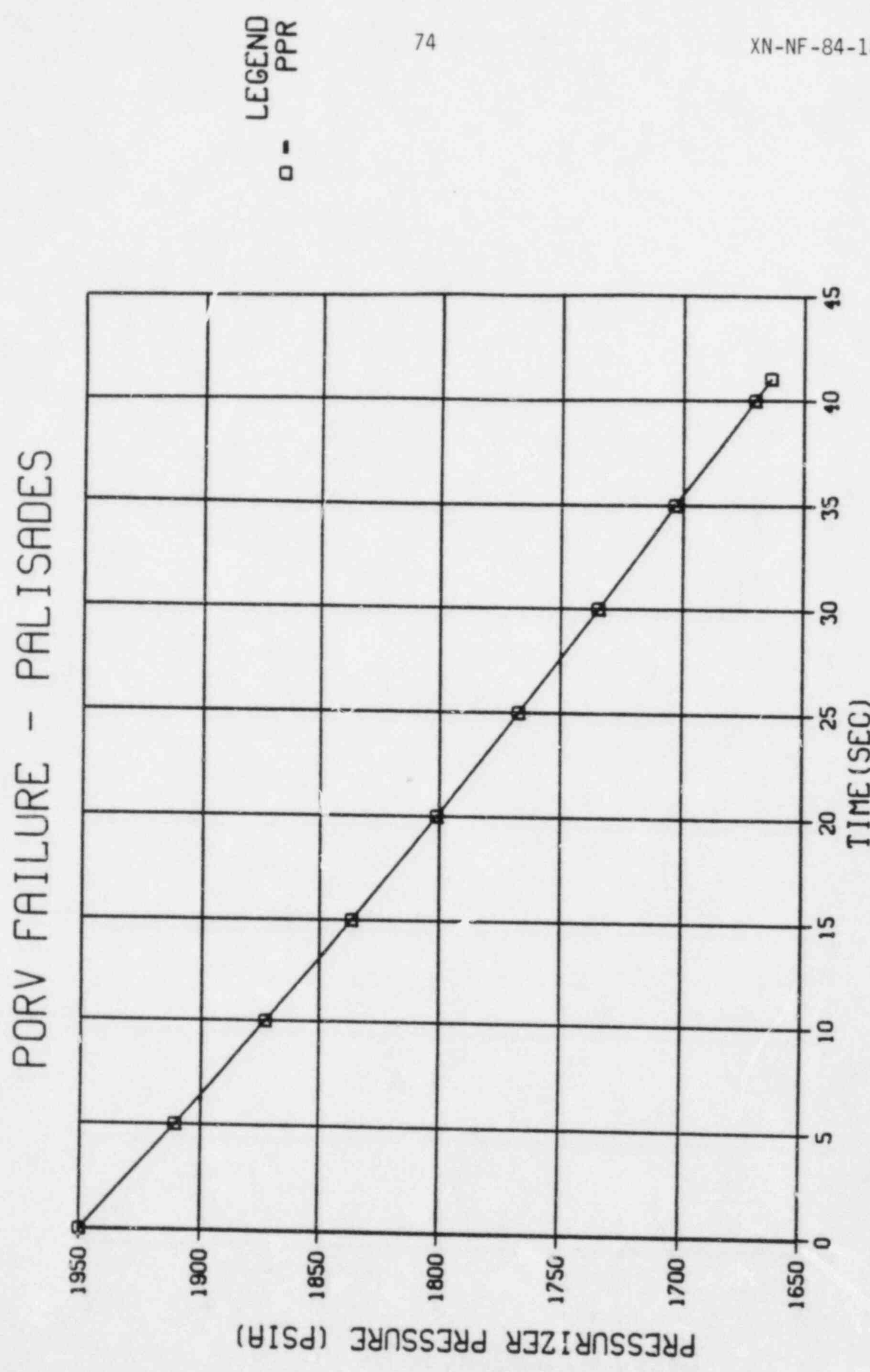

Figure 3.19 Pressurizer Pressure for the PORV Failure

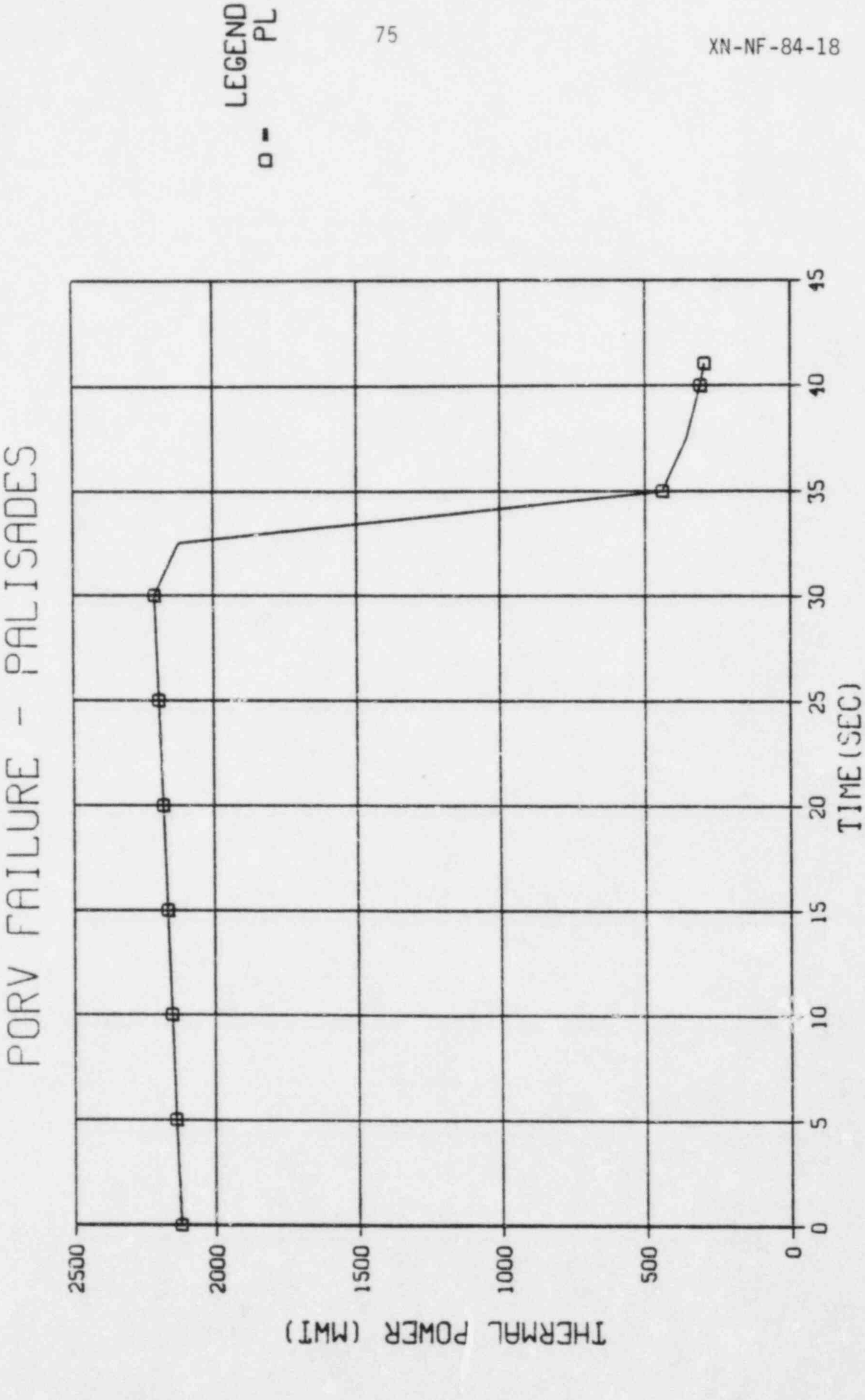

Figure 3.20 Reactor Thermal Power for the PORV Failure

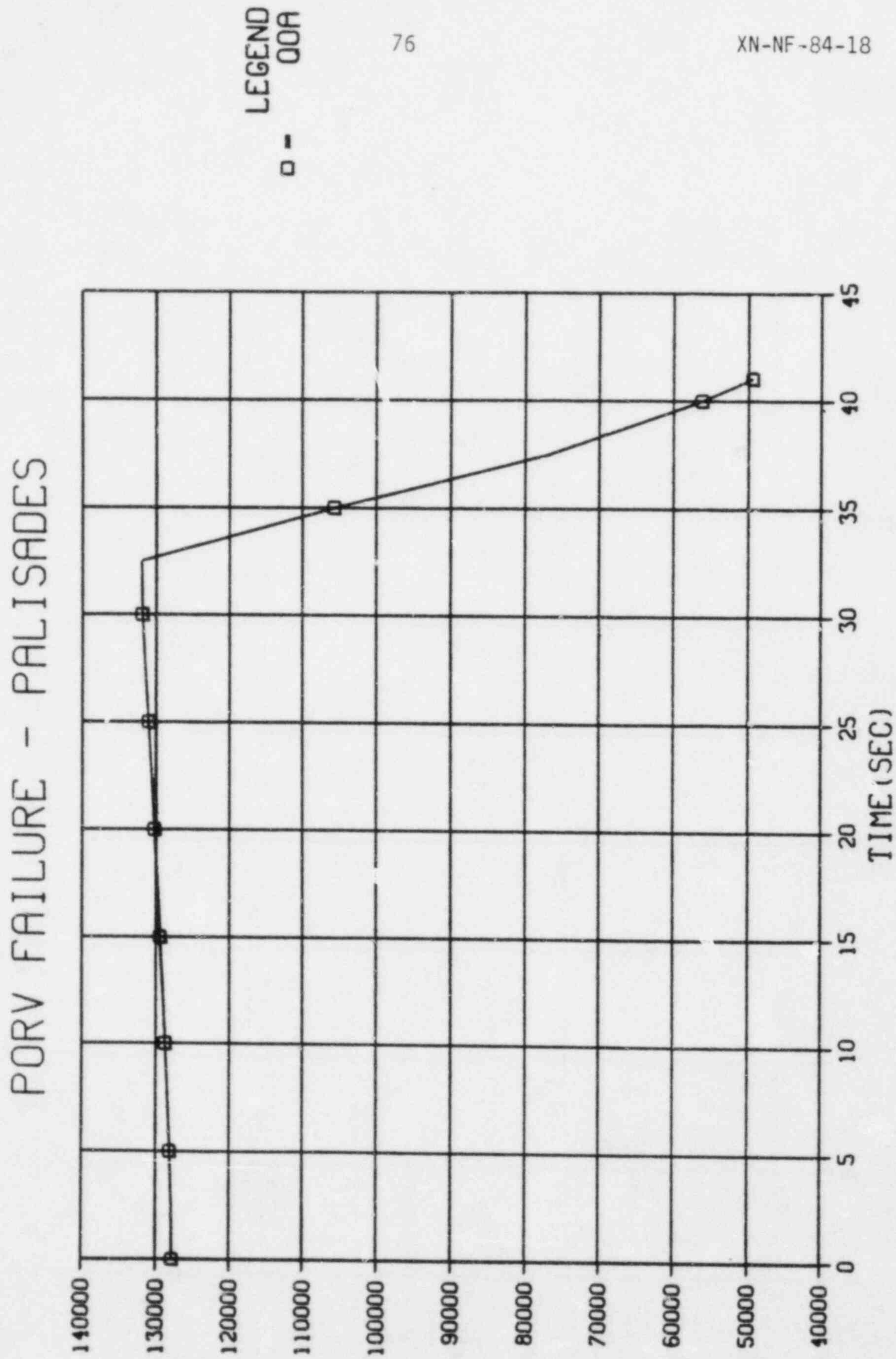

Figure 3.21 Reactor Heat Flux for the PORV Failure

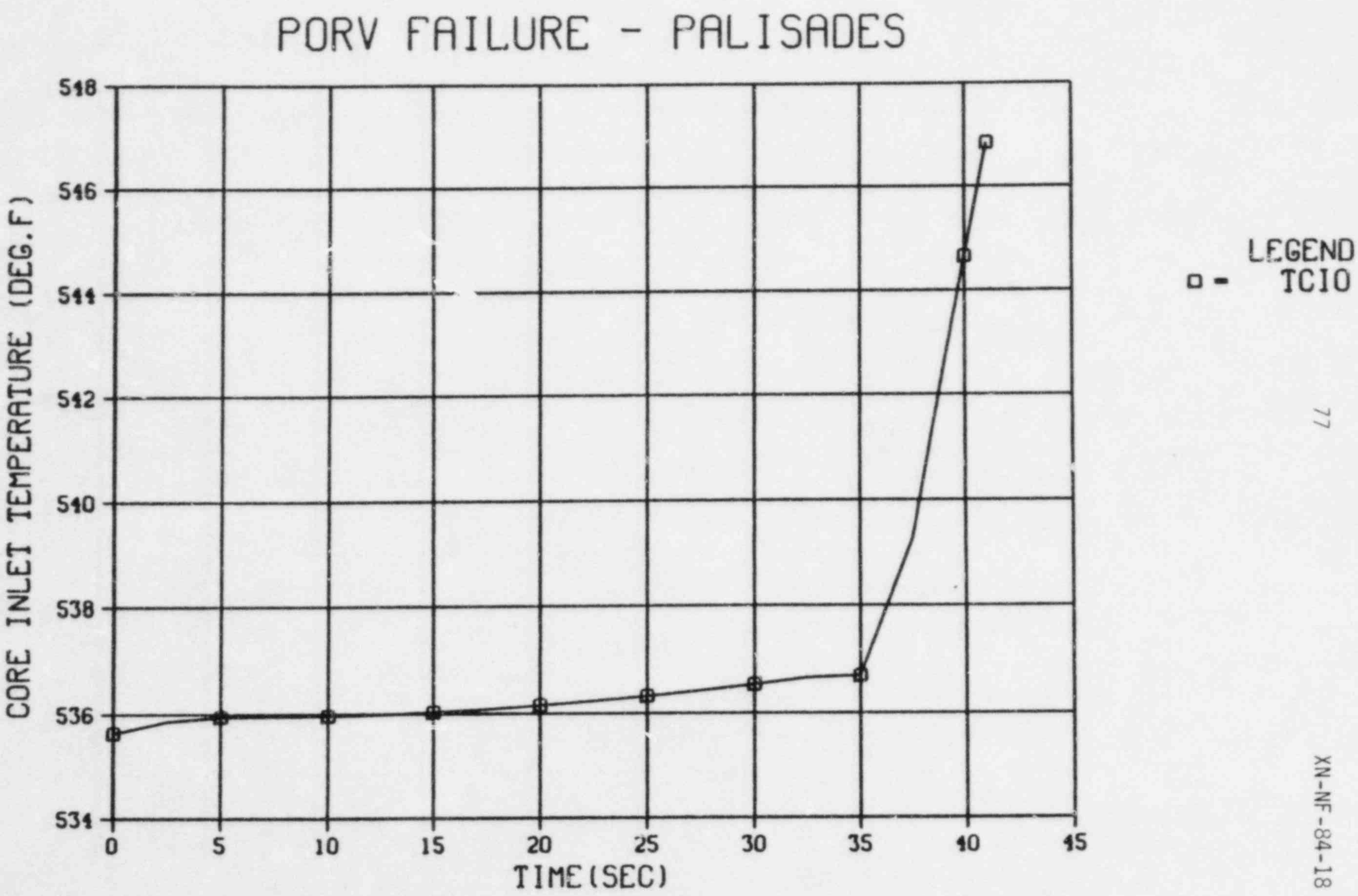

Figure 3.22 Core Inlet Temperature for the PORV Failure

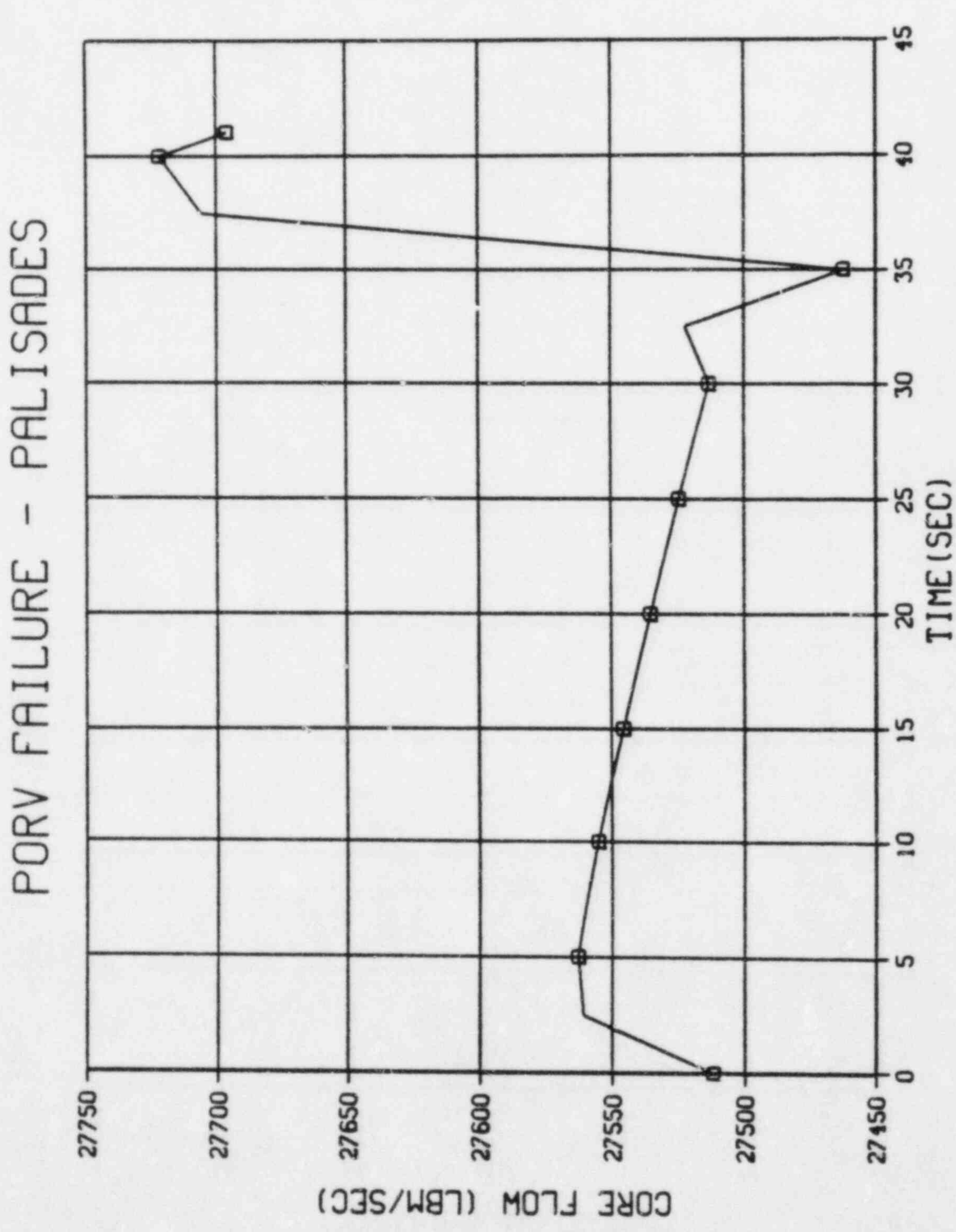

Figure 3.23 Core Flow for the PORV Failure

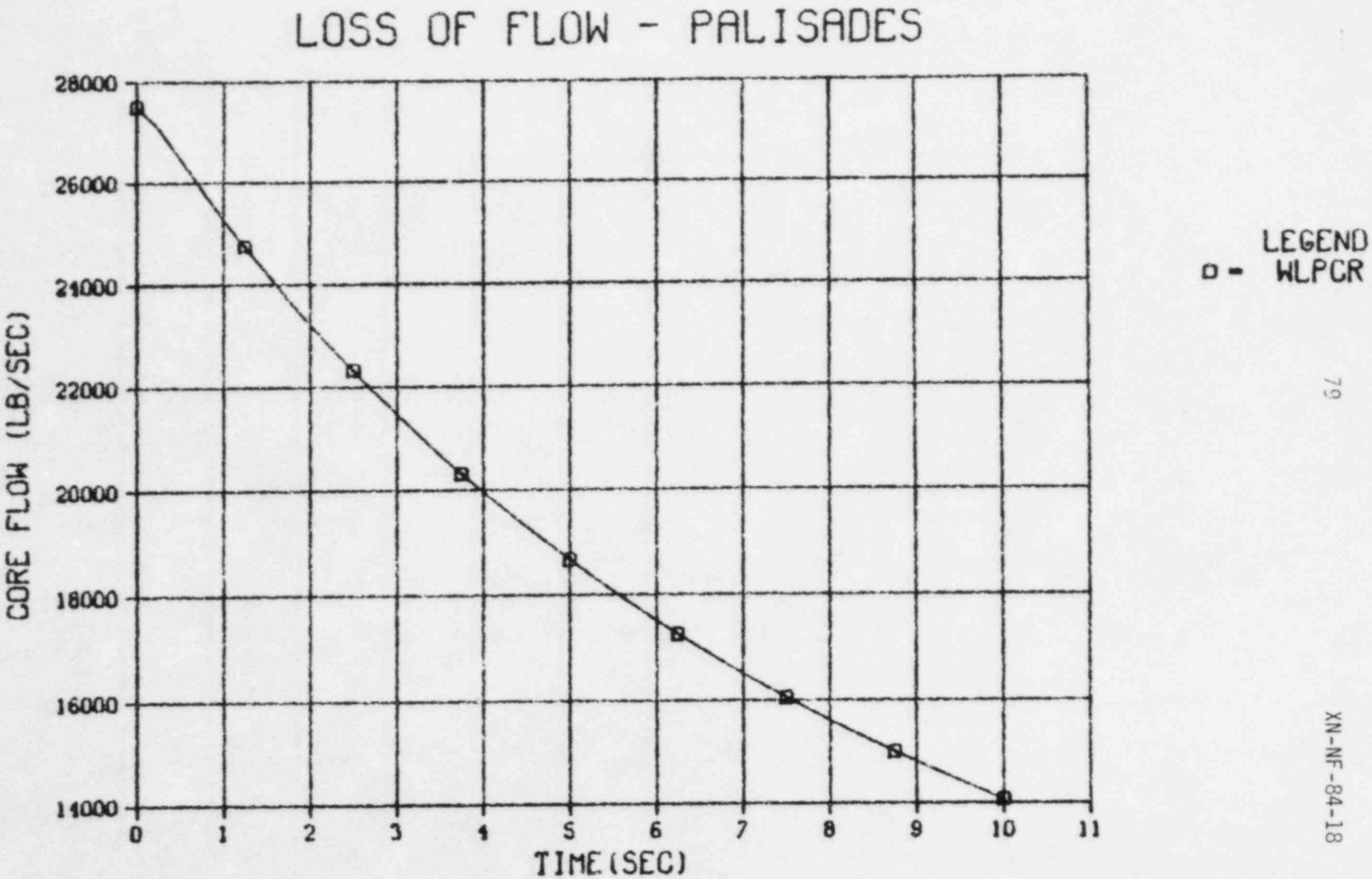

Figure 3.24 Core Flow for the Four-Pump Coastdown

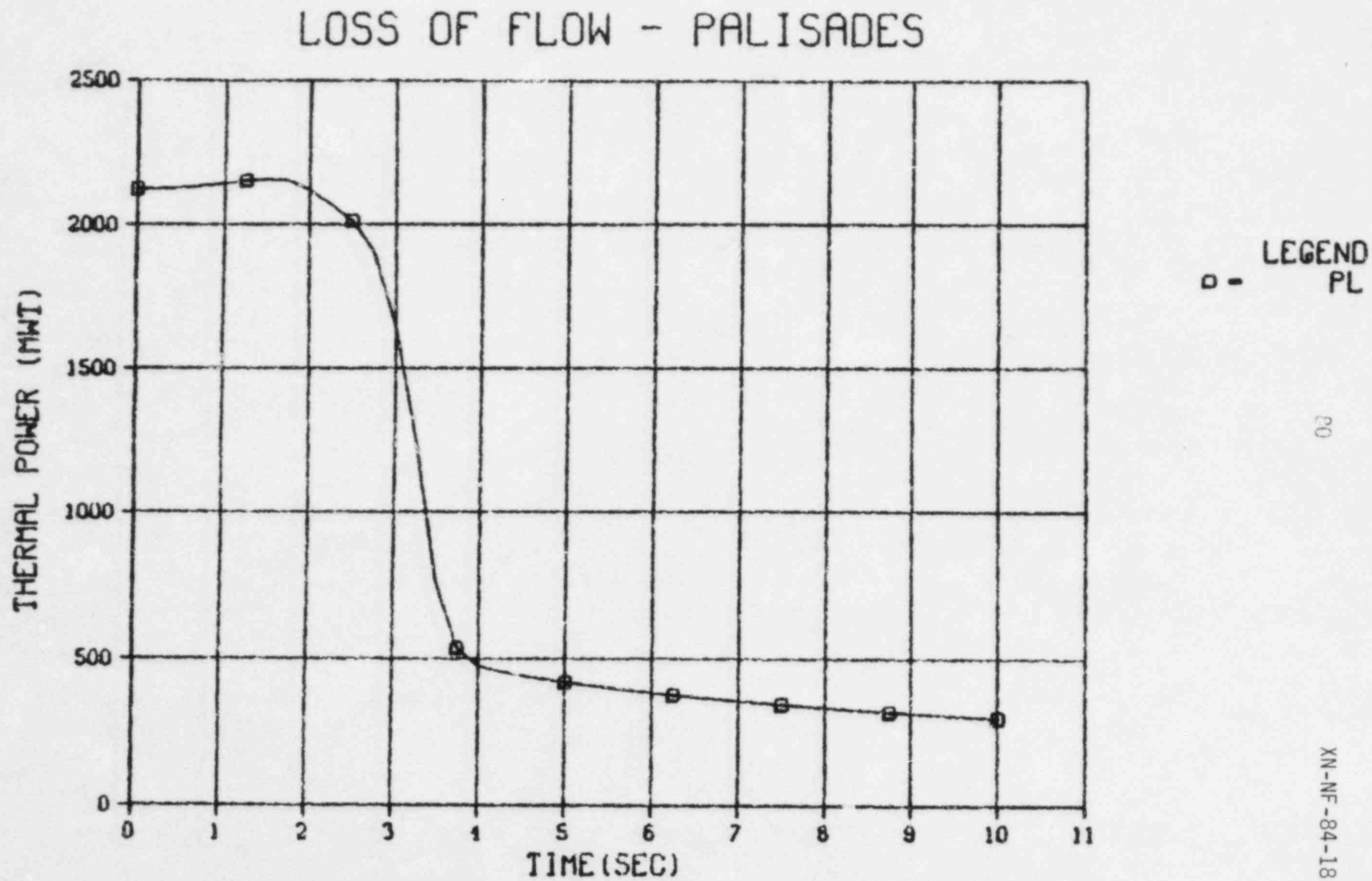

Figure 3.25 Reactor Thermal Power for the Four-Pump Coastdown

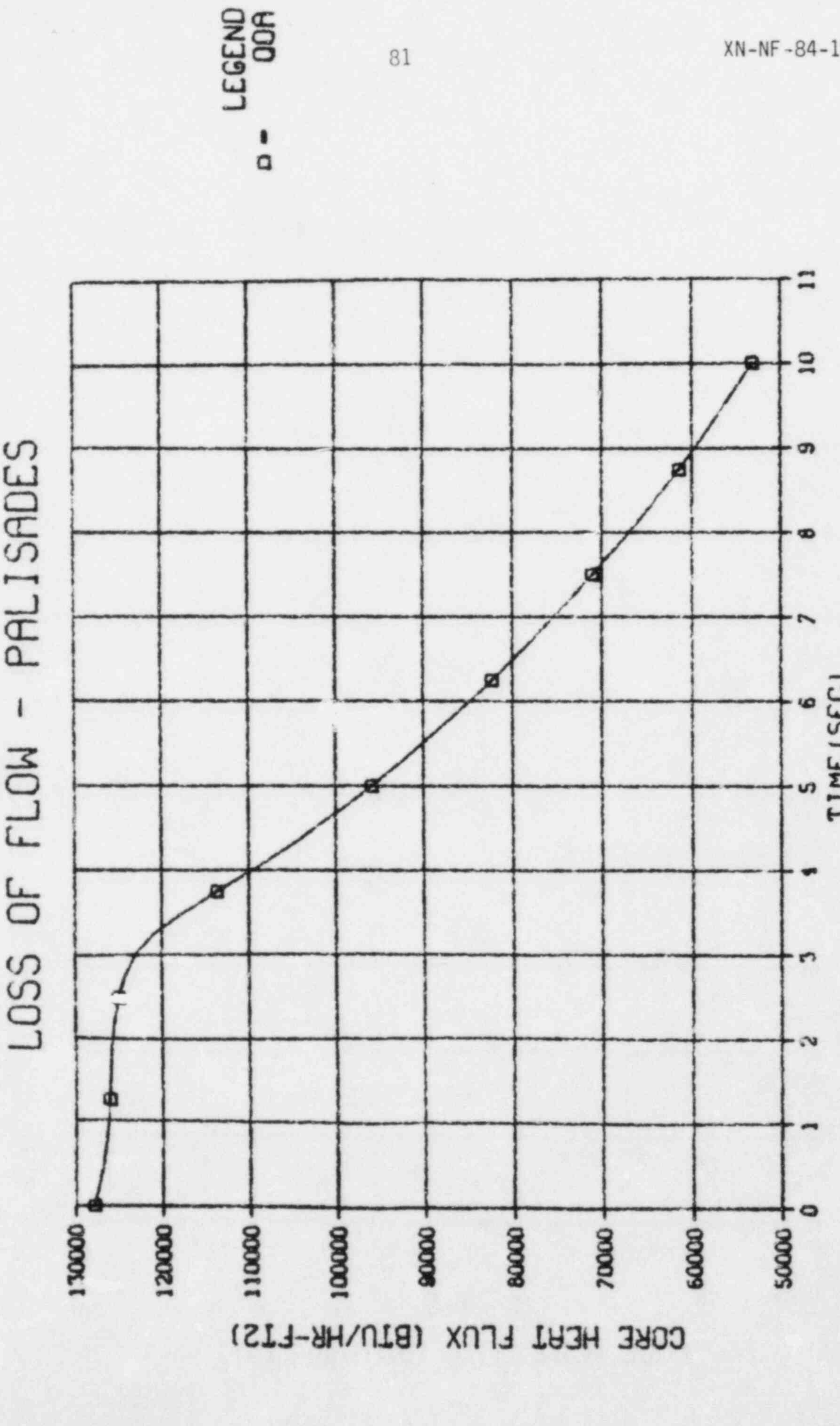

Figure 3.26 Core Heat Flux for the Four-Pump Coastdown

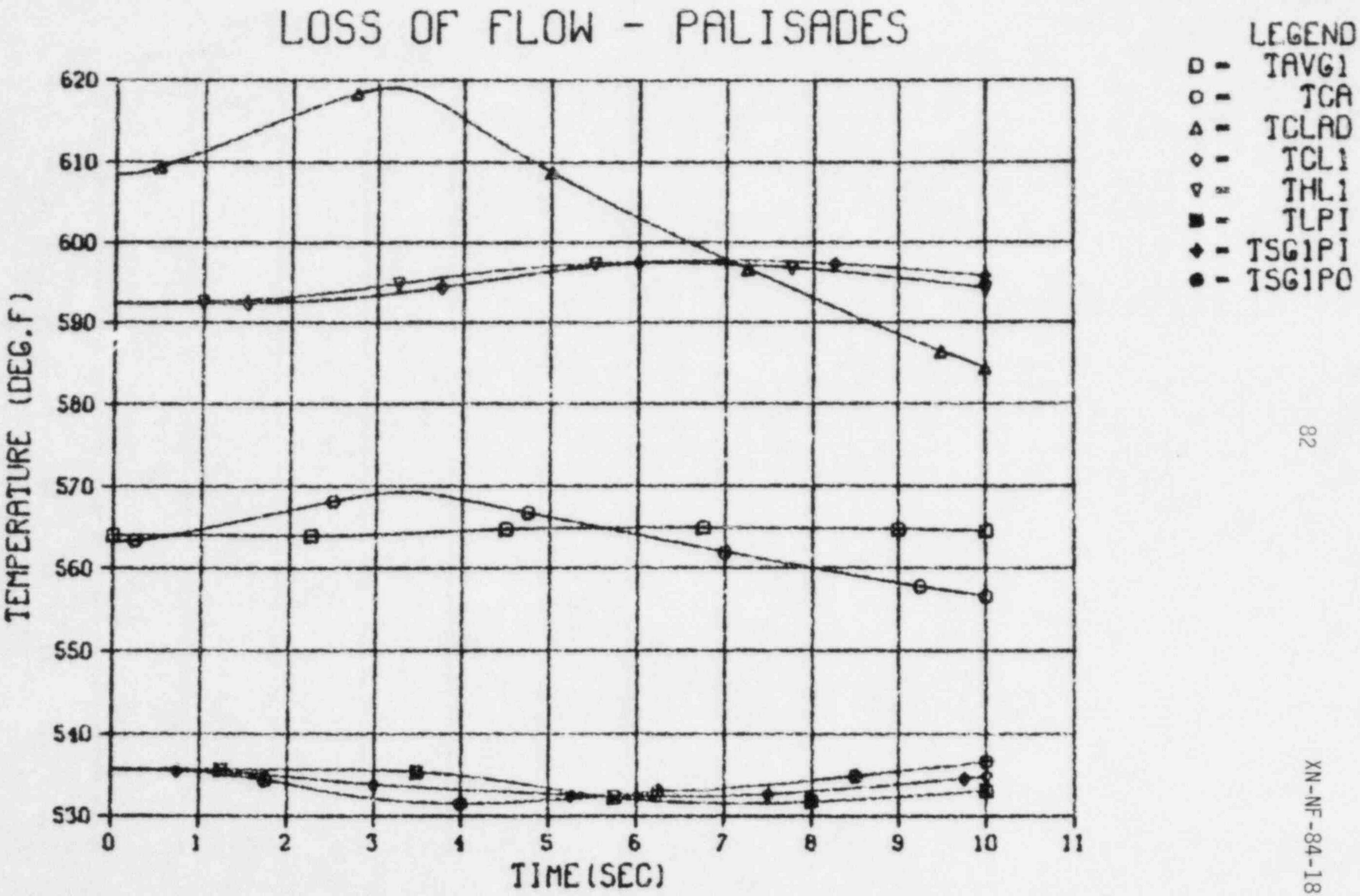

Figure 3.27 Primary Loop Temperatures for the Four-Pump Coastdown

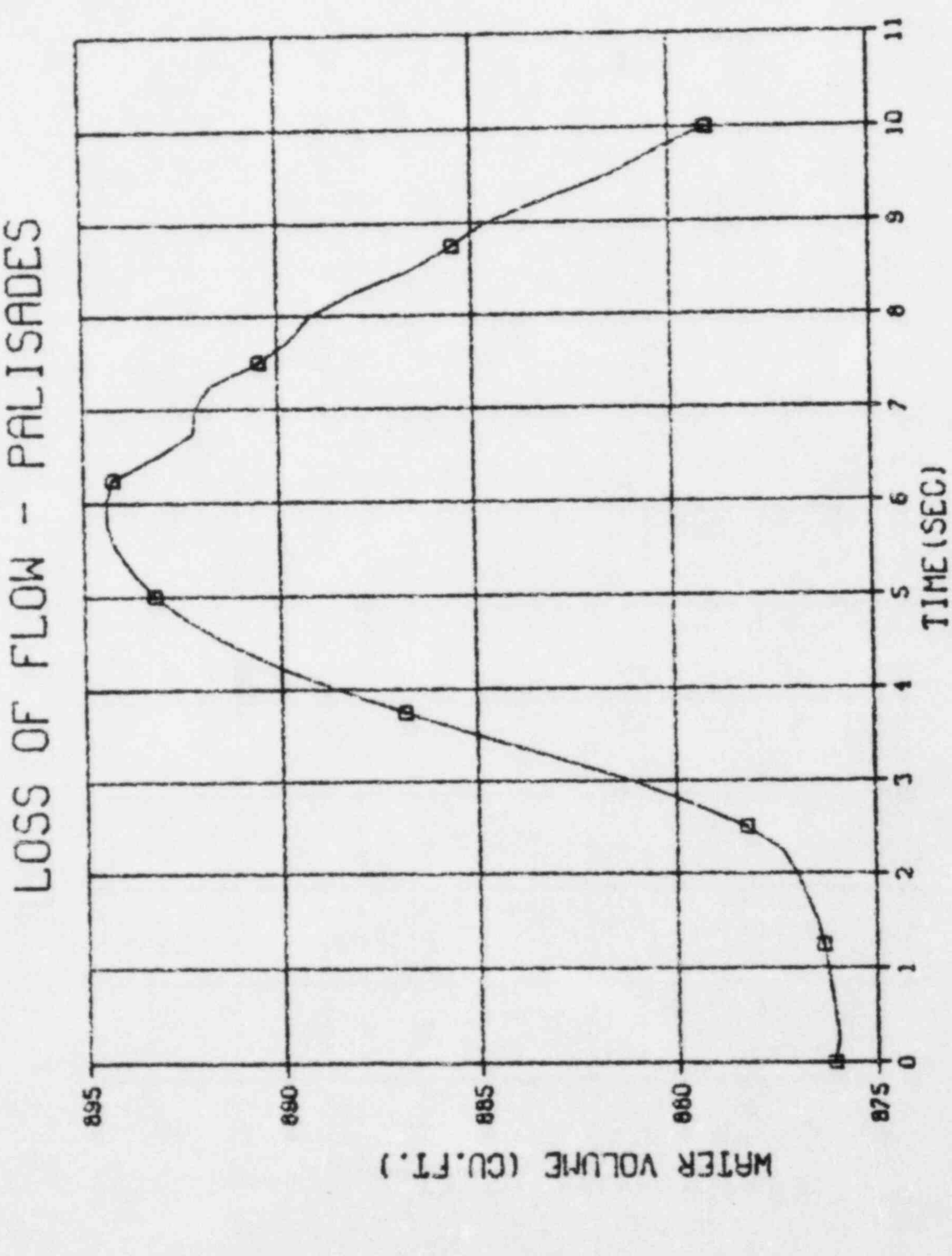

Figure 3.28 Liquid Volume in Pressurizer for the Four-Pump Coastdown

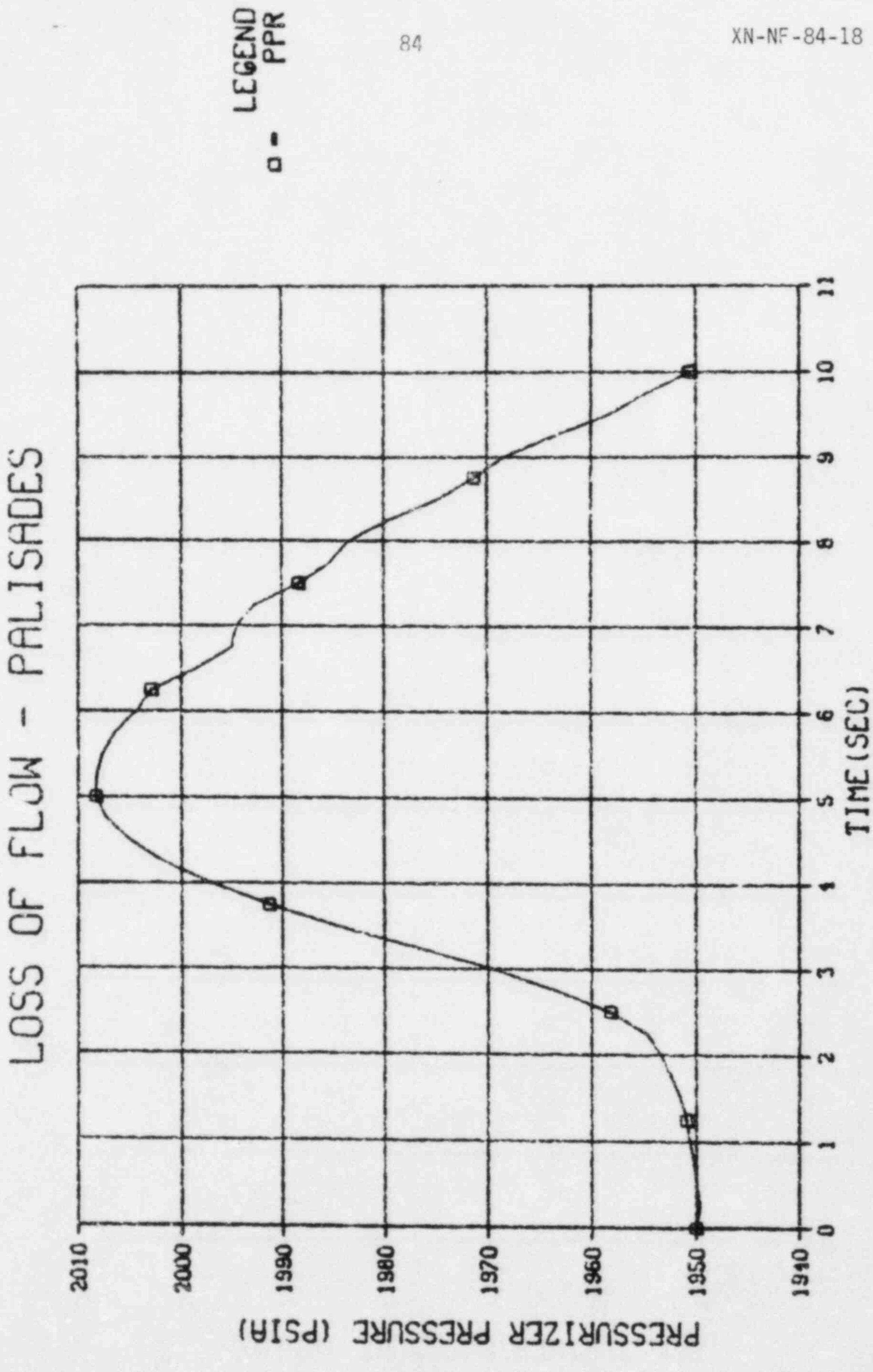

Figure 3.29 Pressurizer Pressure for the Four-Pump Coastdown

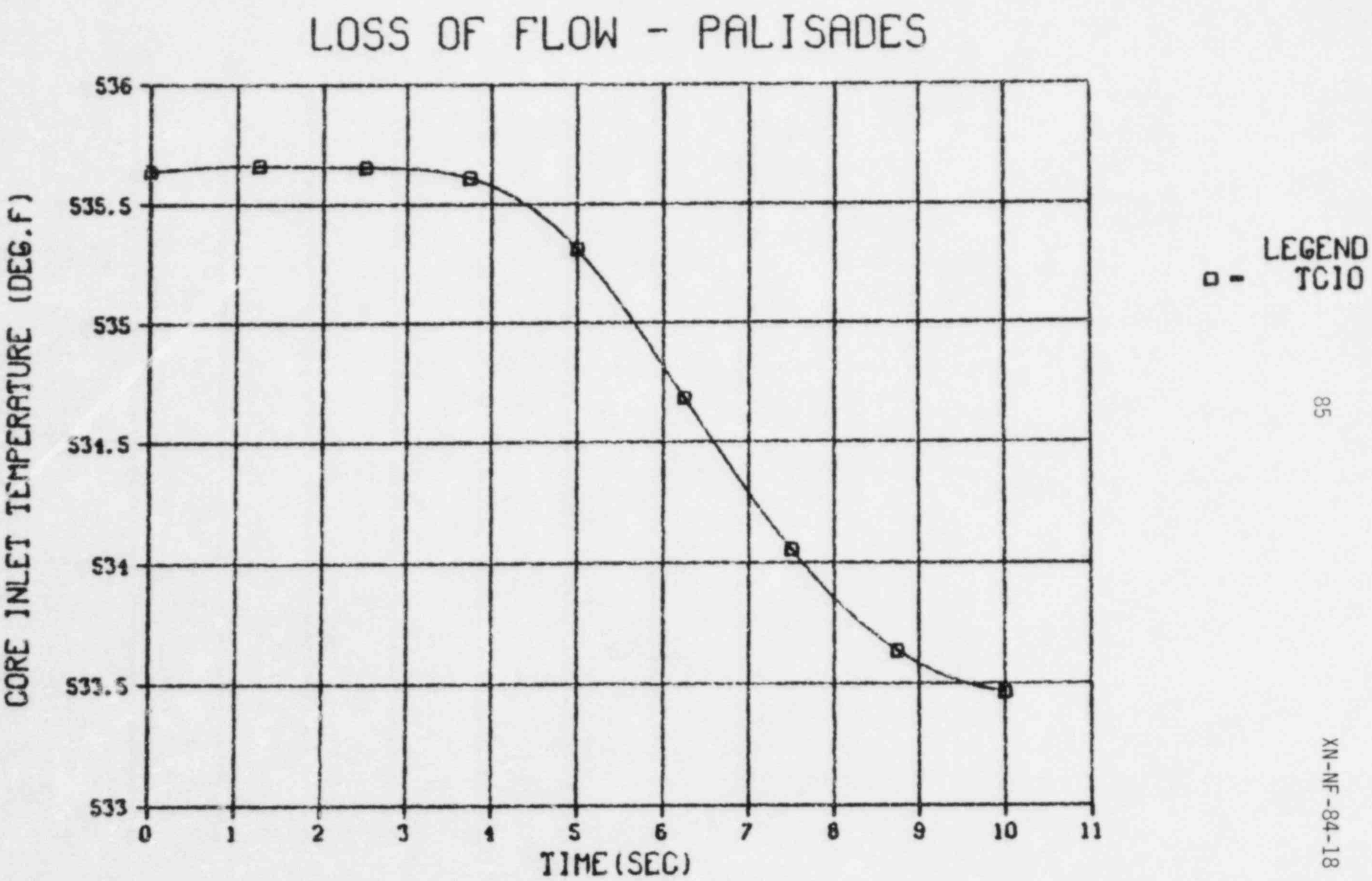

Figure 3.30 Core Inlet Temperature for the Four-Pump Coastdown

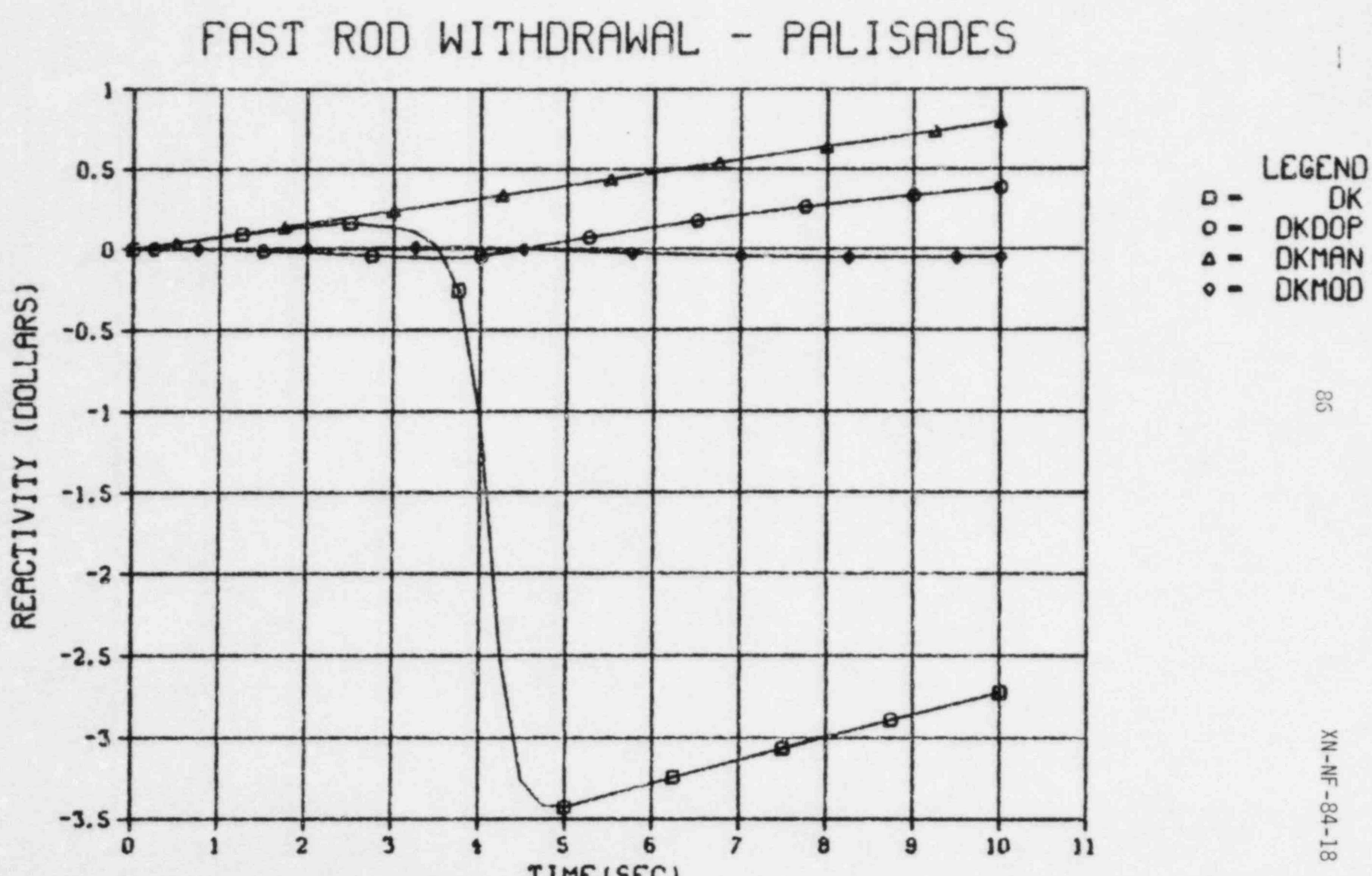

Figure 3.31 Reactivities for Fast Rod Withdrawal from 100% Power

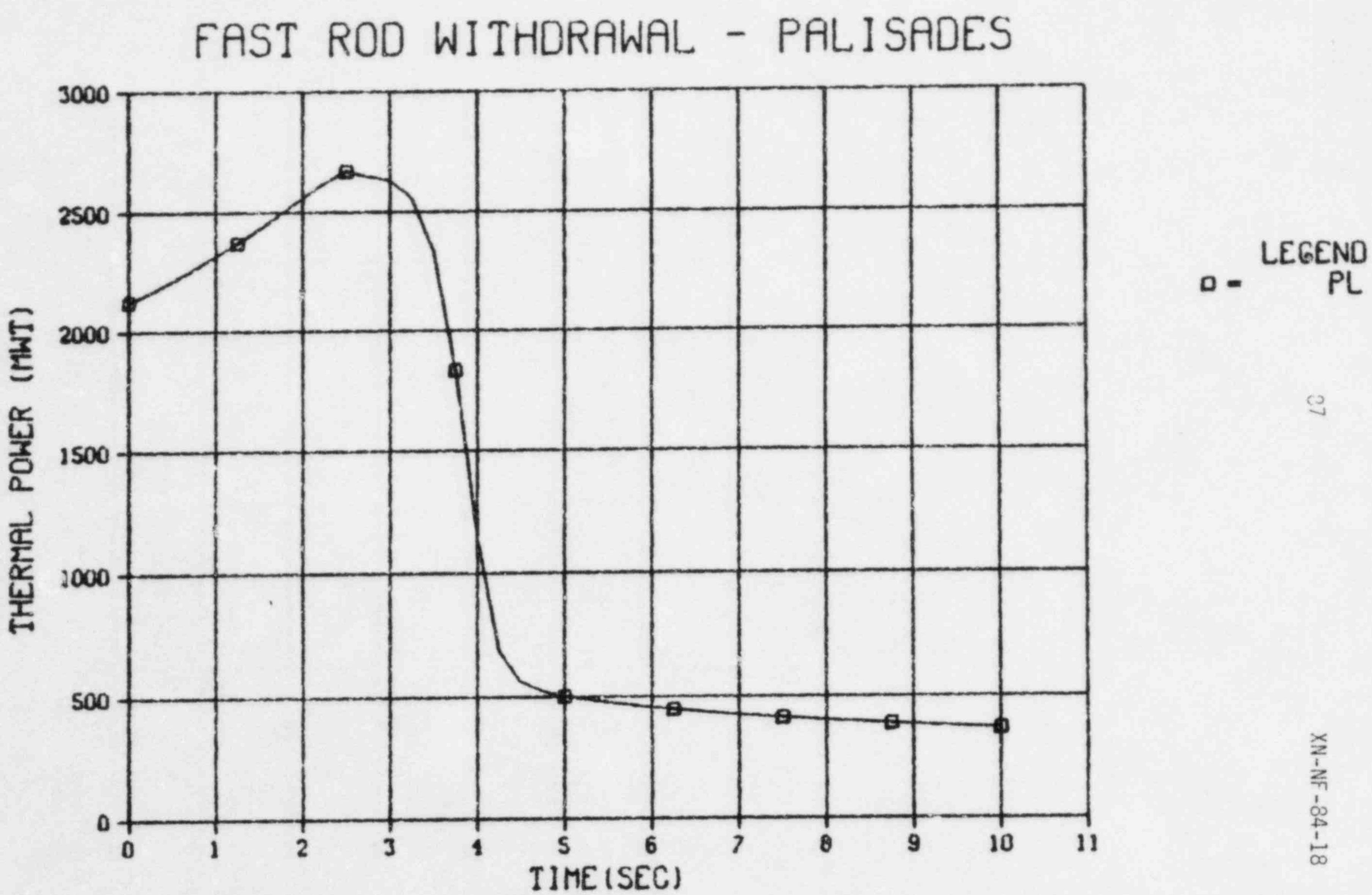

Figure 3.32 Reactor Thermal Power for Fast Rod Withdrawal from 100% Power

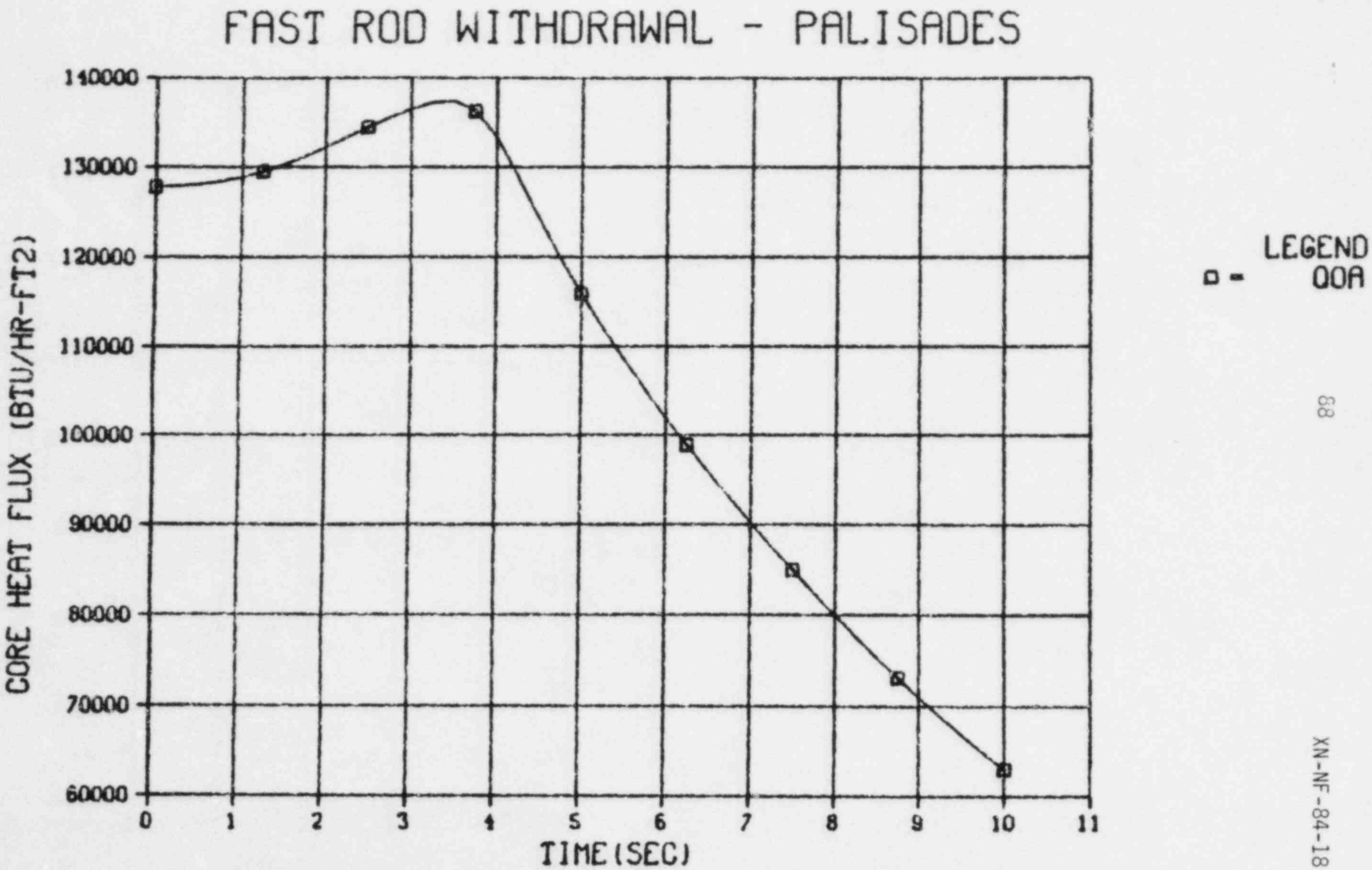

Figure 3.33 Core Heat Flux for Fast Rod Withdrawal from 100% Power

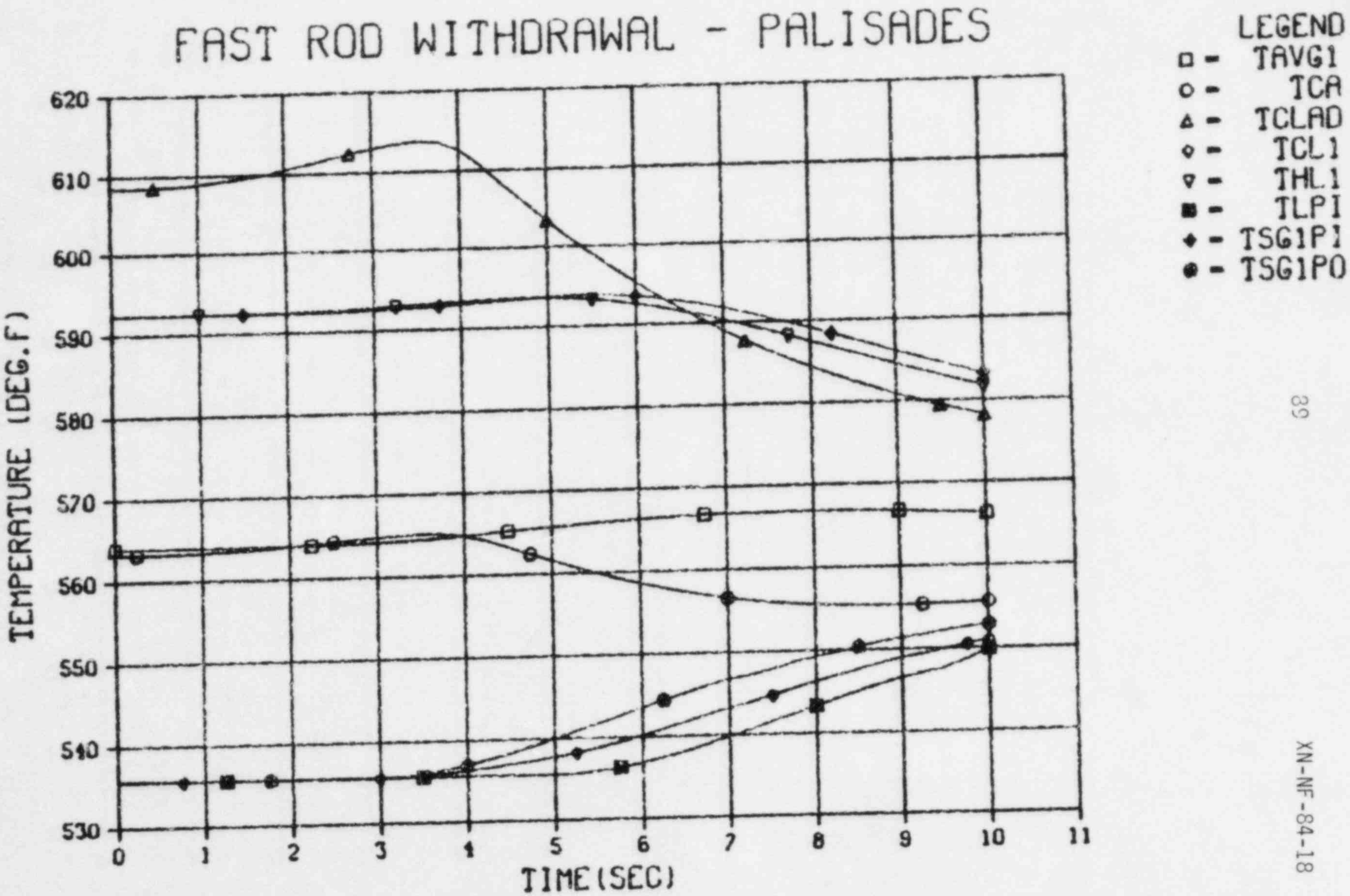

Figure 3.34 Primary Loop Temperatures for Fast Rod Withdrawal at 100% Power

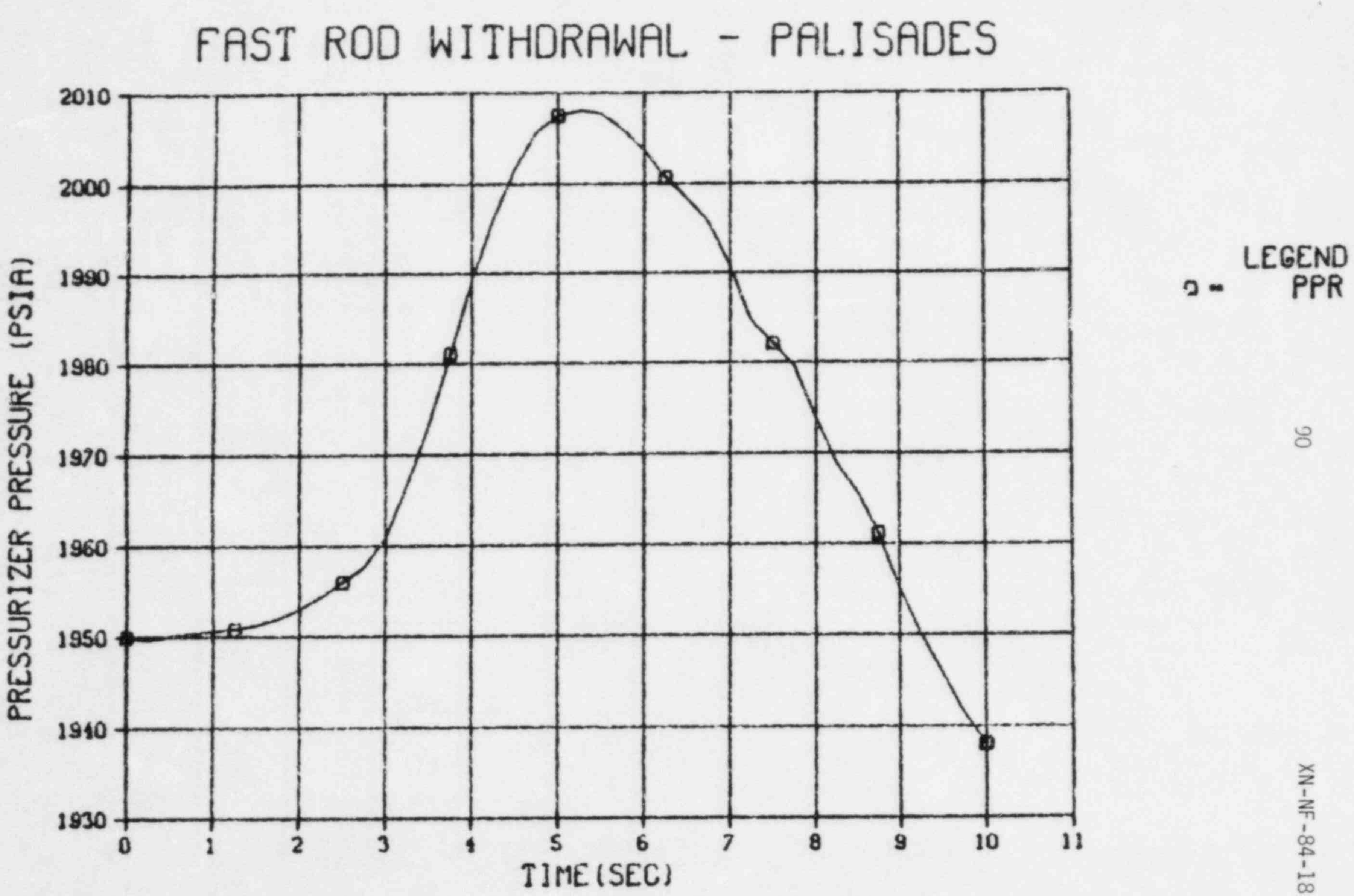

Figure 3.35 Pressurizer Pressure for Fast Rod Withdrawal from 100% Power

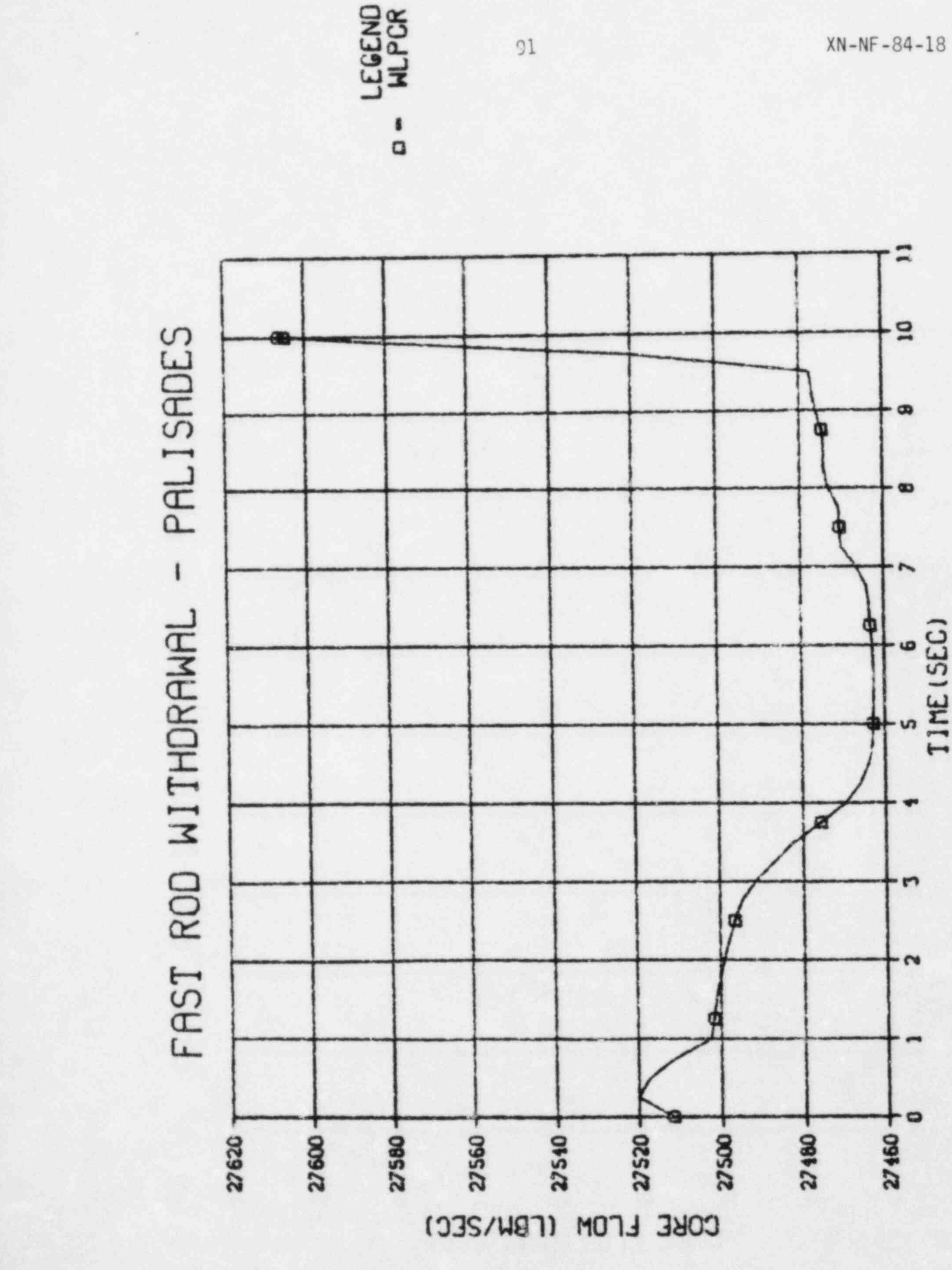

Figure 3.36 Core Flow for Fast Rod Withdrawal from 100% Power

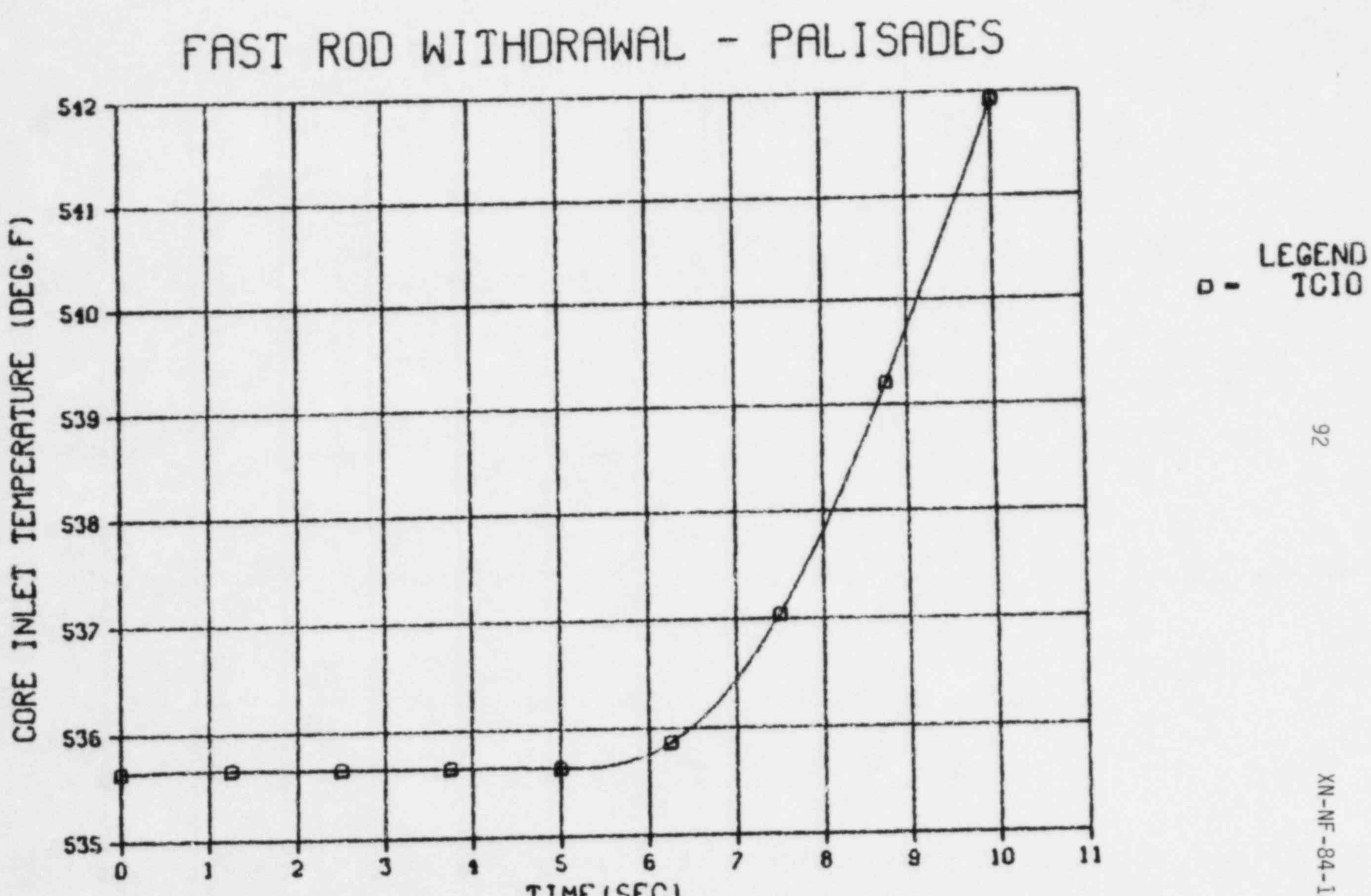

Figure 3.37 Core Inlet Temperature for Fast Rod Withdrawal from 100% Power

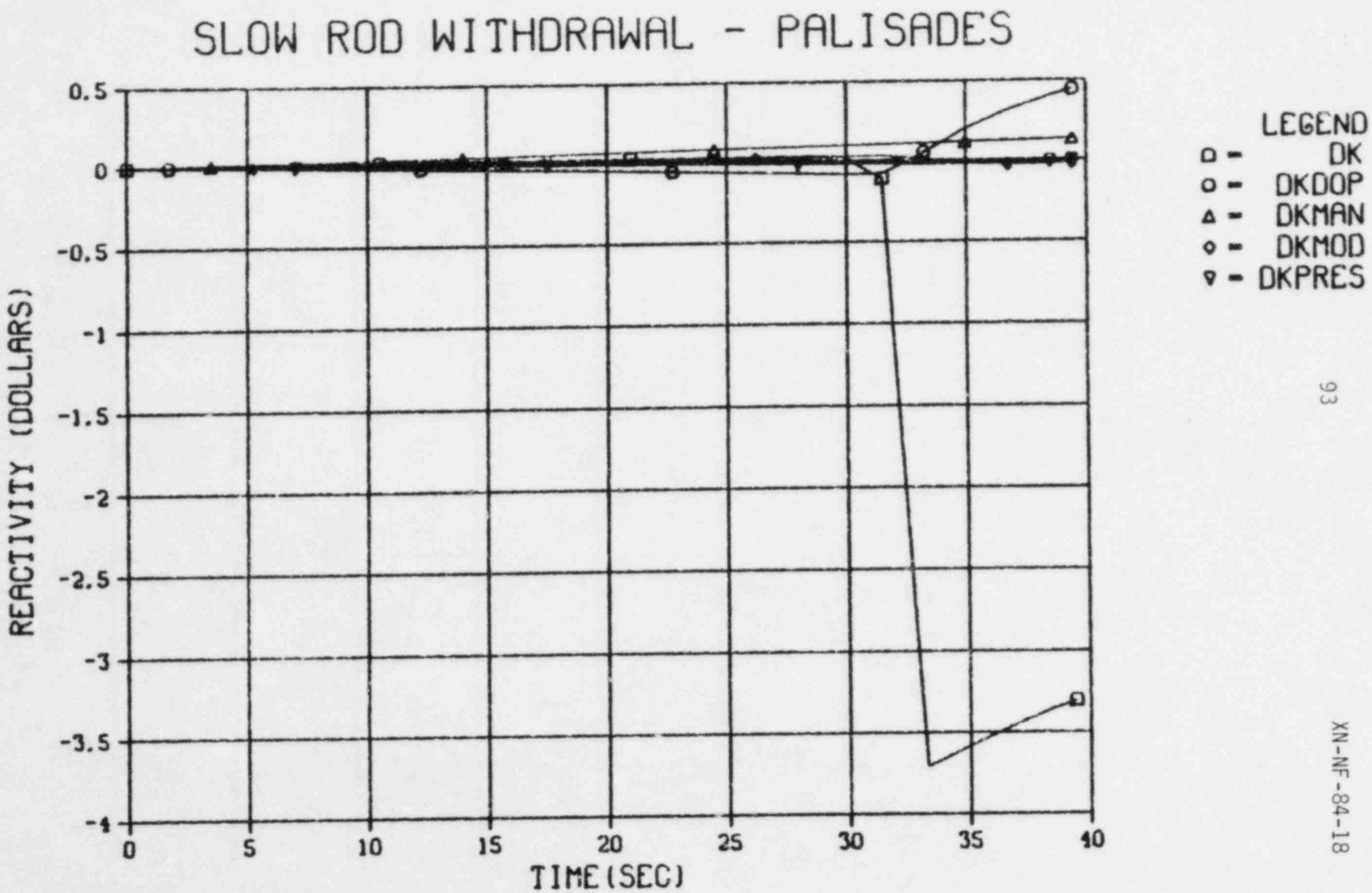

Figure 3.38 Reactivities for Slow Rod Withdrawal at 100% Power

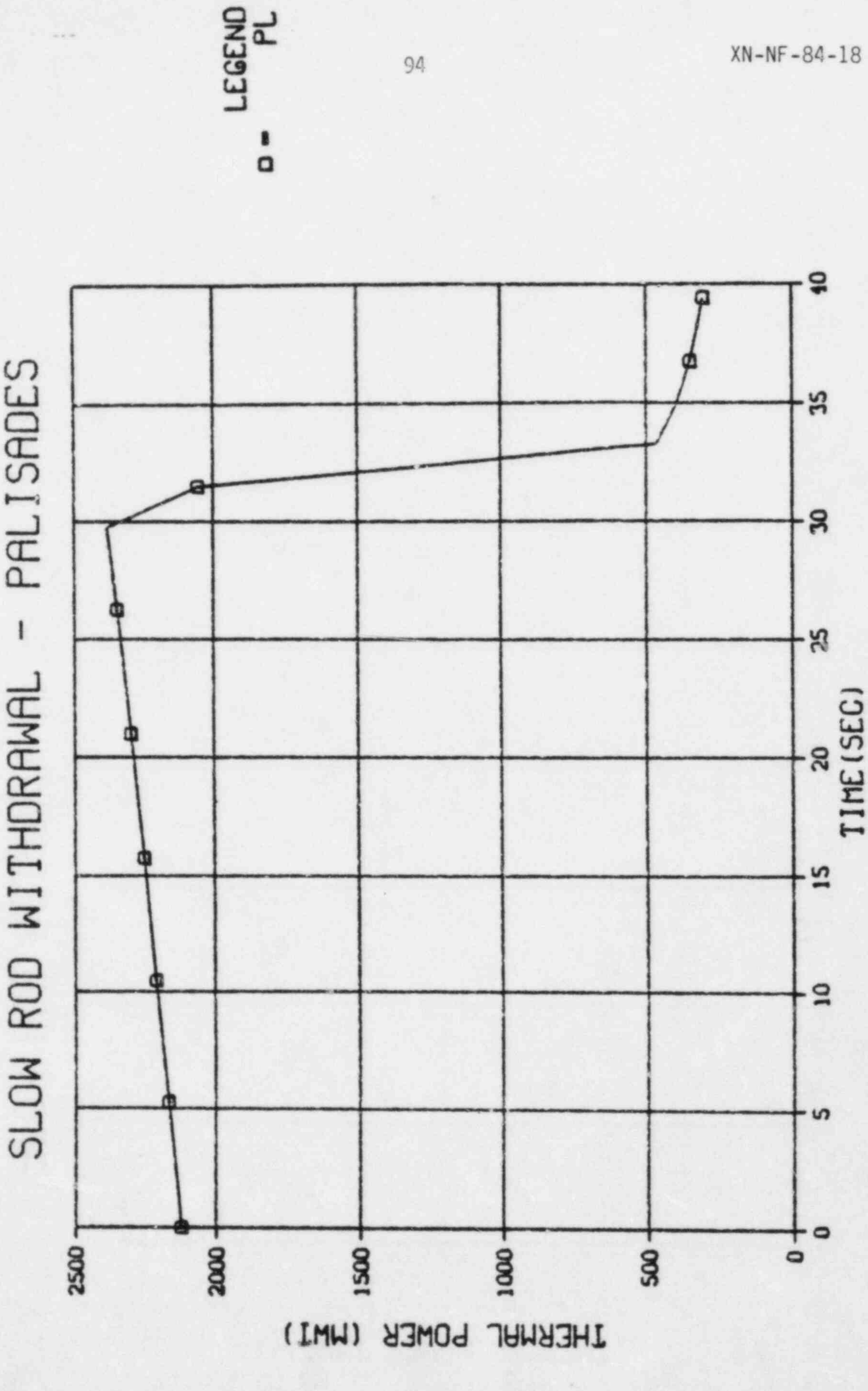

Figure 3.39 Reactor Power for Slow Rod Withdrawal at 100% Power

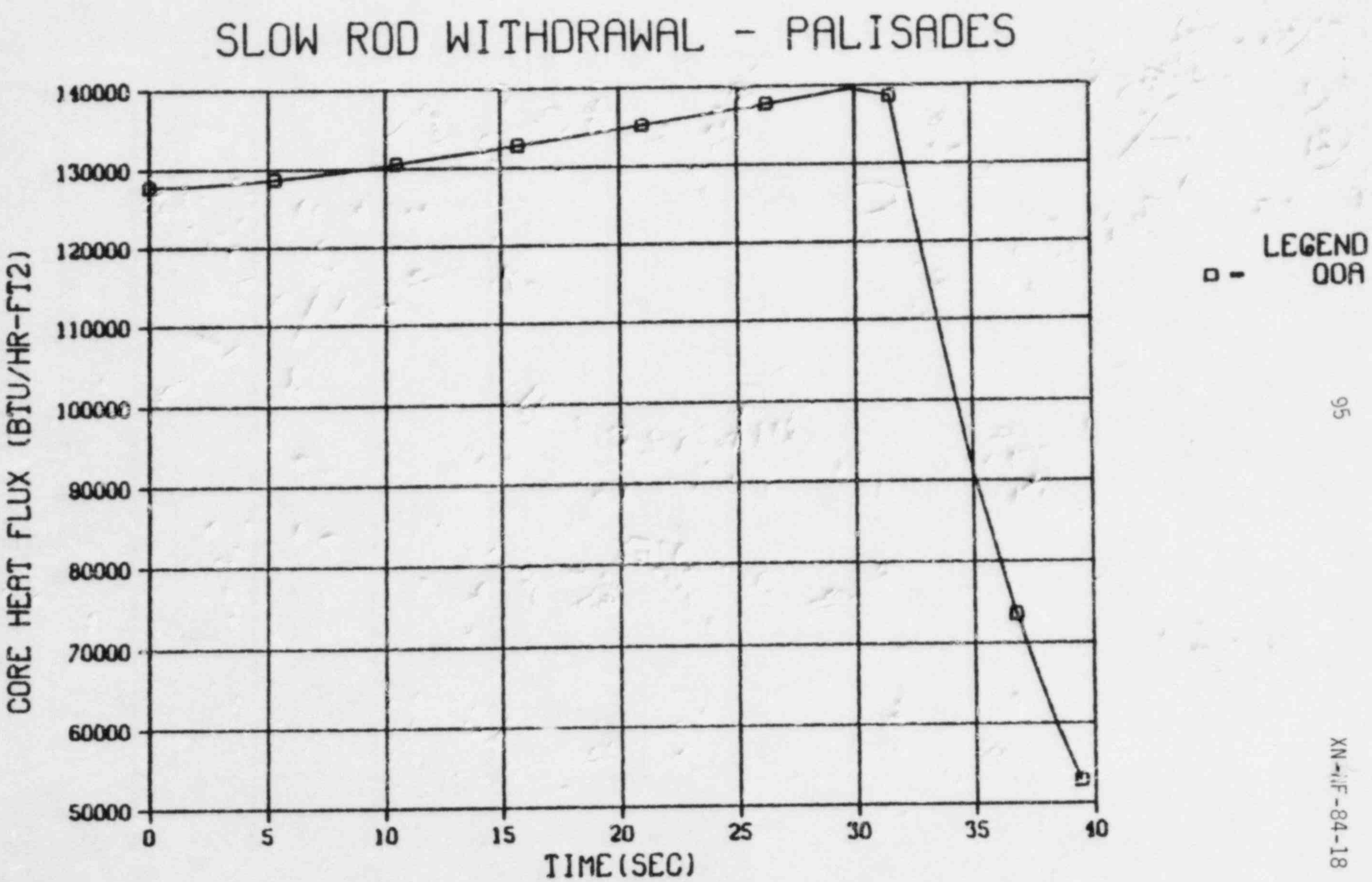

Figure 3.40 Core Heat Flux for Slow Rod Withdrawal at 100% Power

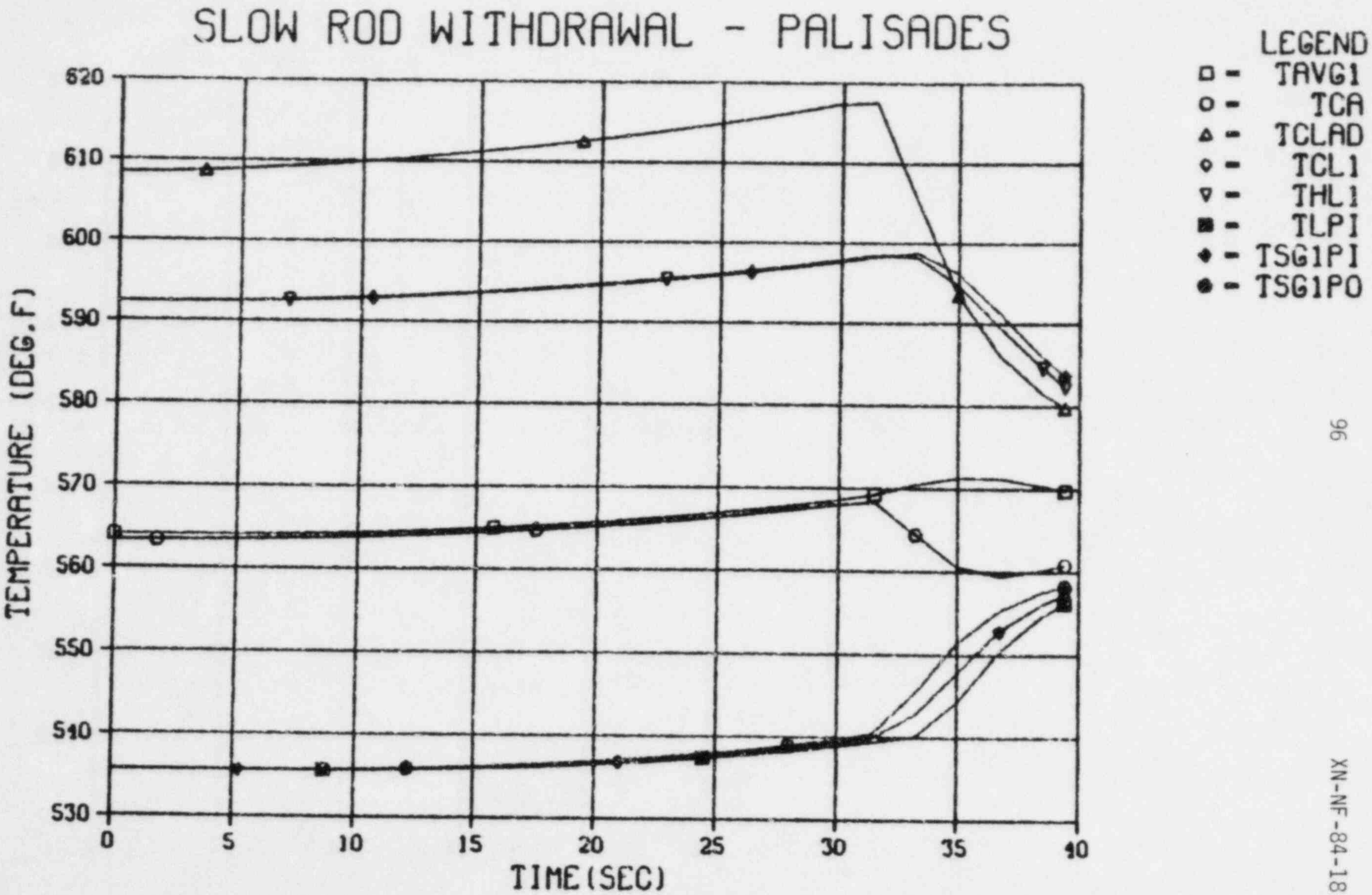

Figure 3.41 Primary Loop Temperatures for Slow Rod Withdrawal at 100% Power

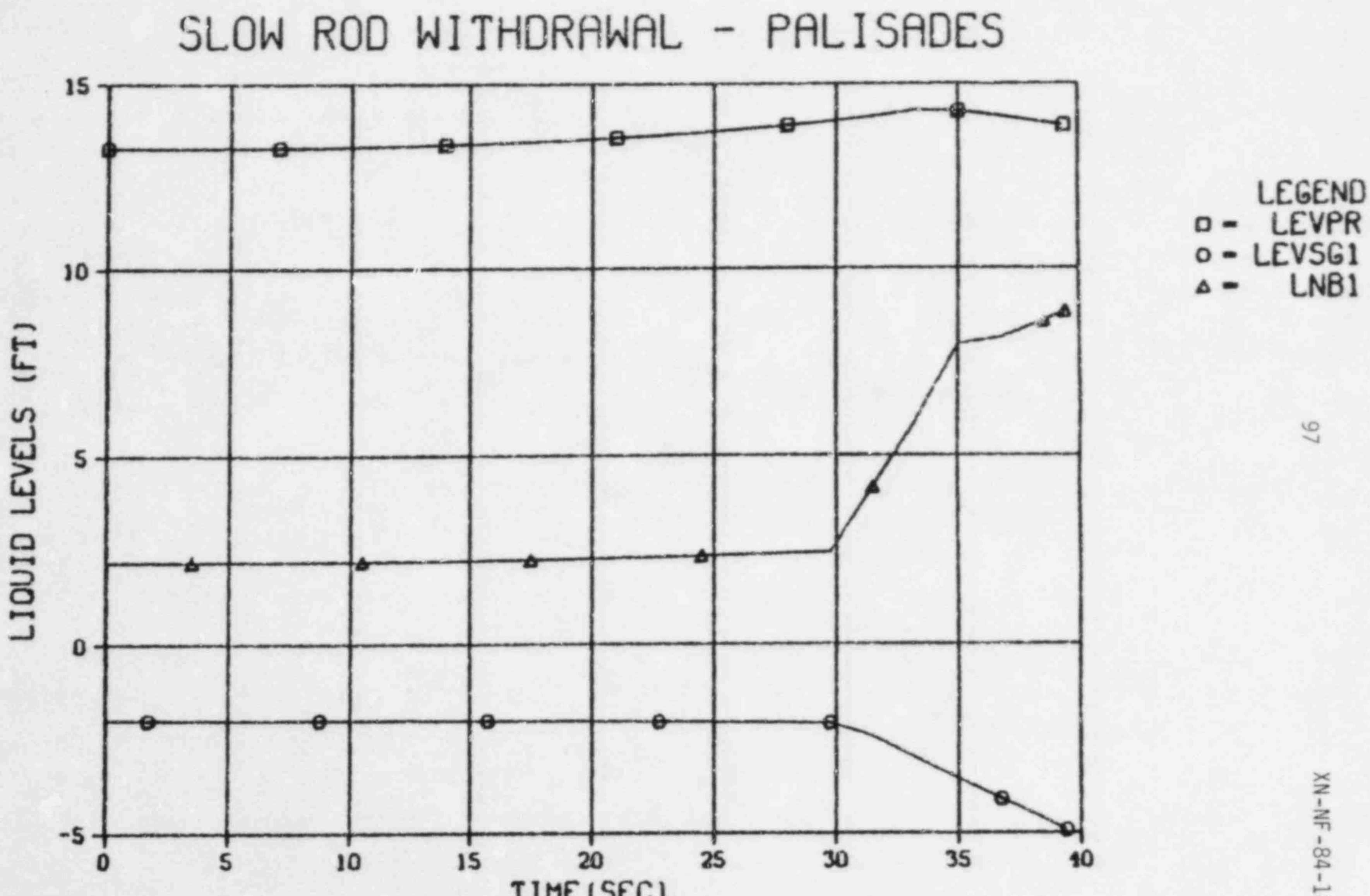

Figure 3.42 Liquid Levels for Slow Rod Withdrawal at 100% Power

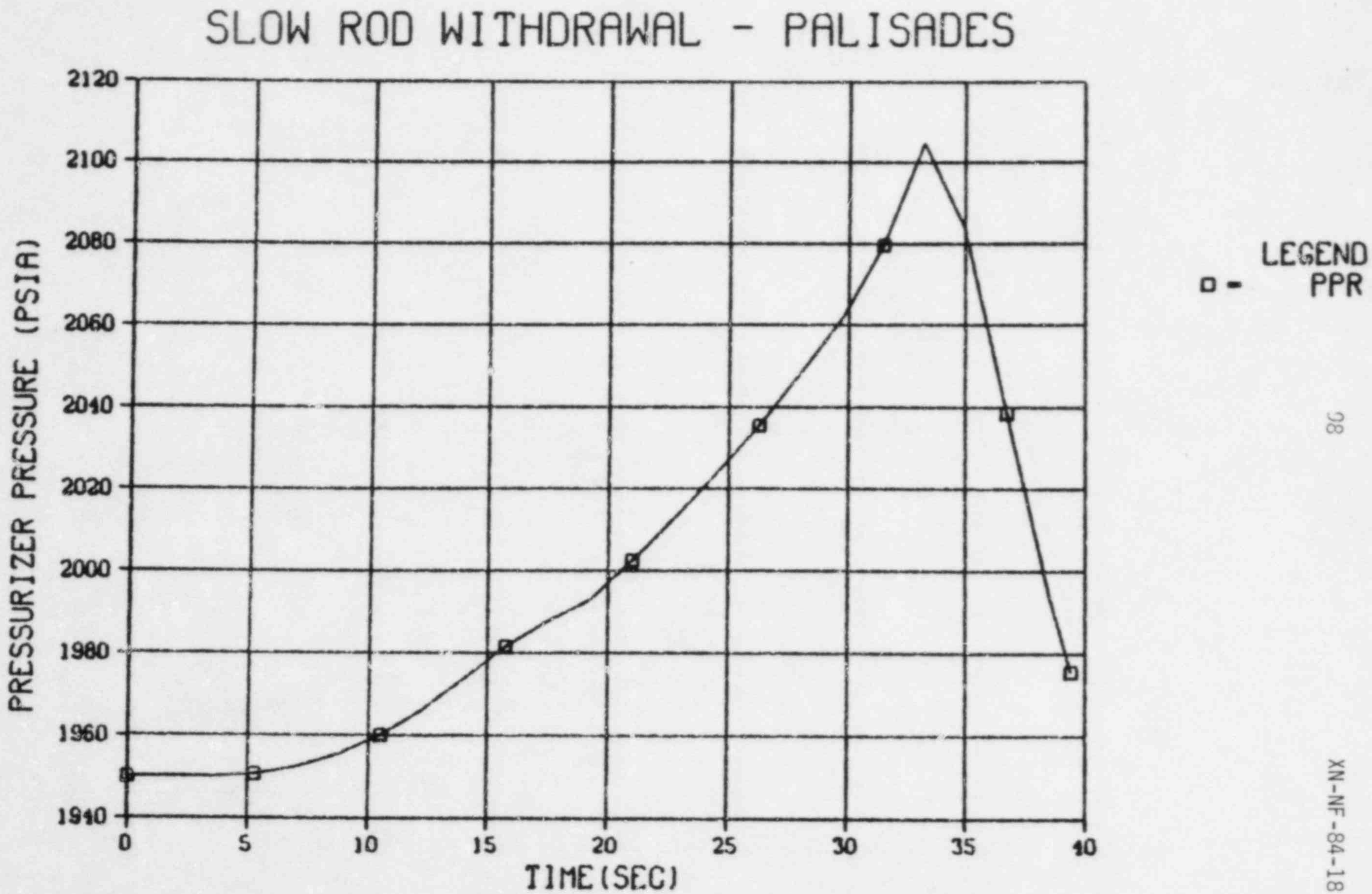

Figure 3.43 Pressurizer Pressure for Slow Rod Withdrawal at 100% Power

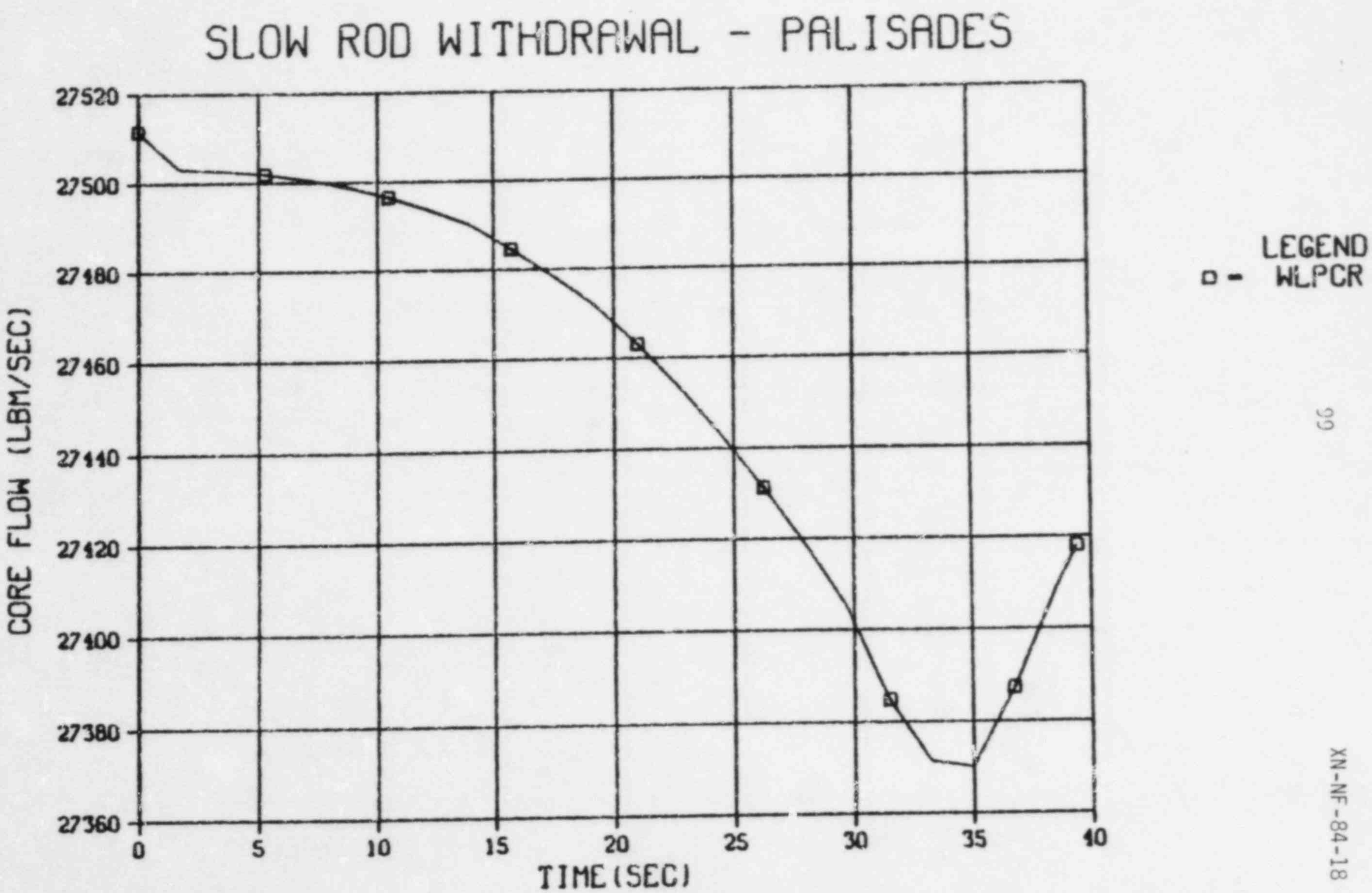

Figure 3.44 Core Flow for Slow Rod Withdrawal at 100% Power

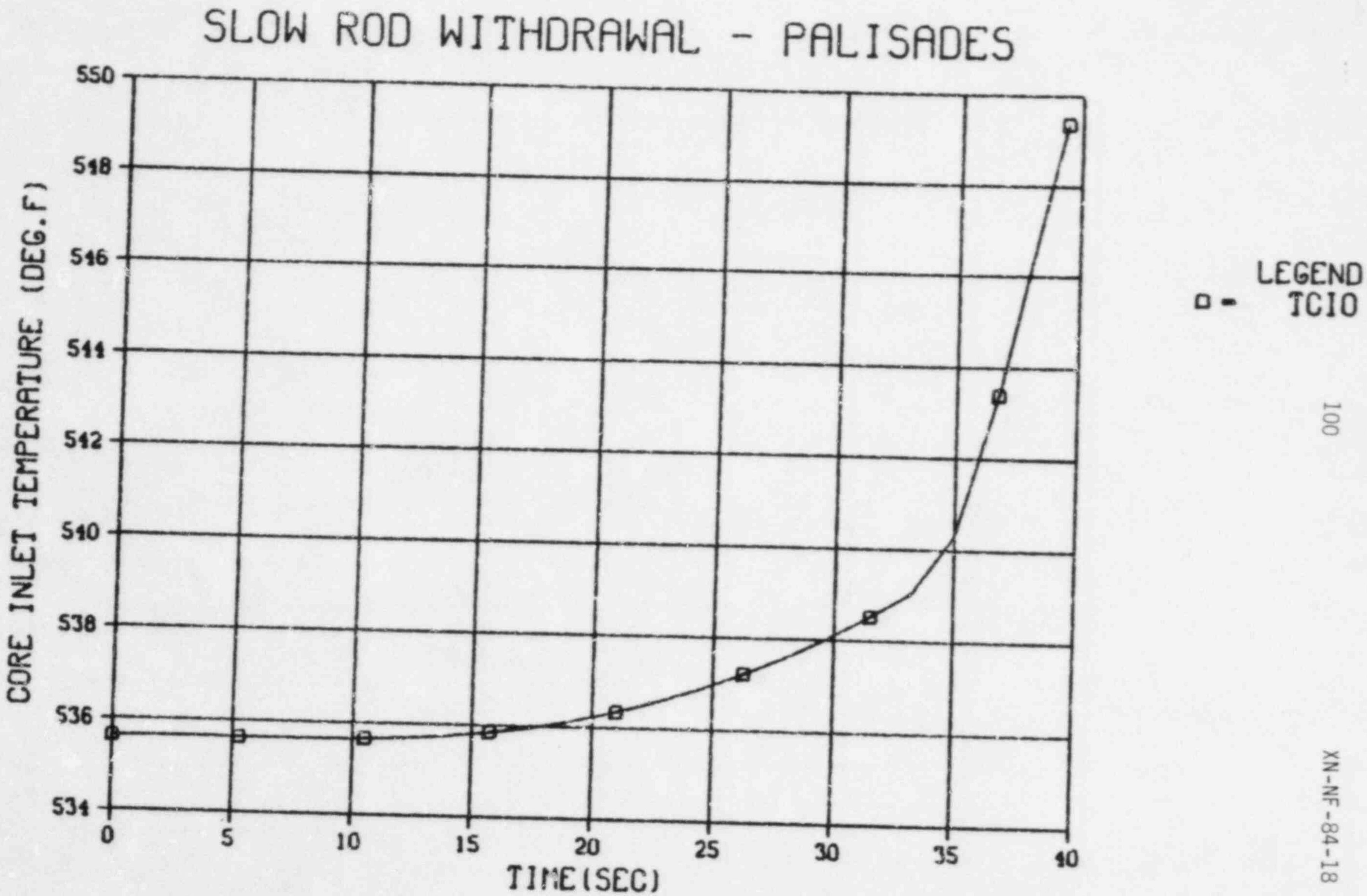

Figure 3.45 Core Inlet Temperature for Slow Rod Withdrawal at 100% Power

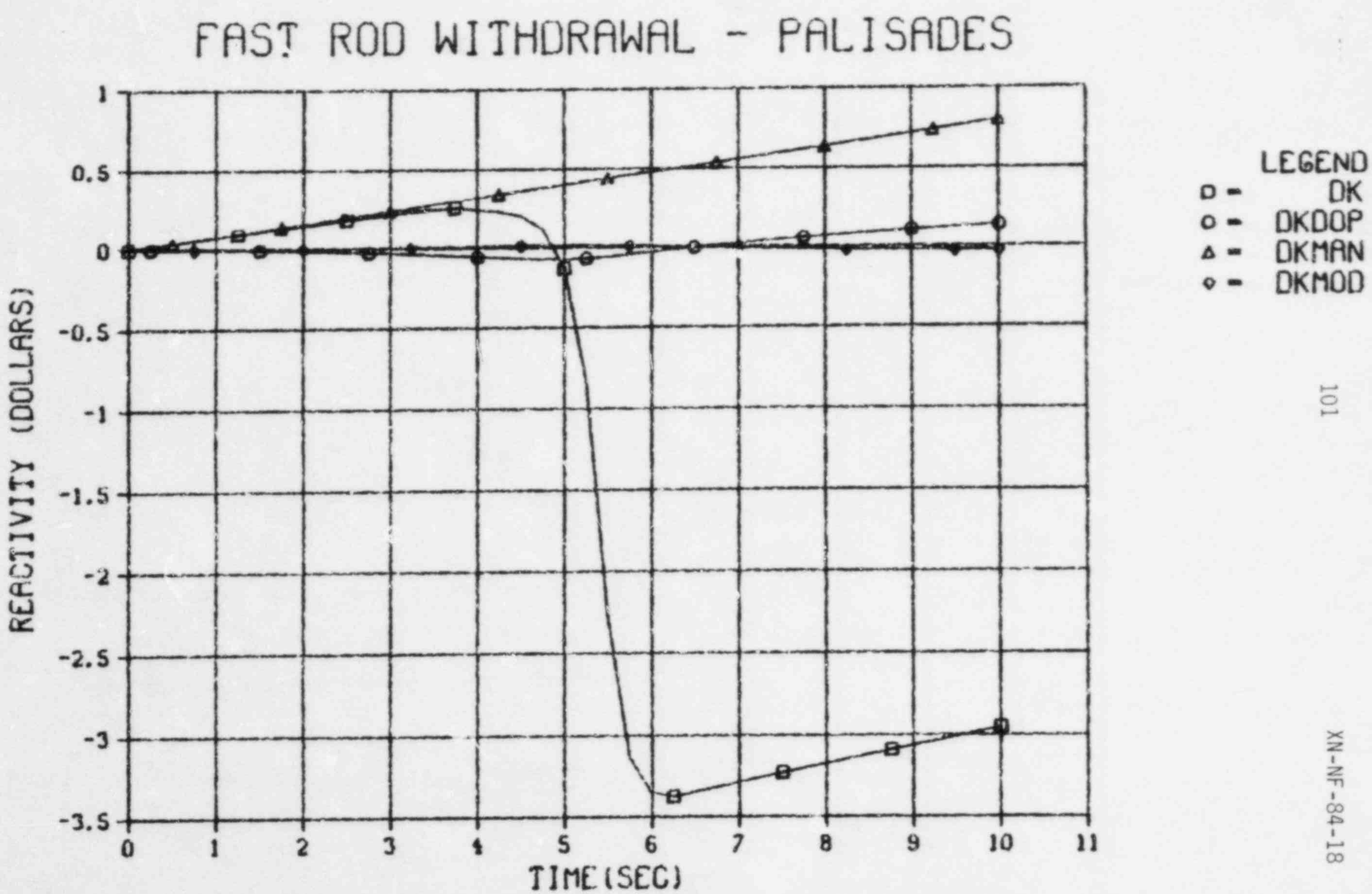

Figure 3.46 Reactivities for Fast Rod Withdrawal from 50% Power

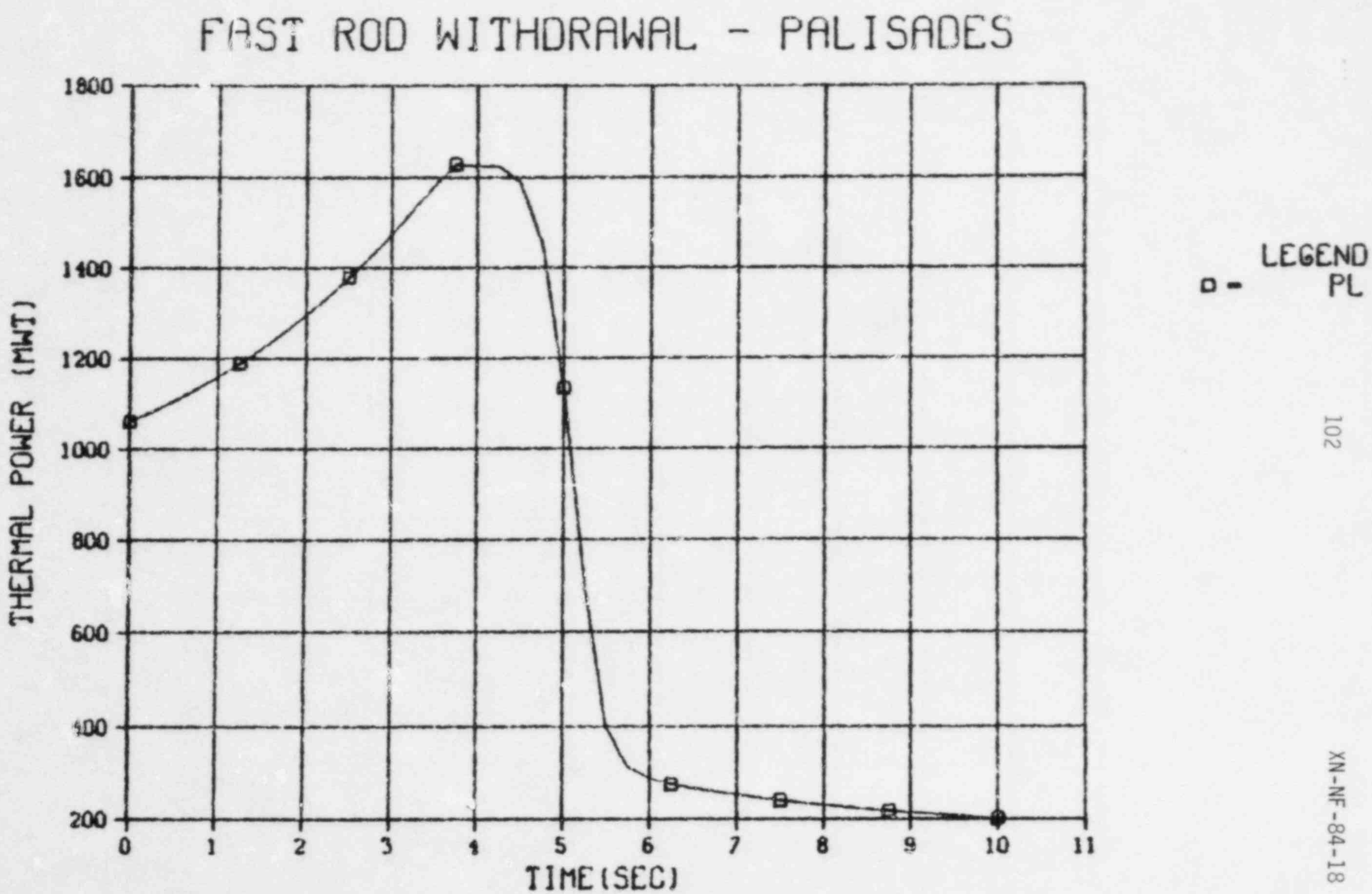

Figure 3.47 Reactor Thermal Power for Fast Rod Withdrawal from 50% Power

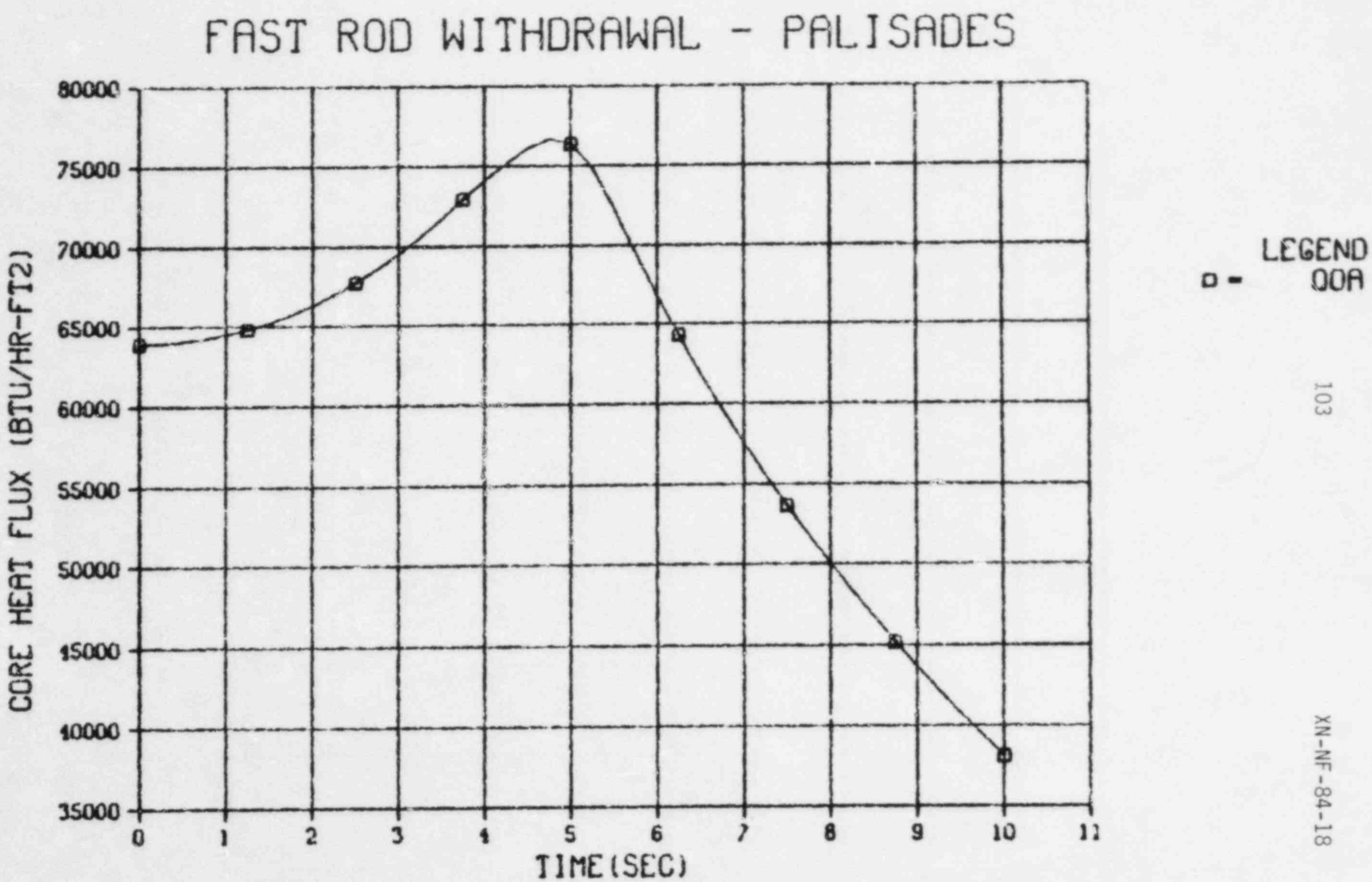

Figure 3.48 Core Heat Flux for Fast Rod Withdrawal from 50% Power

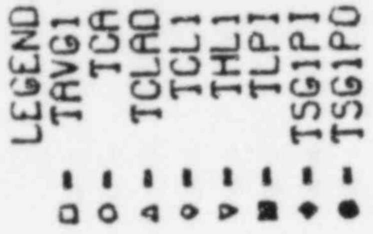

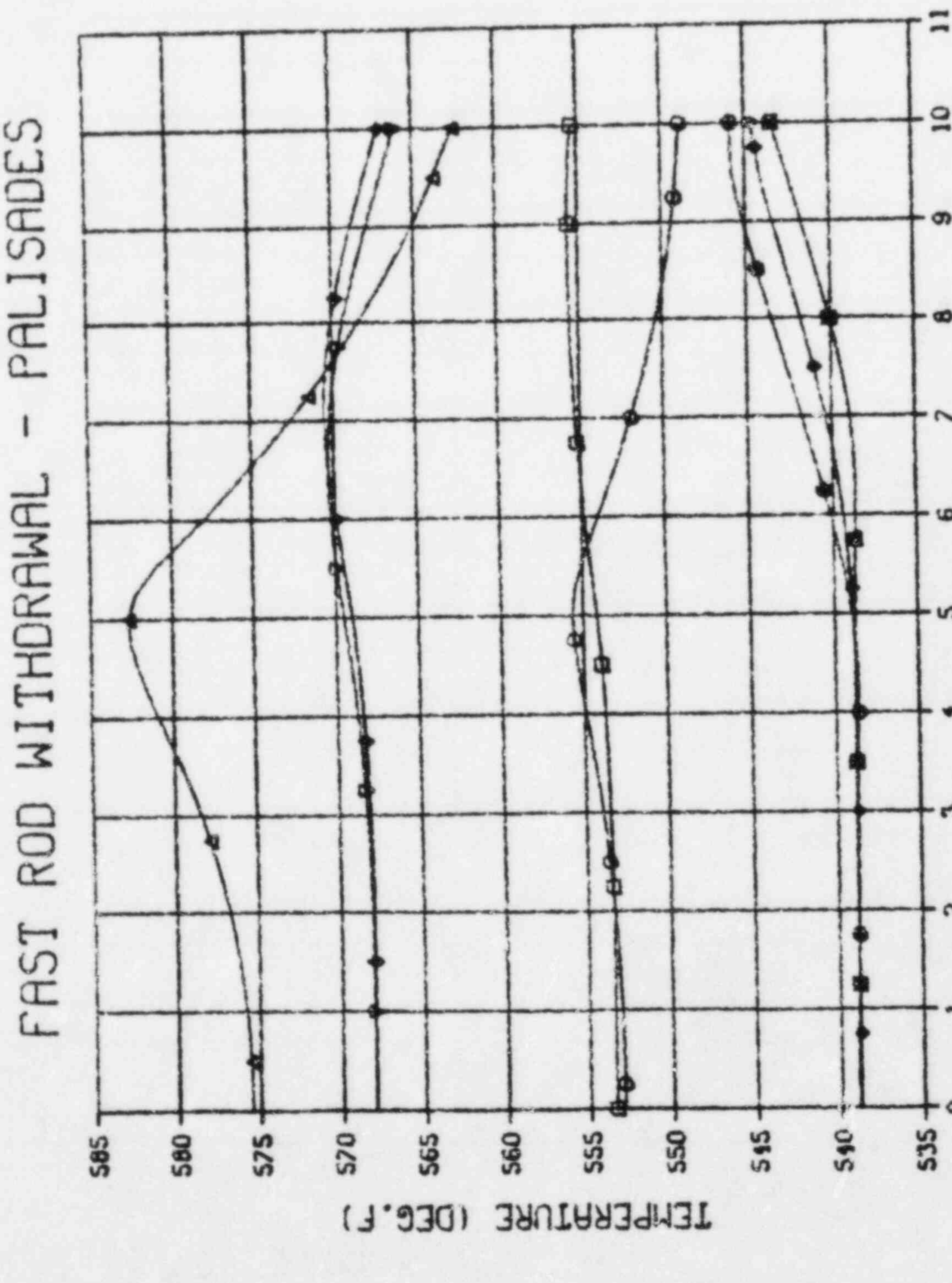

Figure 3.49 Primary Loop Temperatures for Fast Rod Withdrawal from 50% Power

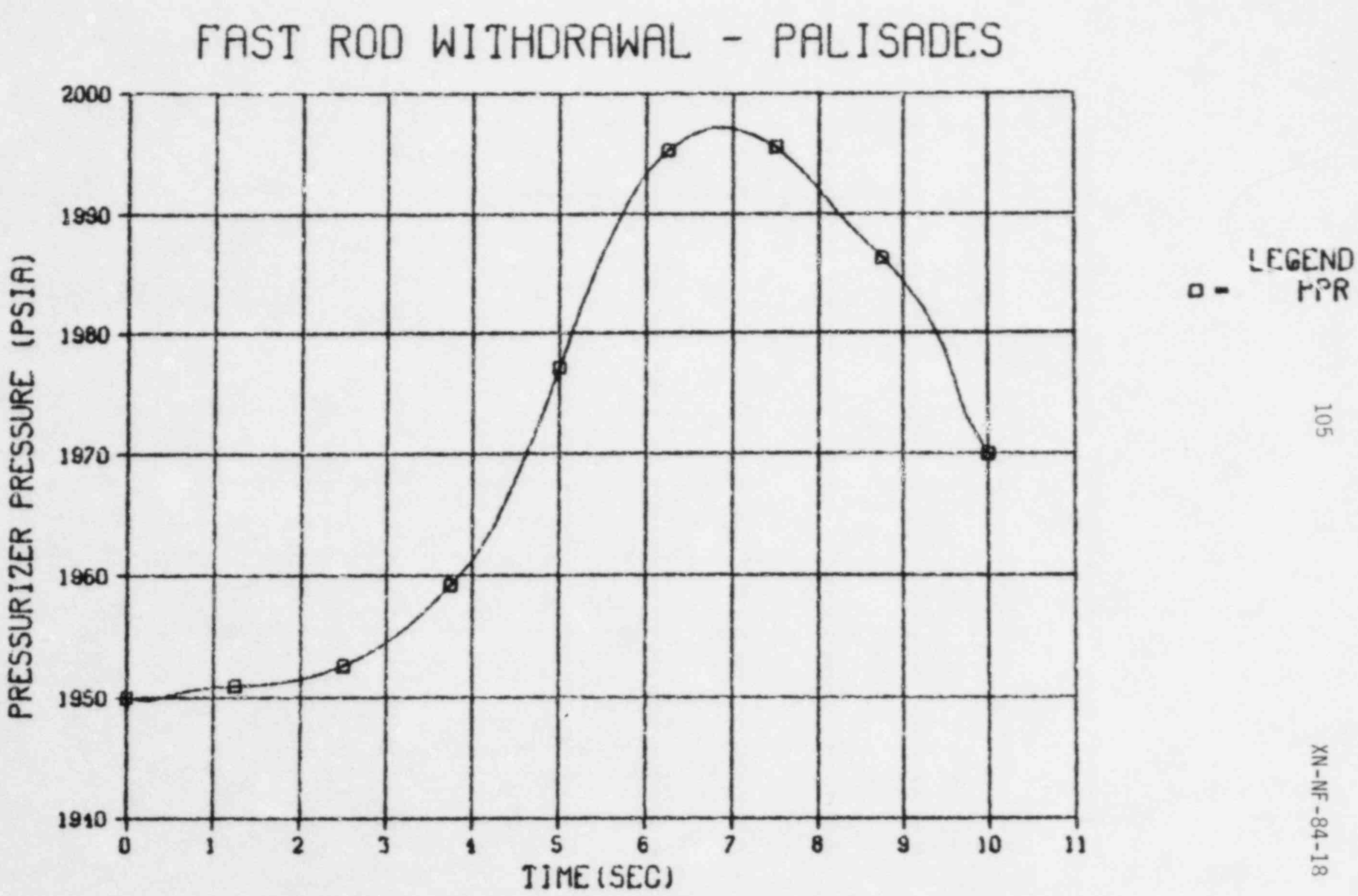

Figure 3.50 Pressurizer Pressure for Fast Rod Withdrawal from 50% Power

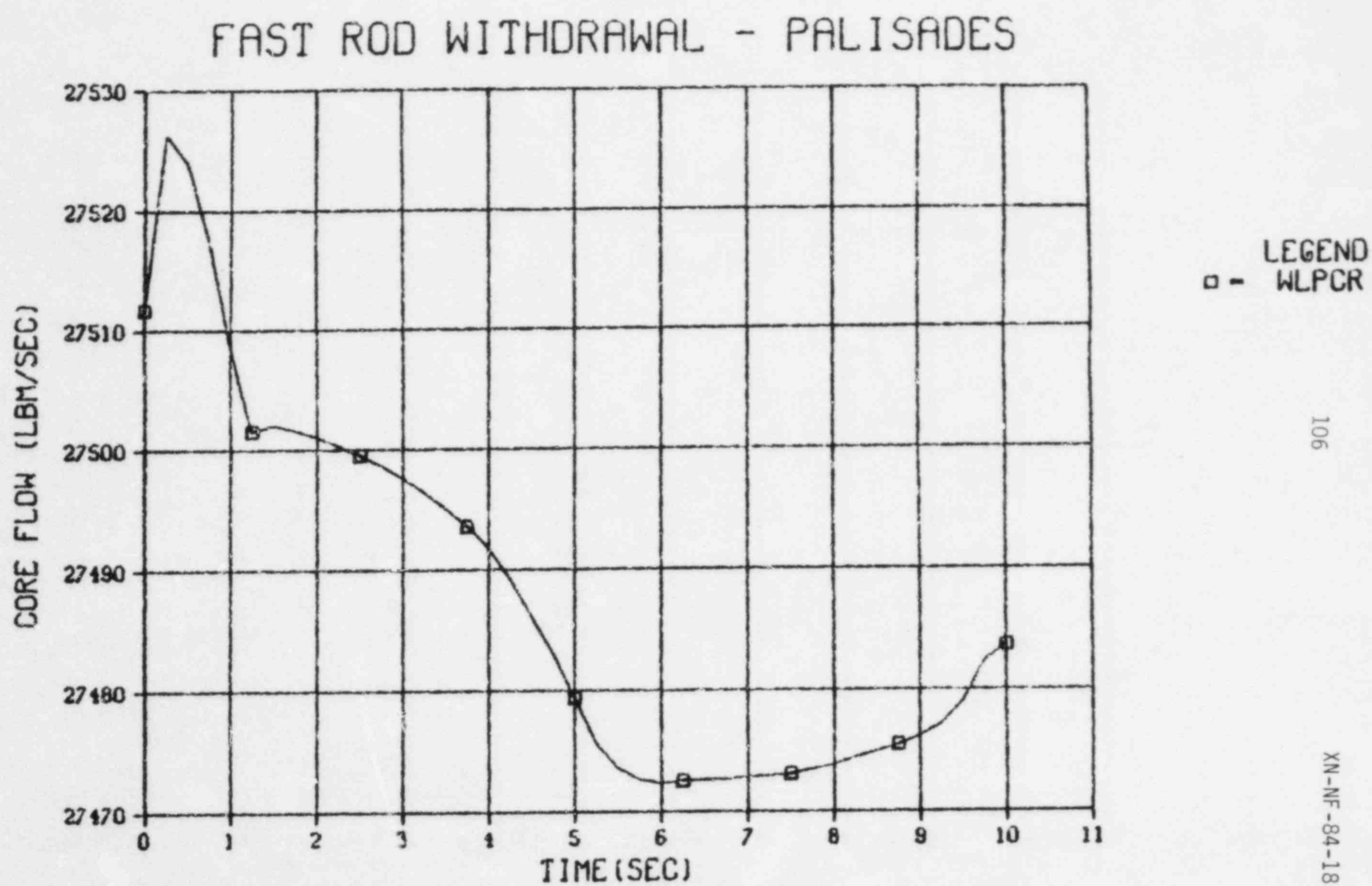

Figure 3.51 Core Flow for Fast Rod Withdrawal from 50% Power

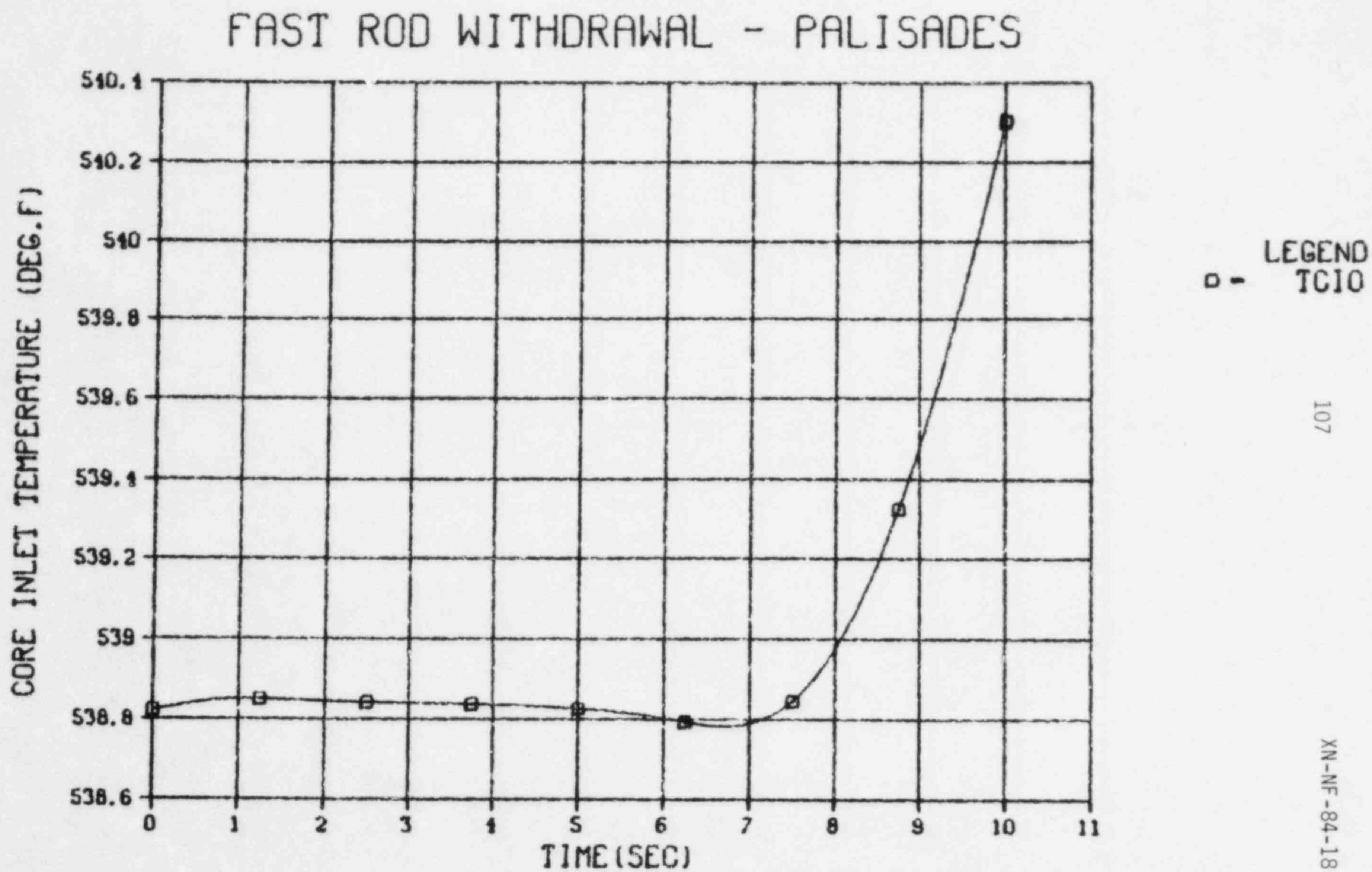

Figure 3.52 Core Inlet Temperature for Fast Rod Withdrawal from 50% Power

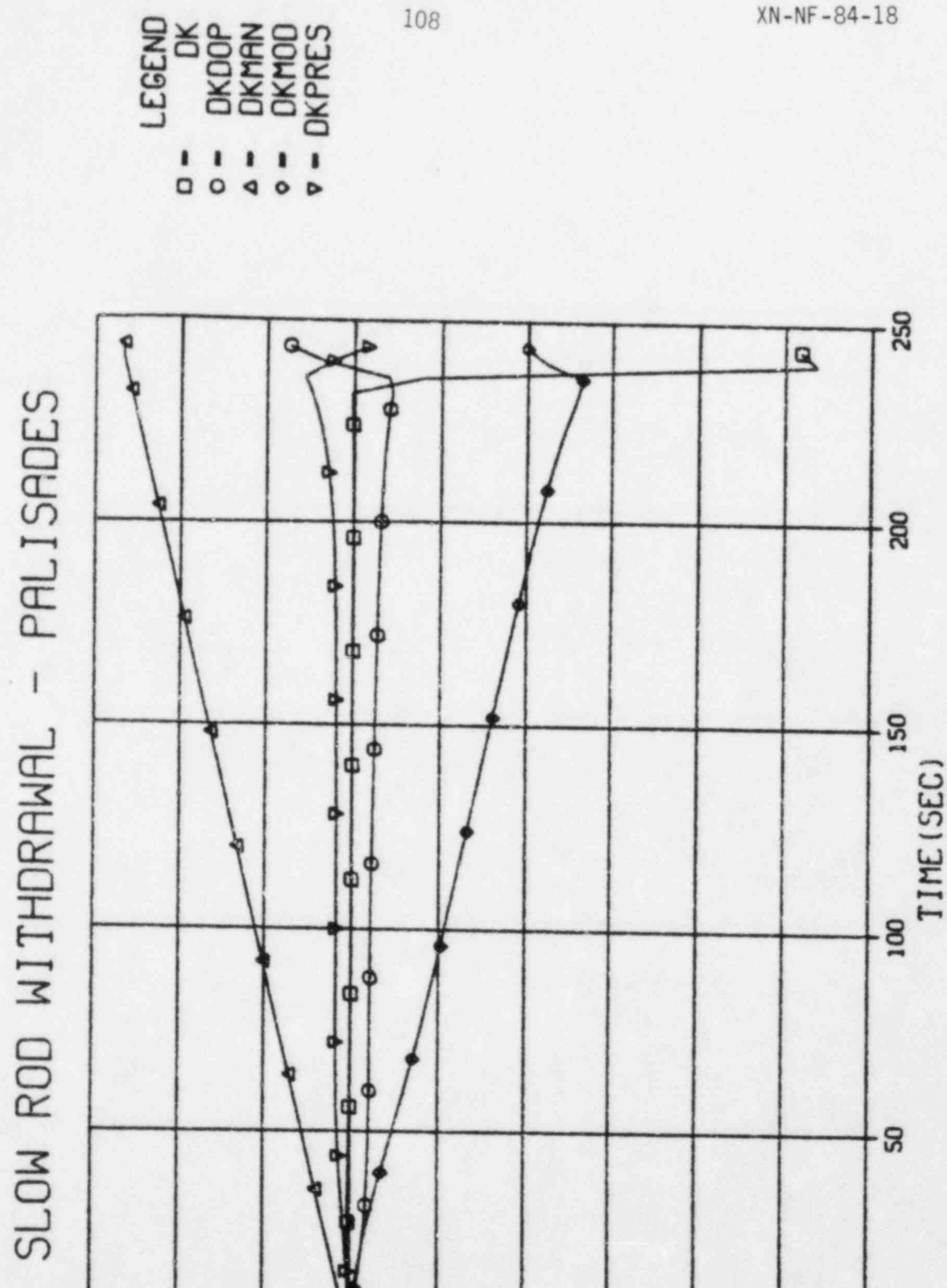

Figure 3.53 Reactivities for Slow Rod Withdrawal from 50% Power

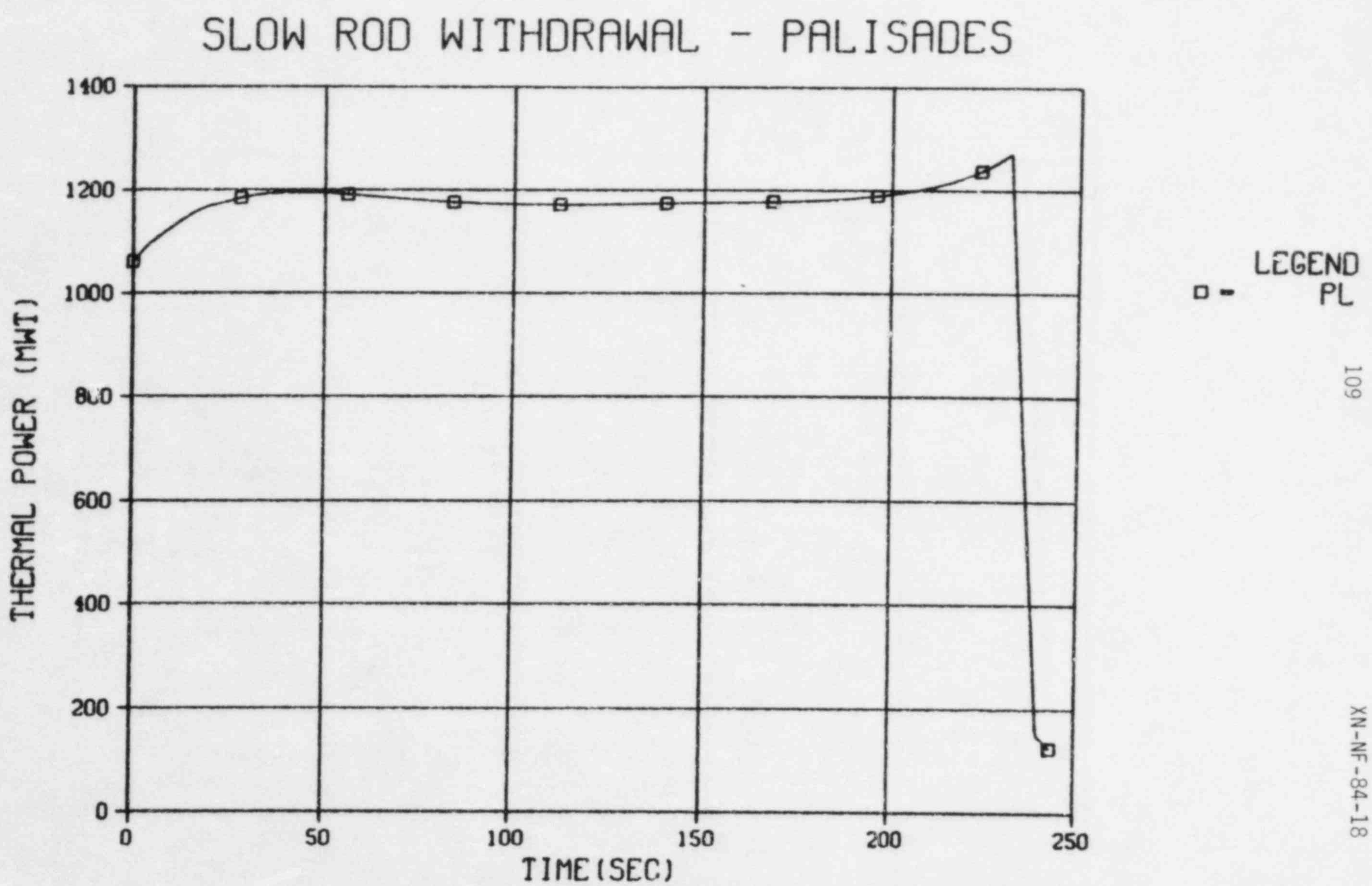

Figure 3.54 Reactor Power for Slow Rod Withdrawal from 50% Power

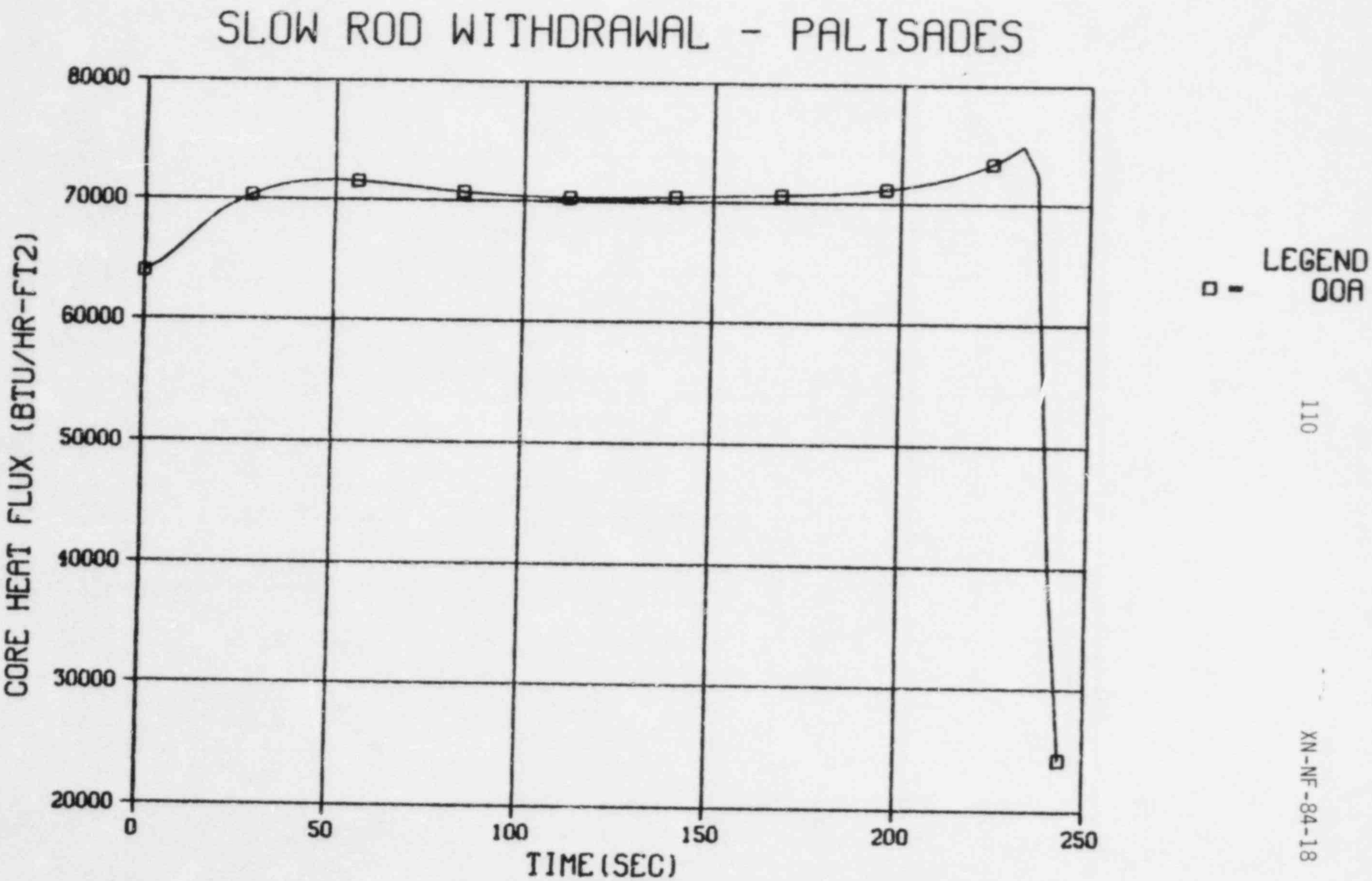

Figure 3.55 Reactor Heat Flux for Slow Rod Withdrawal from 50% Power

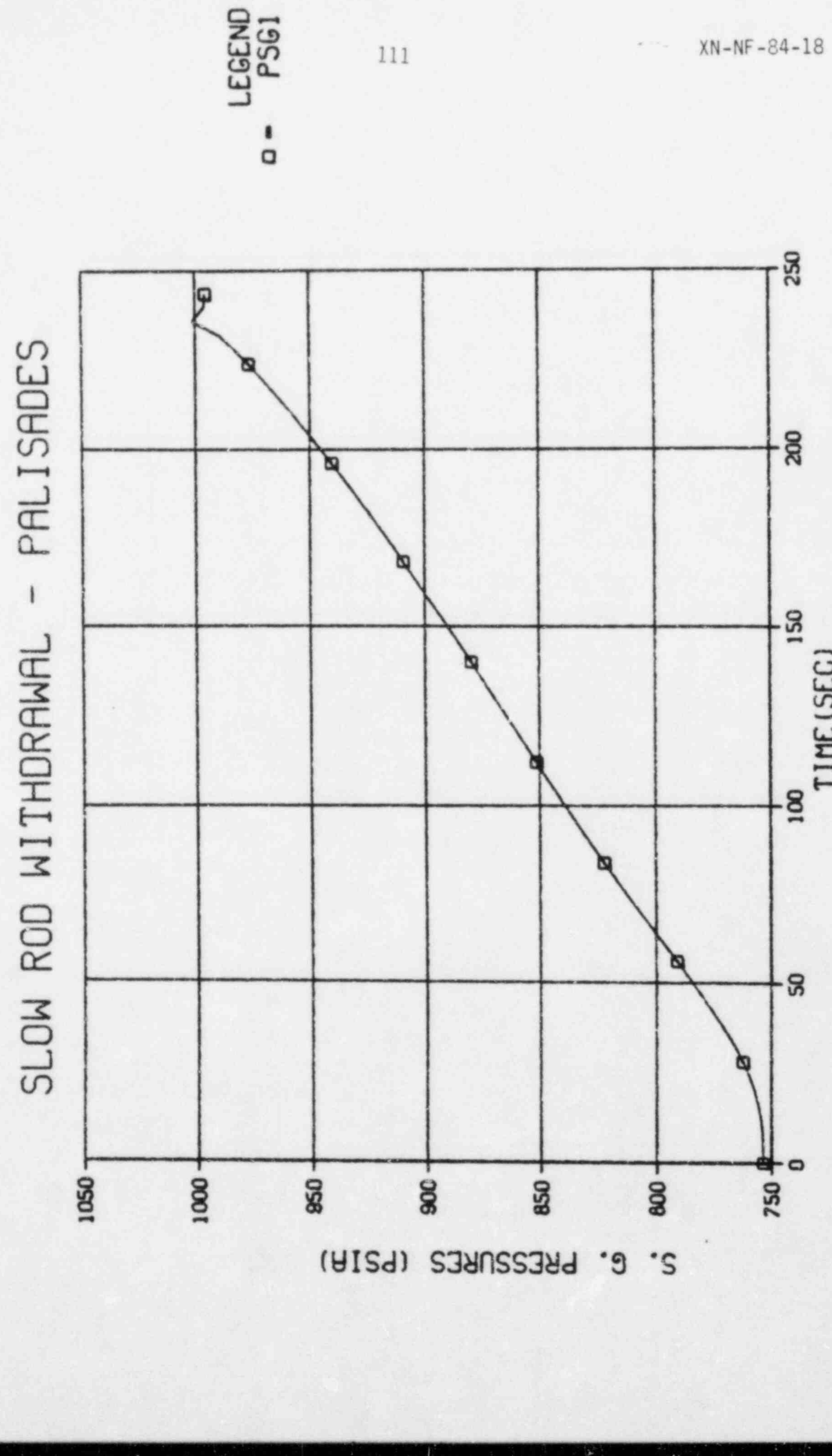

Figure 3.56 Steam Generator Pressure for Slow Rod Withdrawal from 50% Power

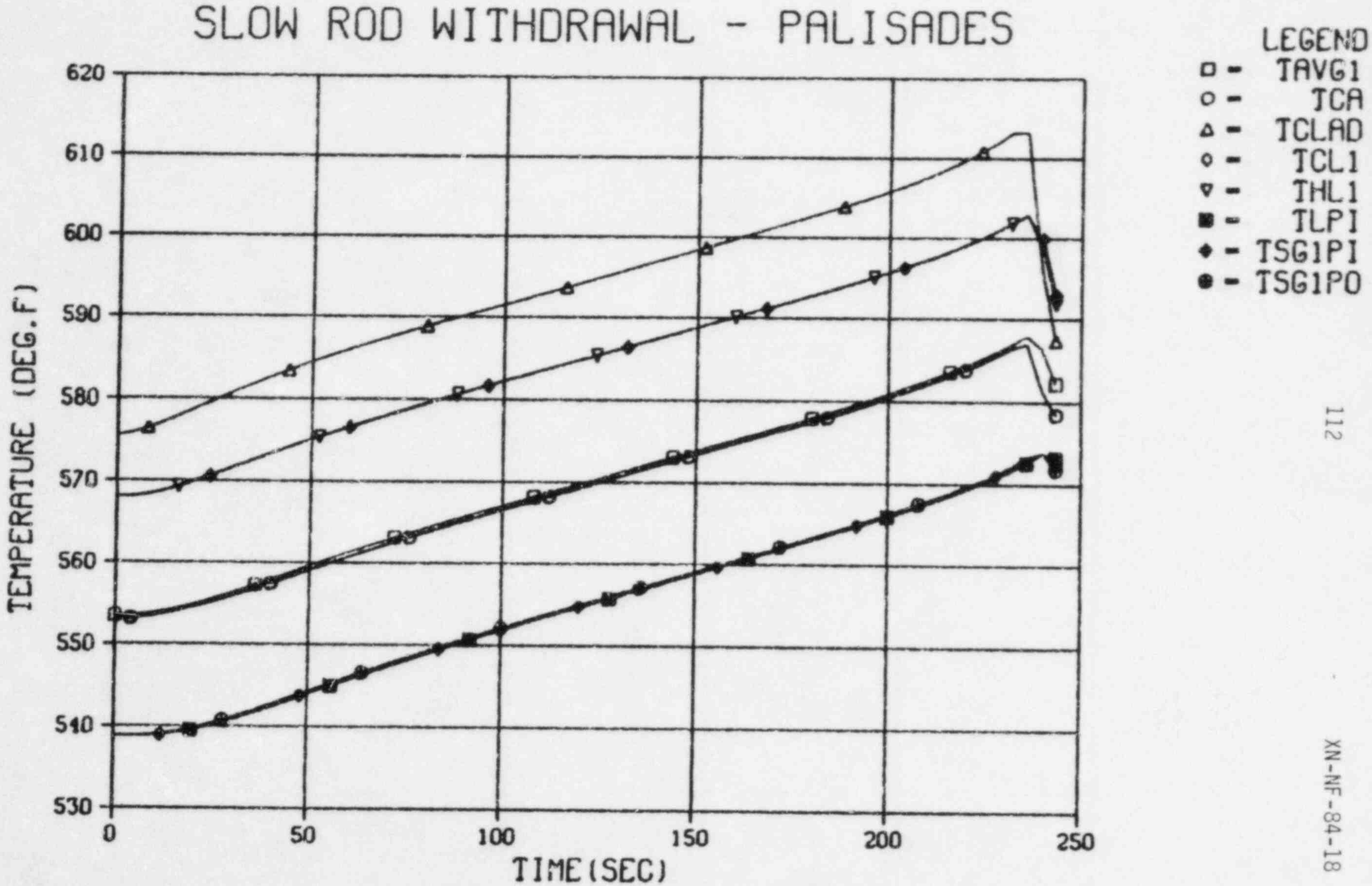

Figure 3.57 Primary Loop Temperatures for Slow Rod Withdrawal from 50% Power

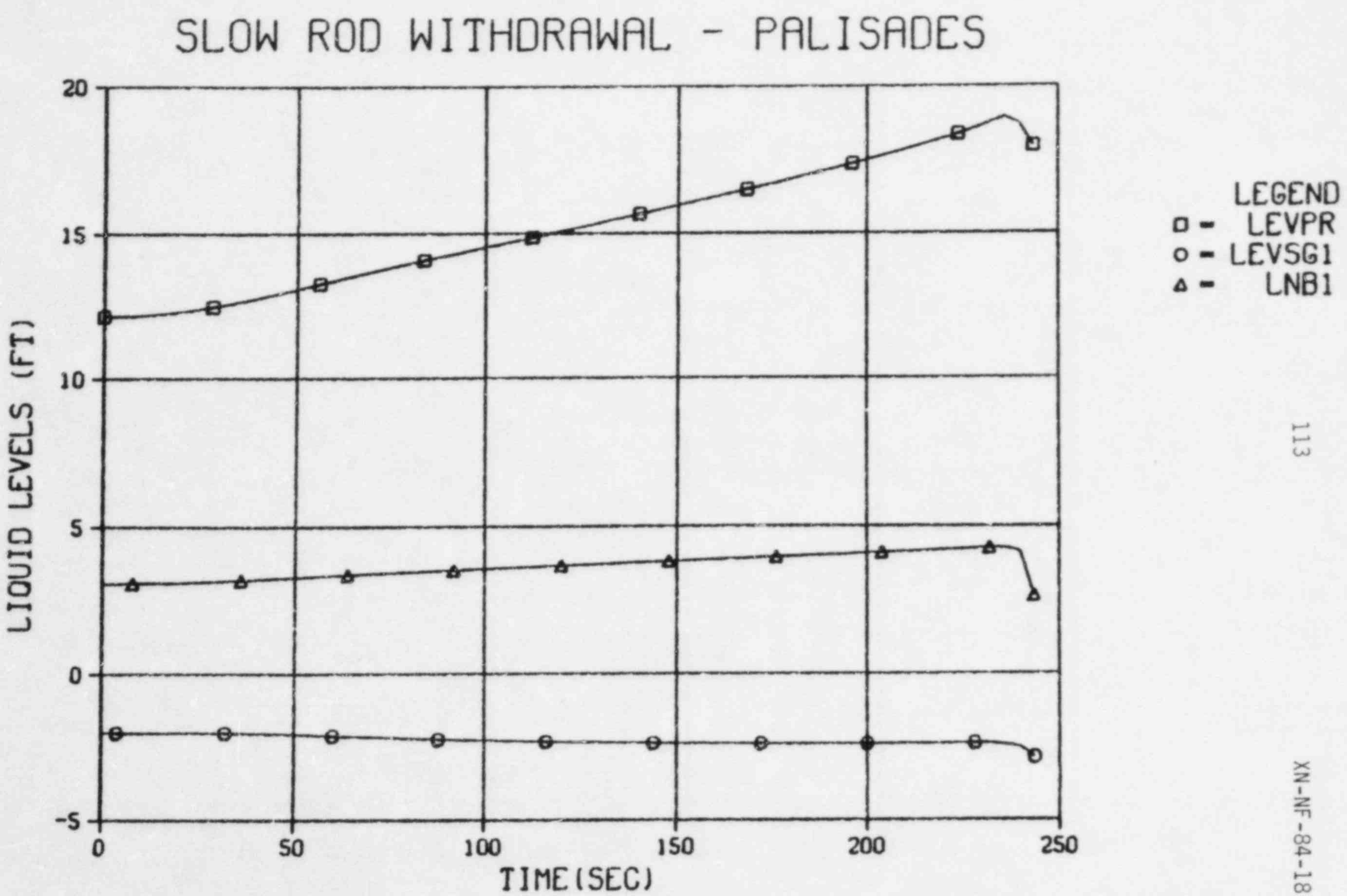

Figure 3.58 Liquid Levels for Slow Rod Withdrawal from 50% Power

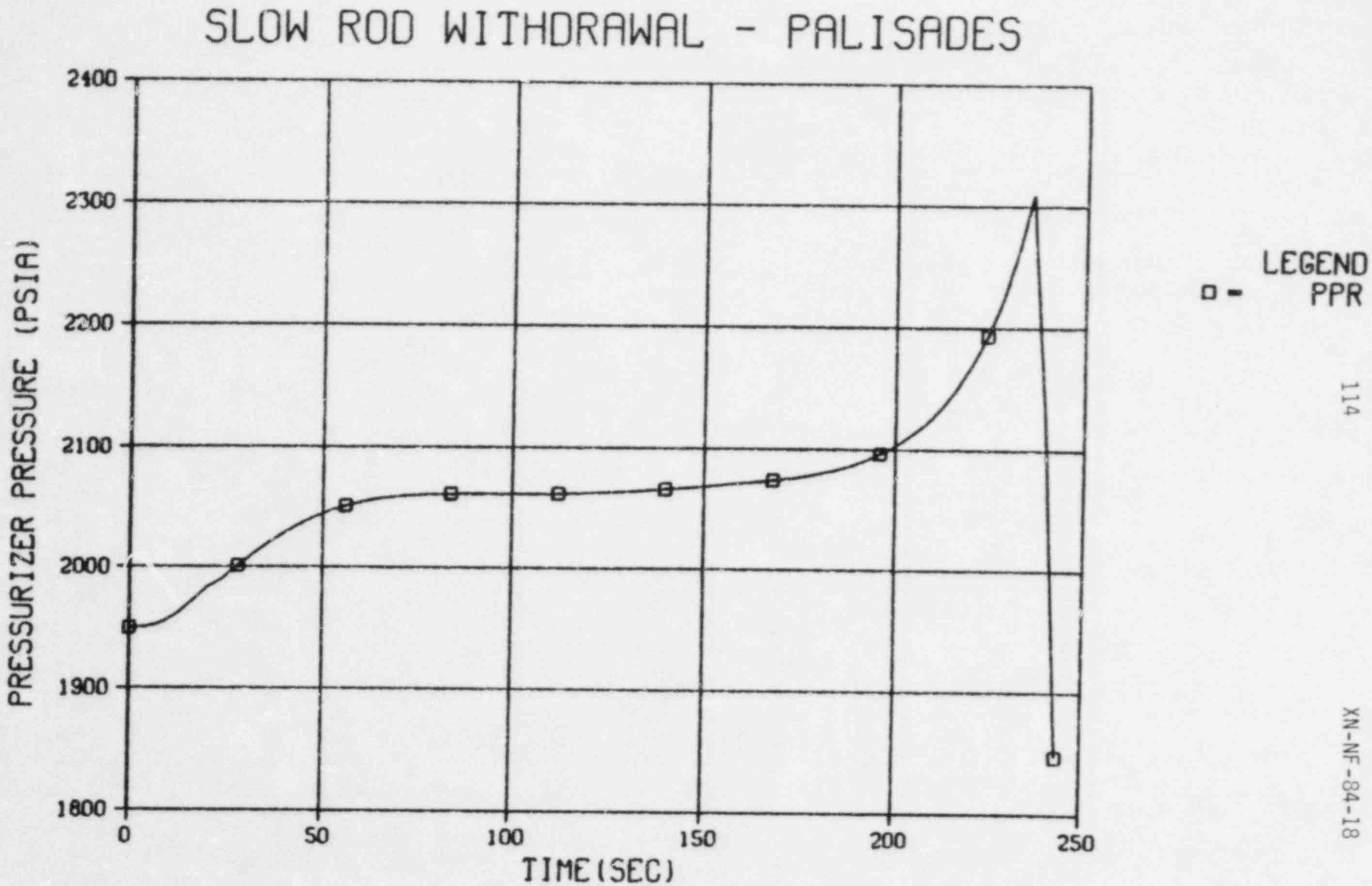

Figure 3.59 Pressurizer Pressure for Slow Rod Withdrawal from 50% Power

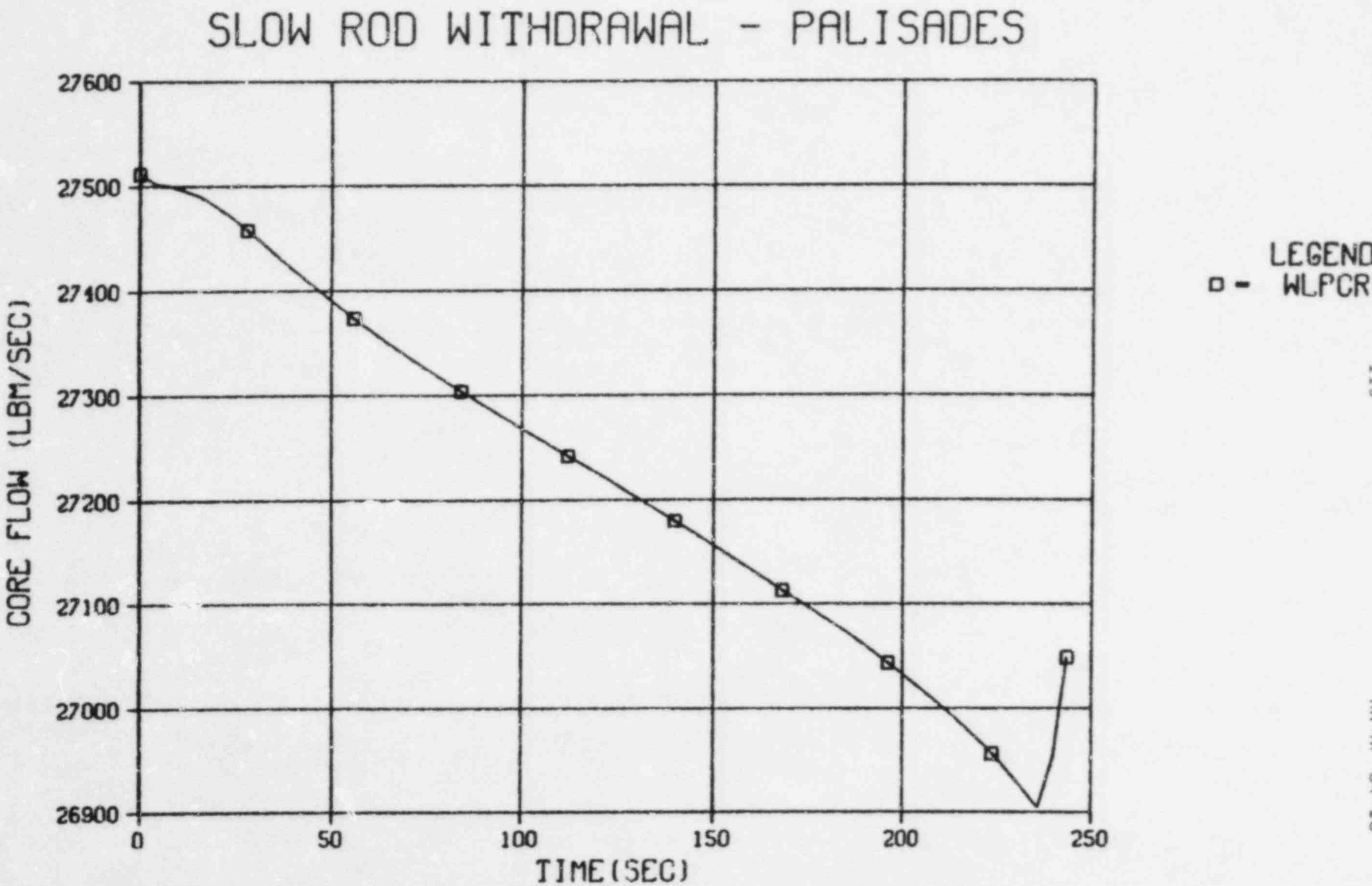

Figure 3.60 Core Flow for Slow Rod Withdrawal from 50% Power

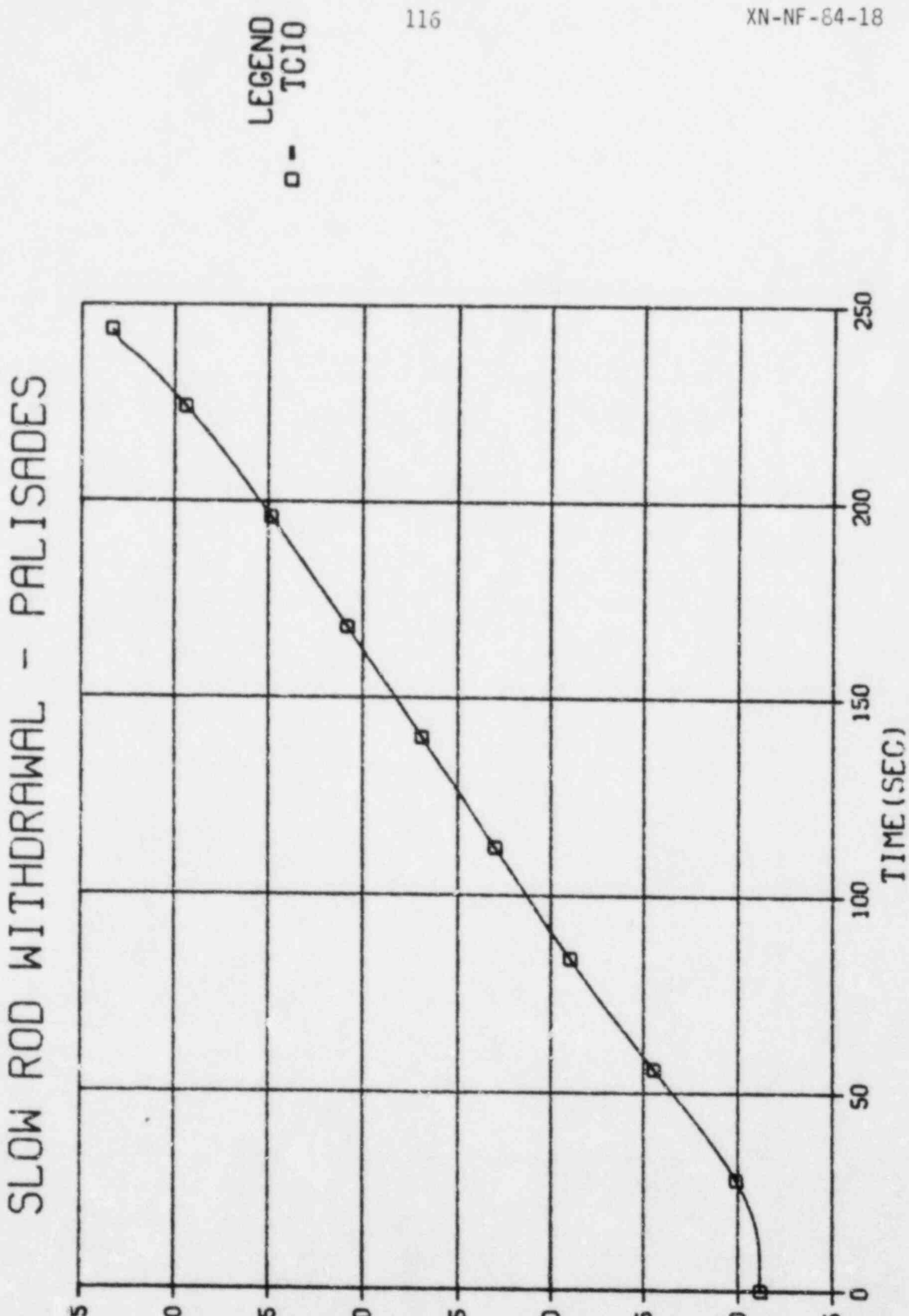

Figure 3.61 Core Inlet Temperature for Slow Rod Withdrawal from 50% Power

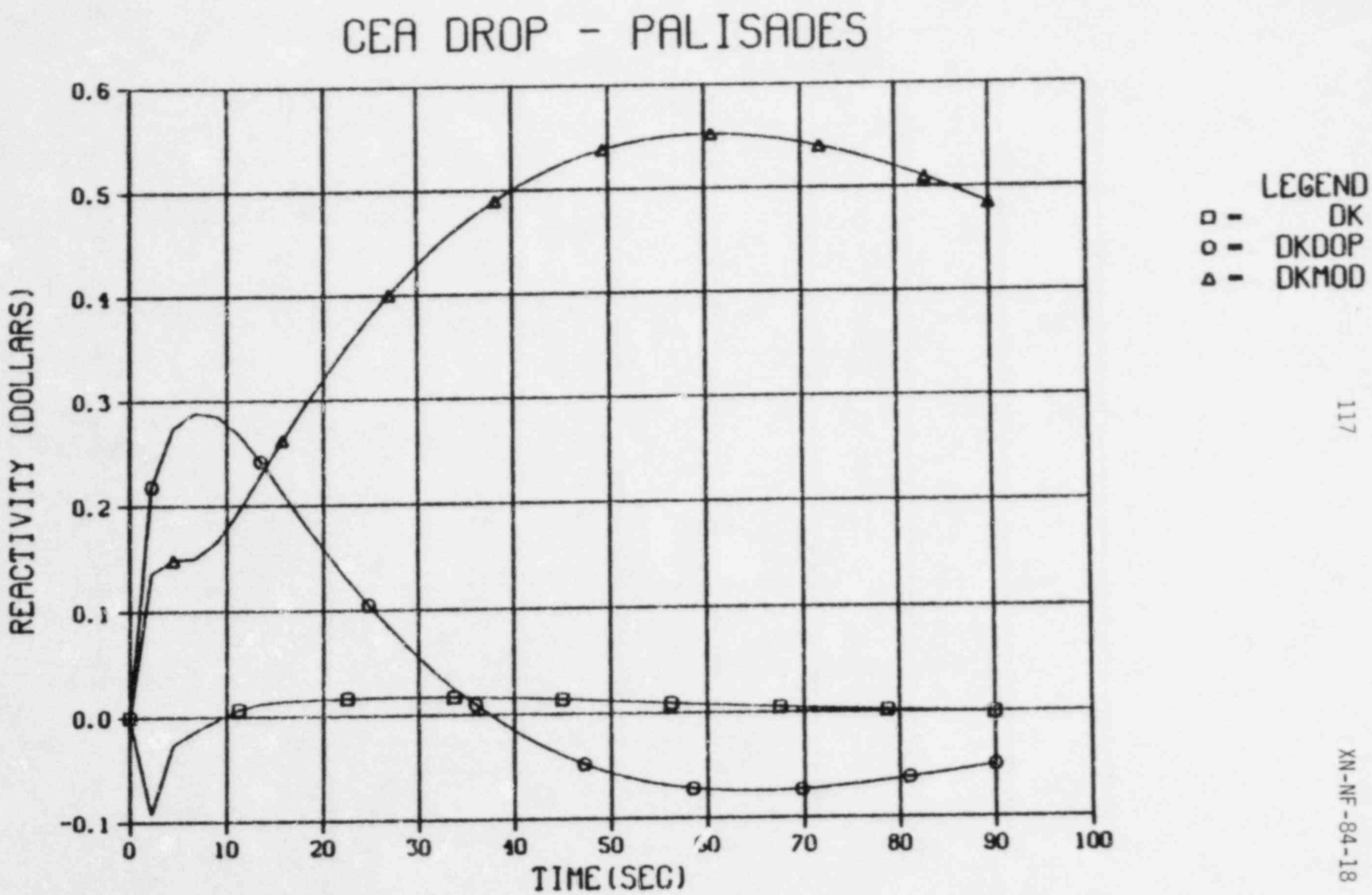

Figure 3.62 Reactivities for CEA Drop

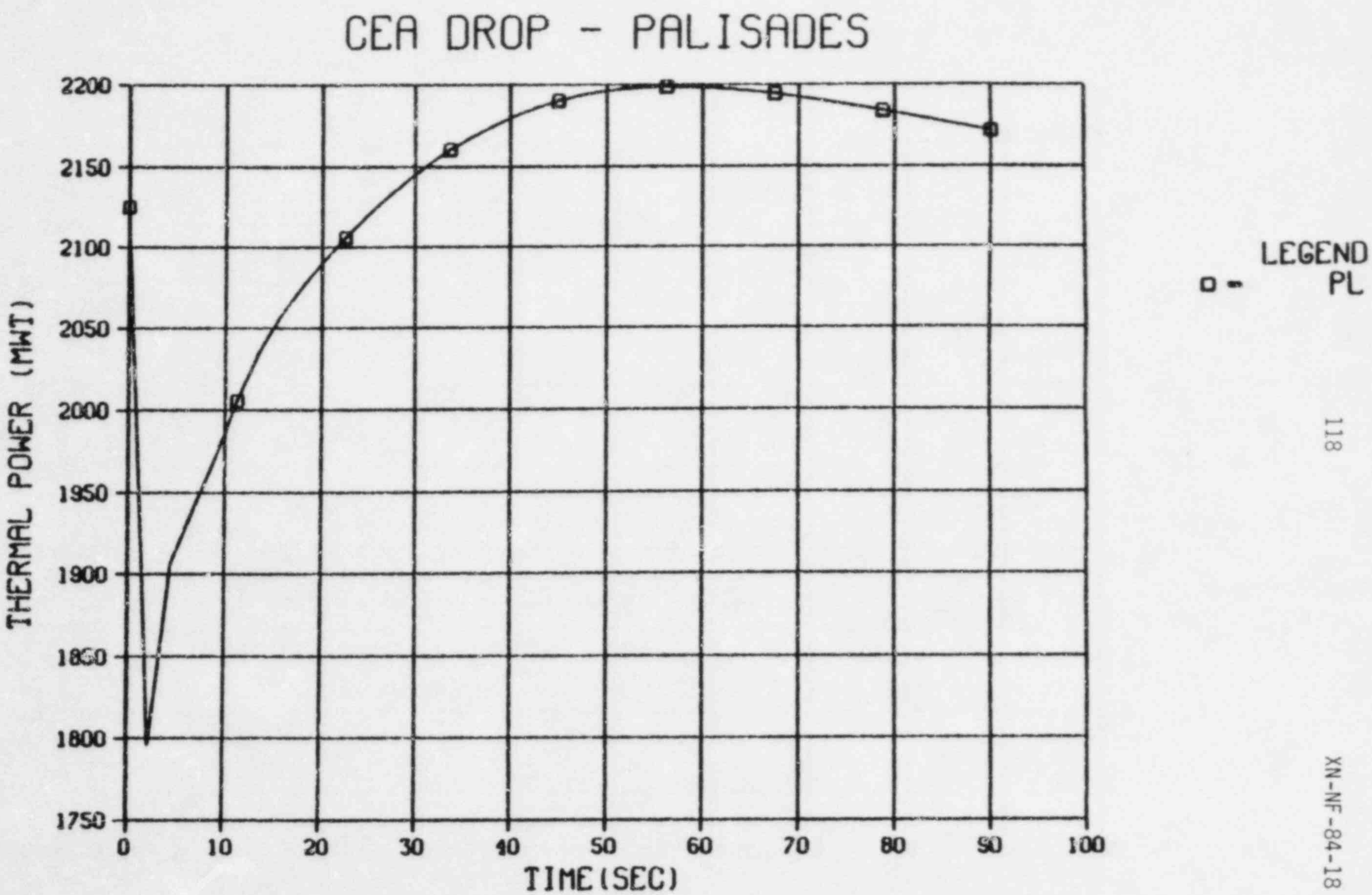

Figure 3.63 Reactor Power for CEA Drop

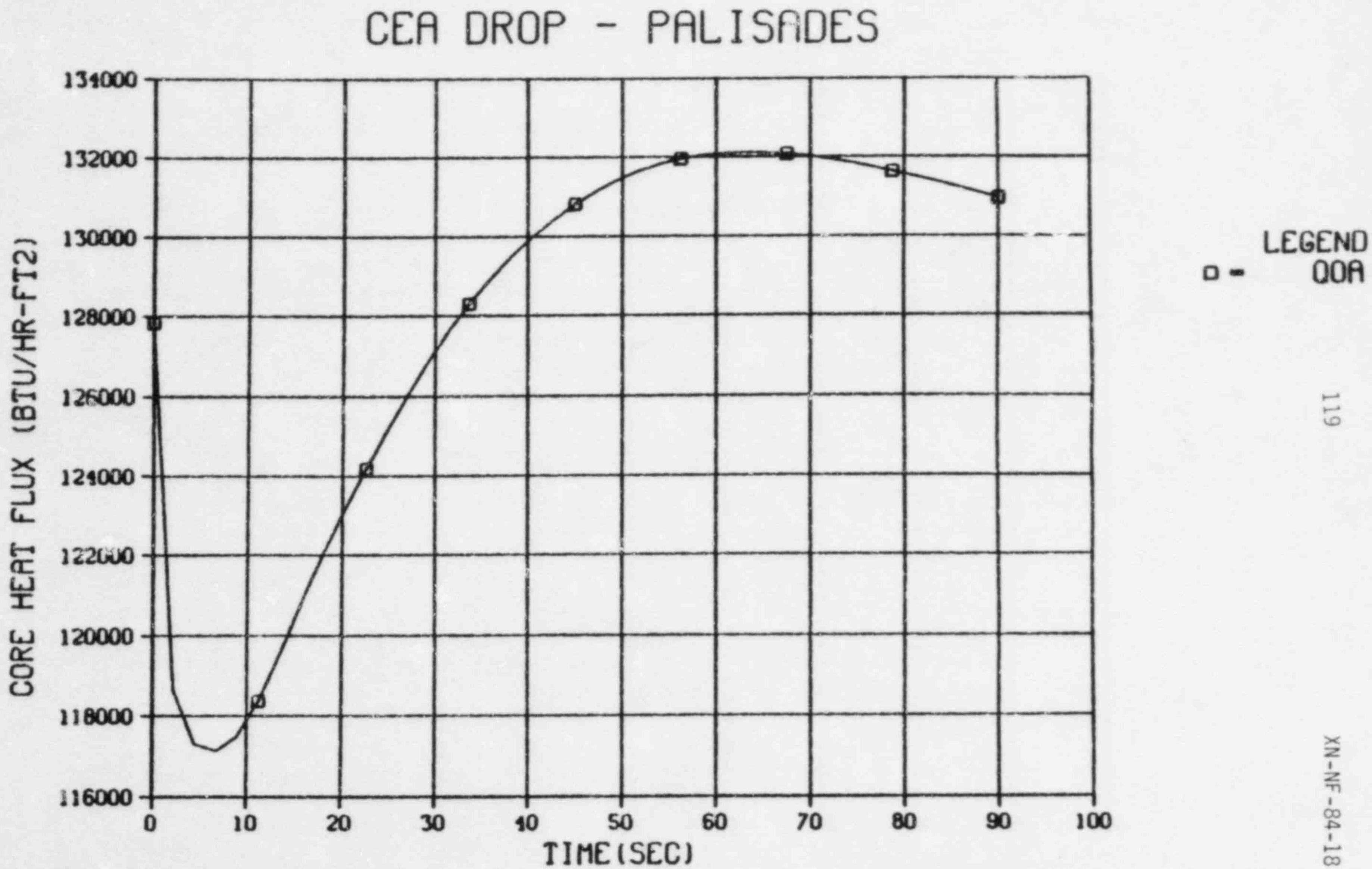

Figure 3.64 Reactor Heat Flux for CEA Drop

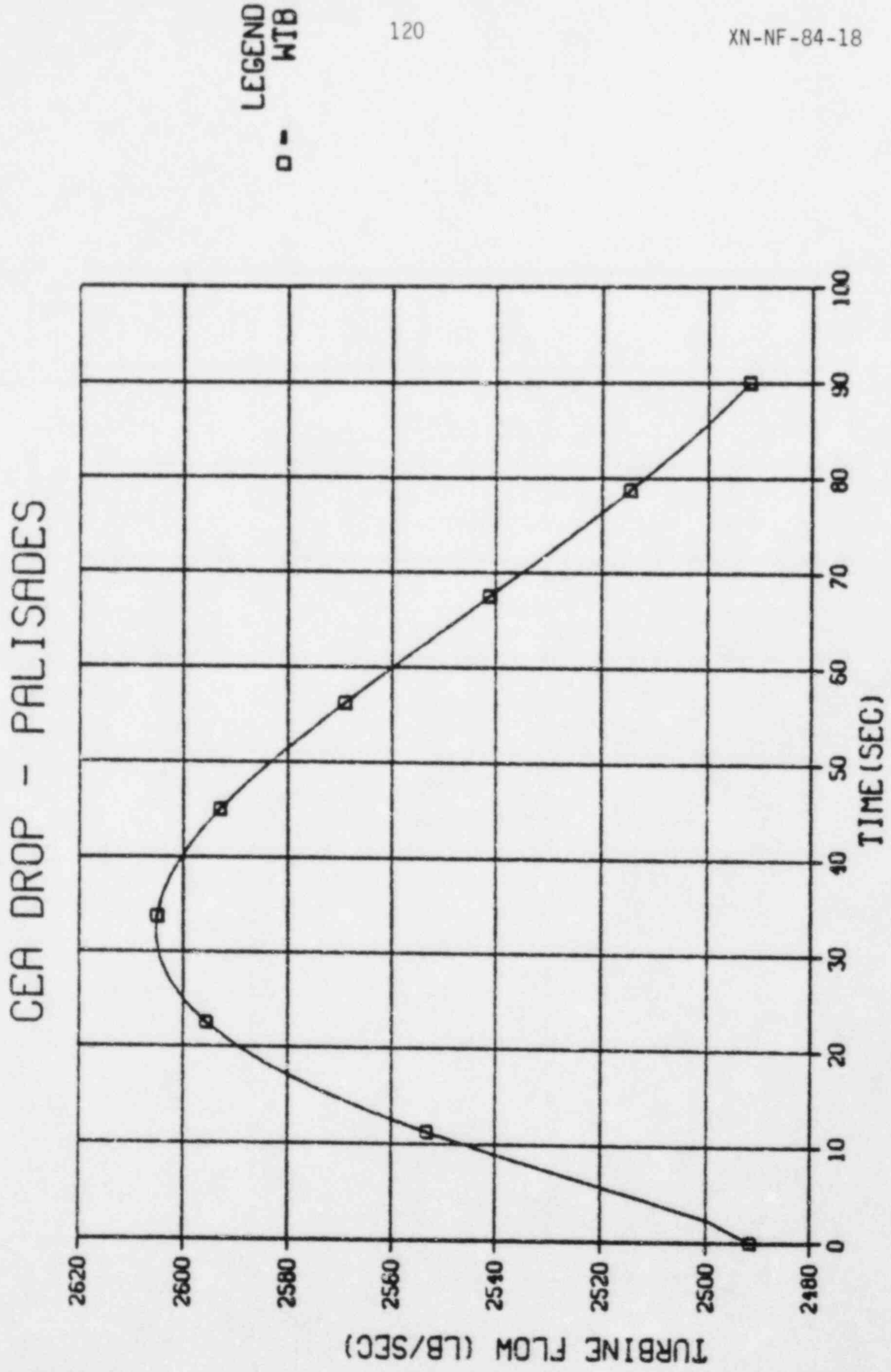

Figure 3.65 Turbine Flow for CEA Drop

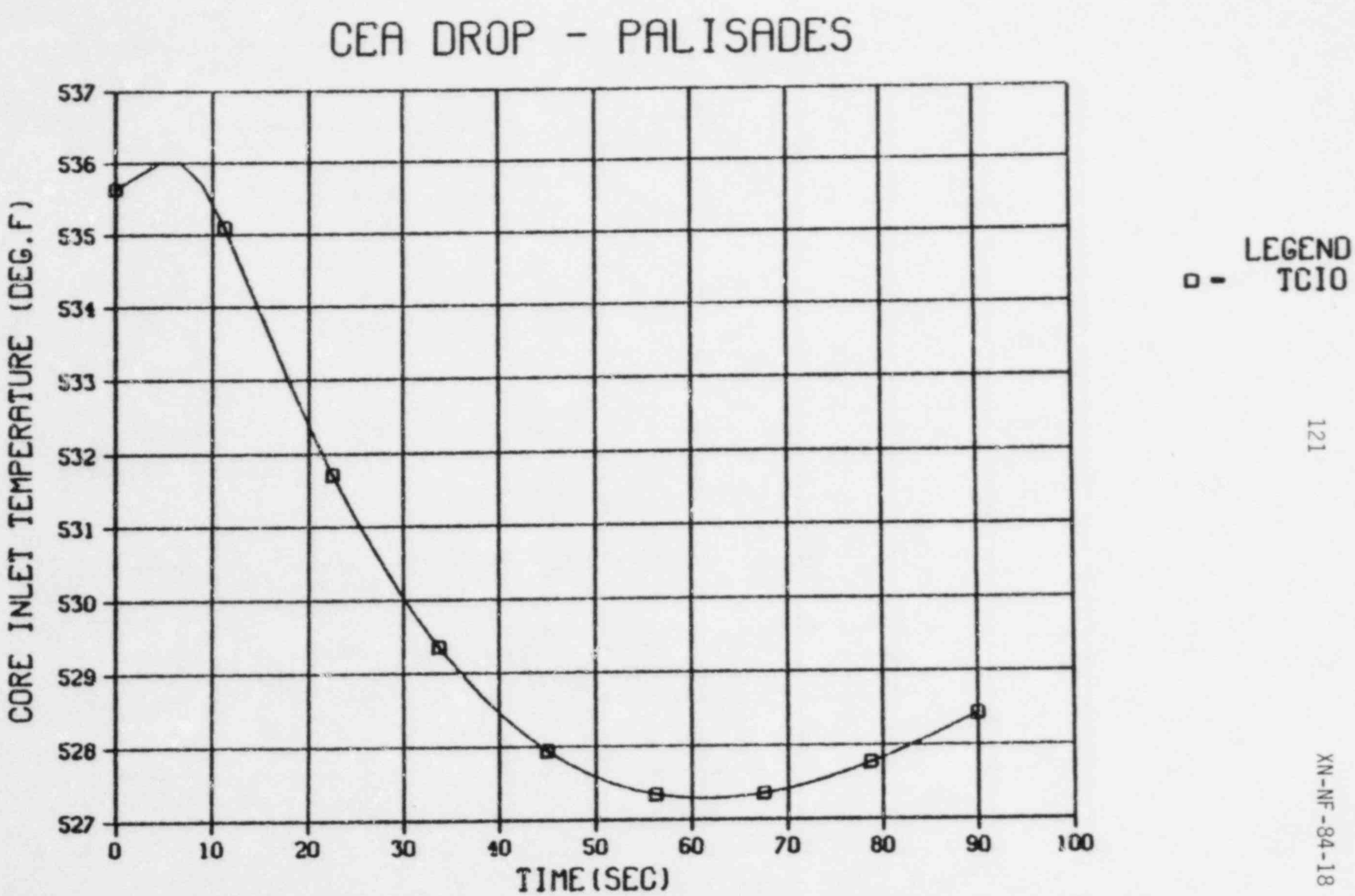

Figure 3.66 Core Inlet Temperature for CEA Drop

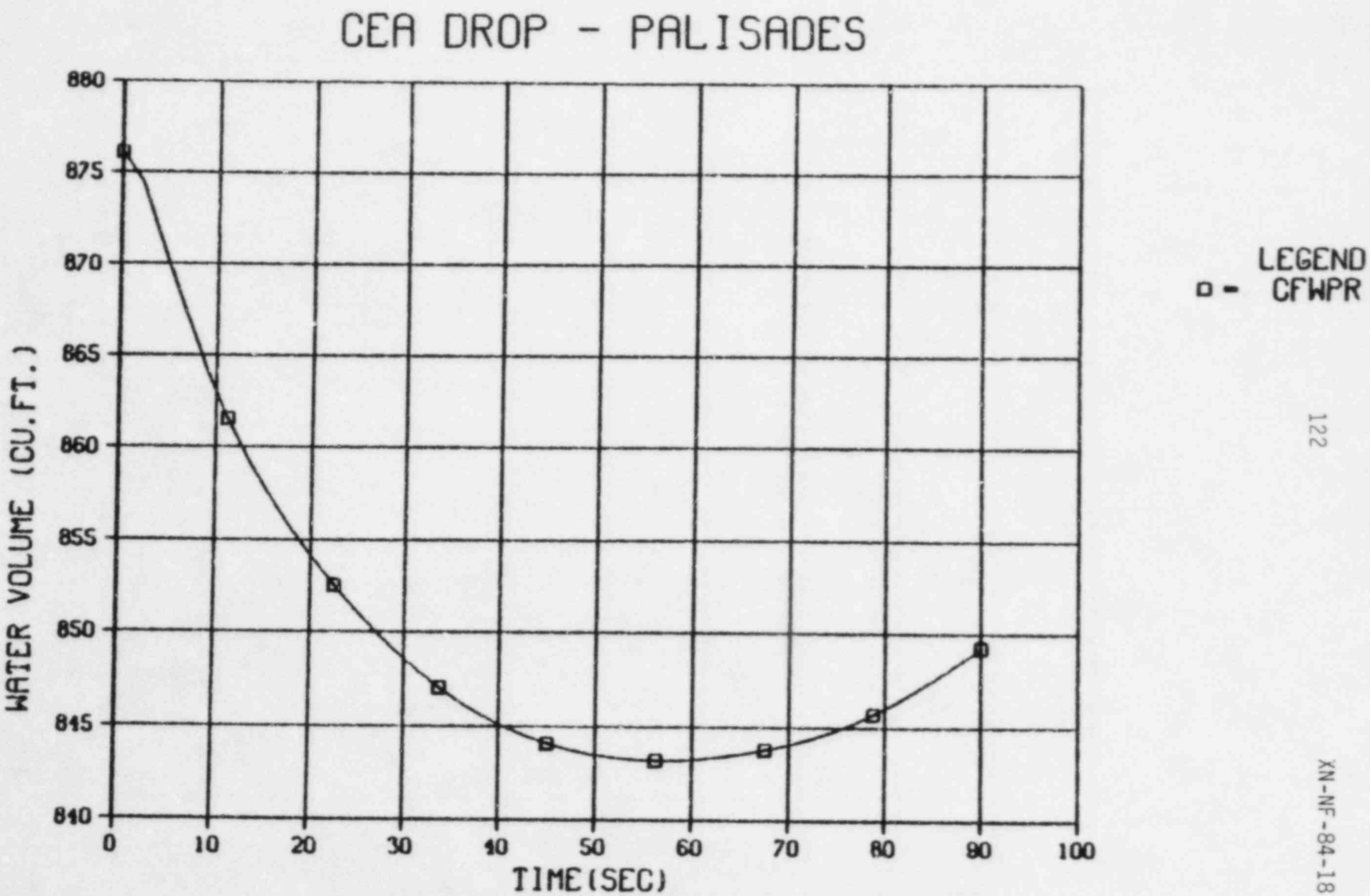

Figure 3.67 Volume of Water in Pressurizer for CEA Drop

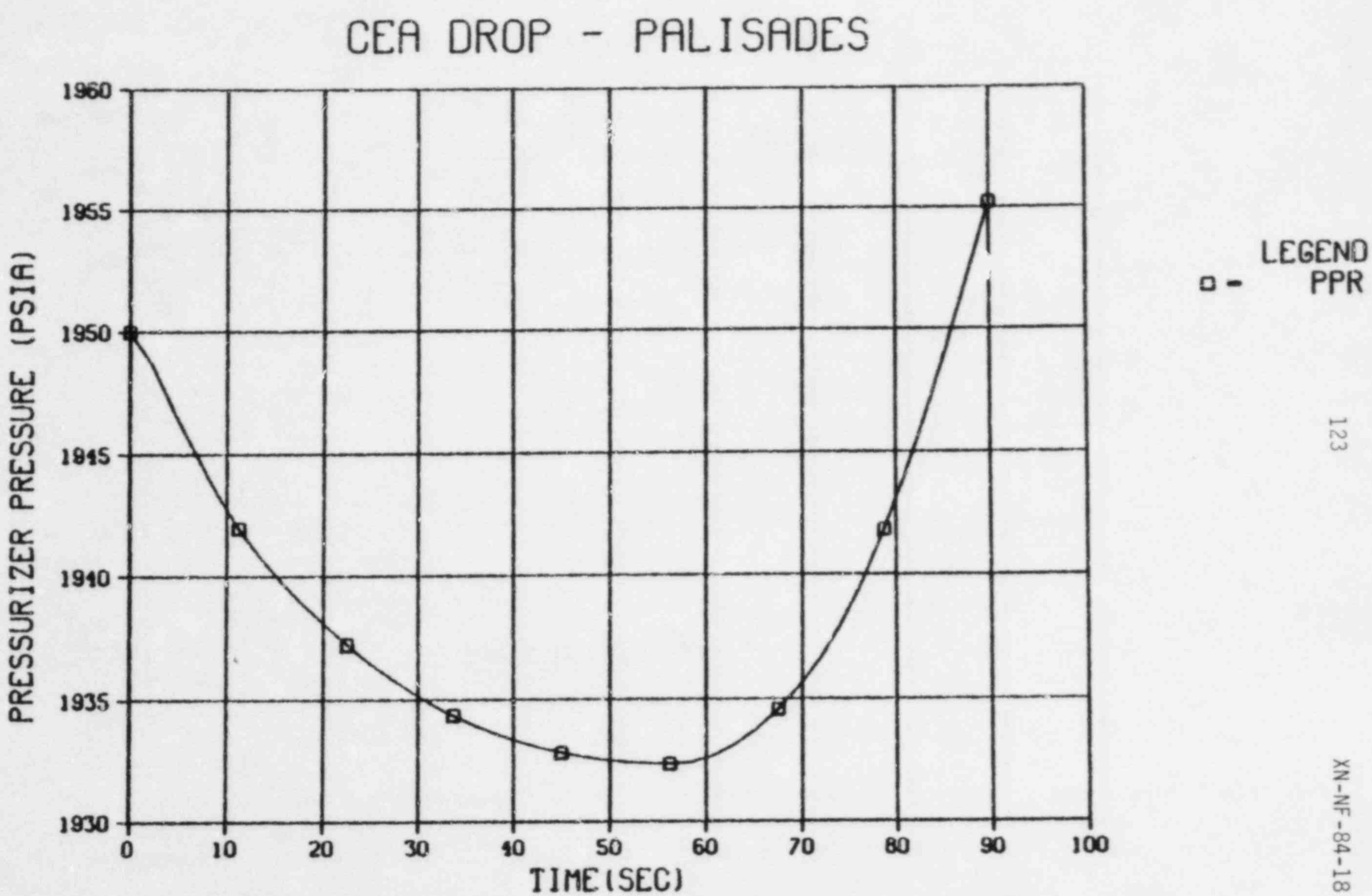

Figure 3.68 Pressurizer Pressure for CEA Drop

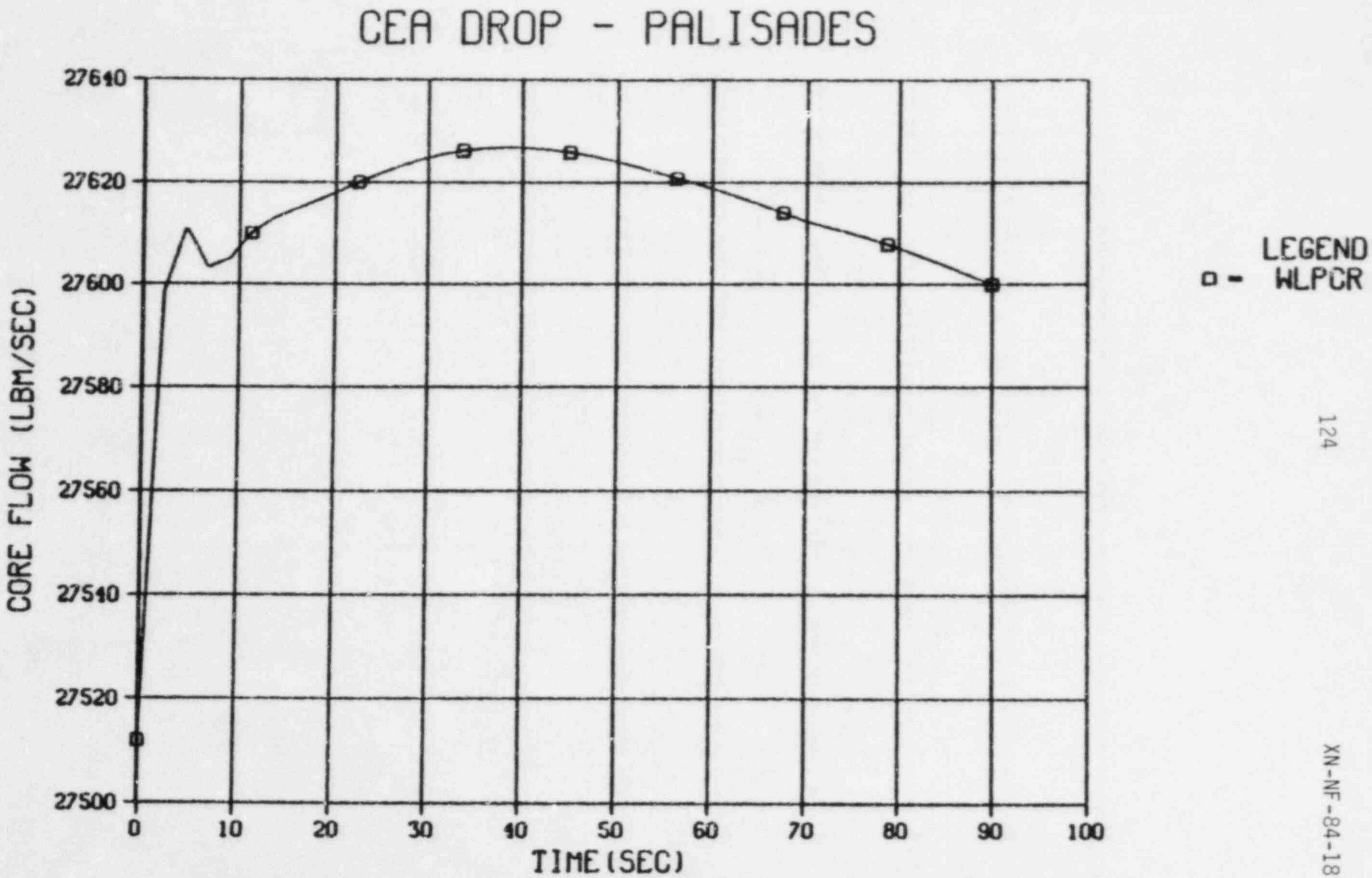

Figure 3.69 Core Flow for CEA Drop

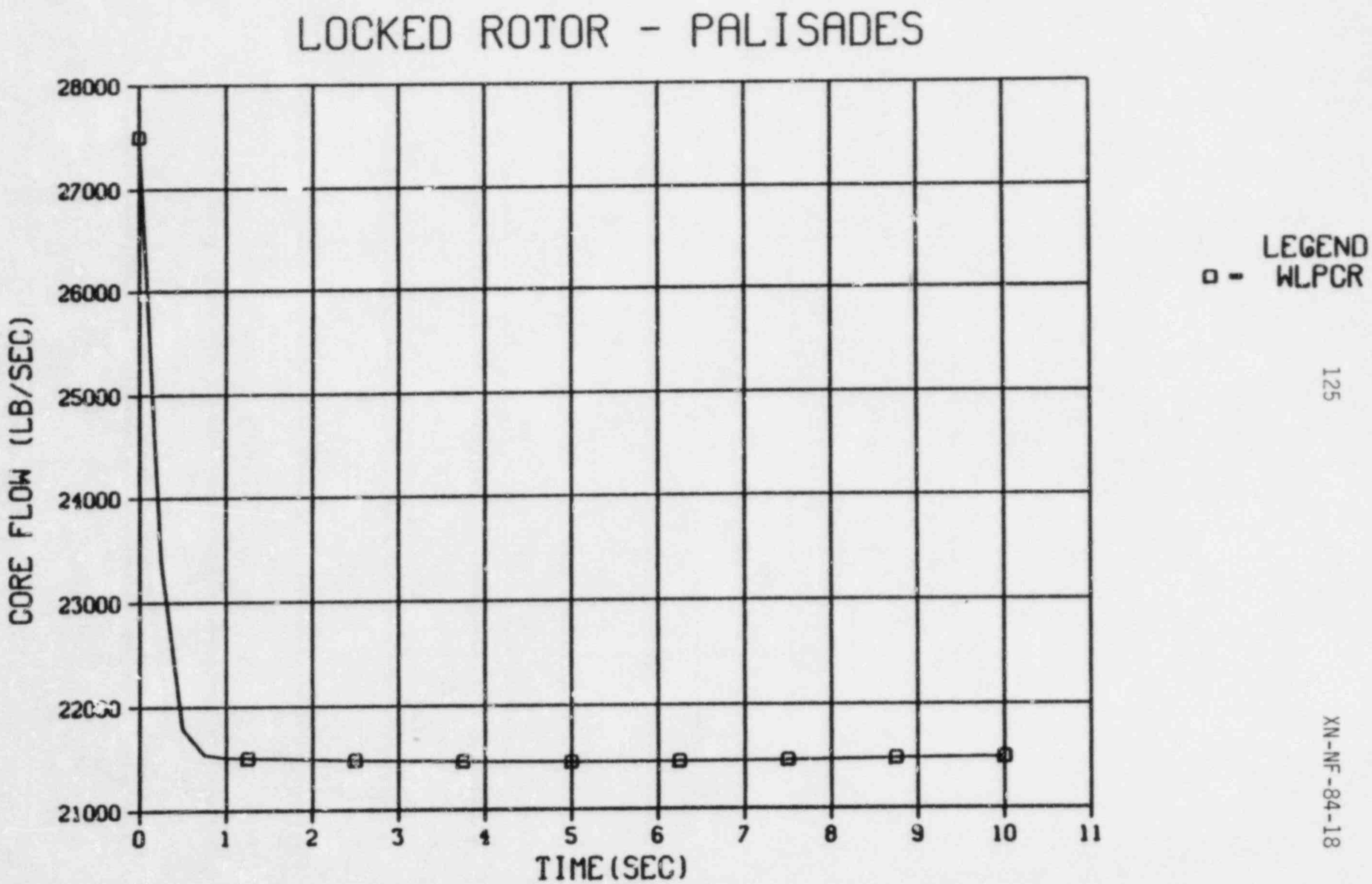

Figure 3.70 Core Flow for the Locked Rotor

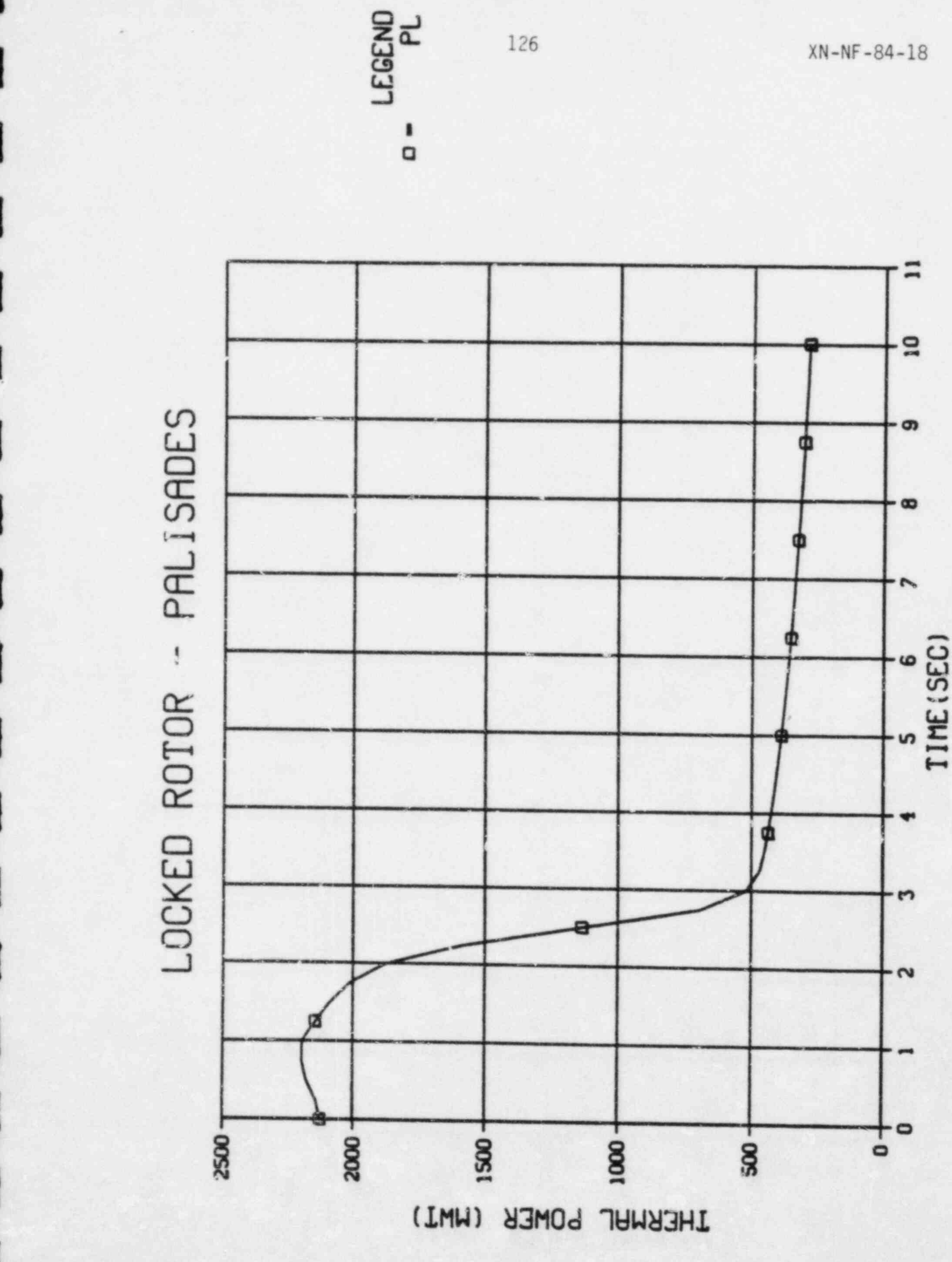

Figure 3.71 Reactor Power for the Locked Rotcr

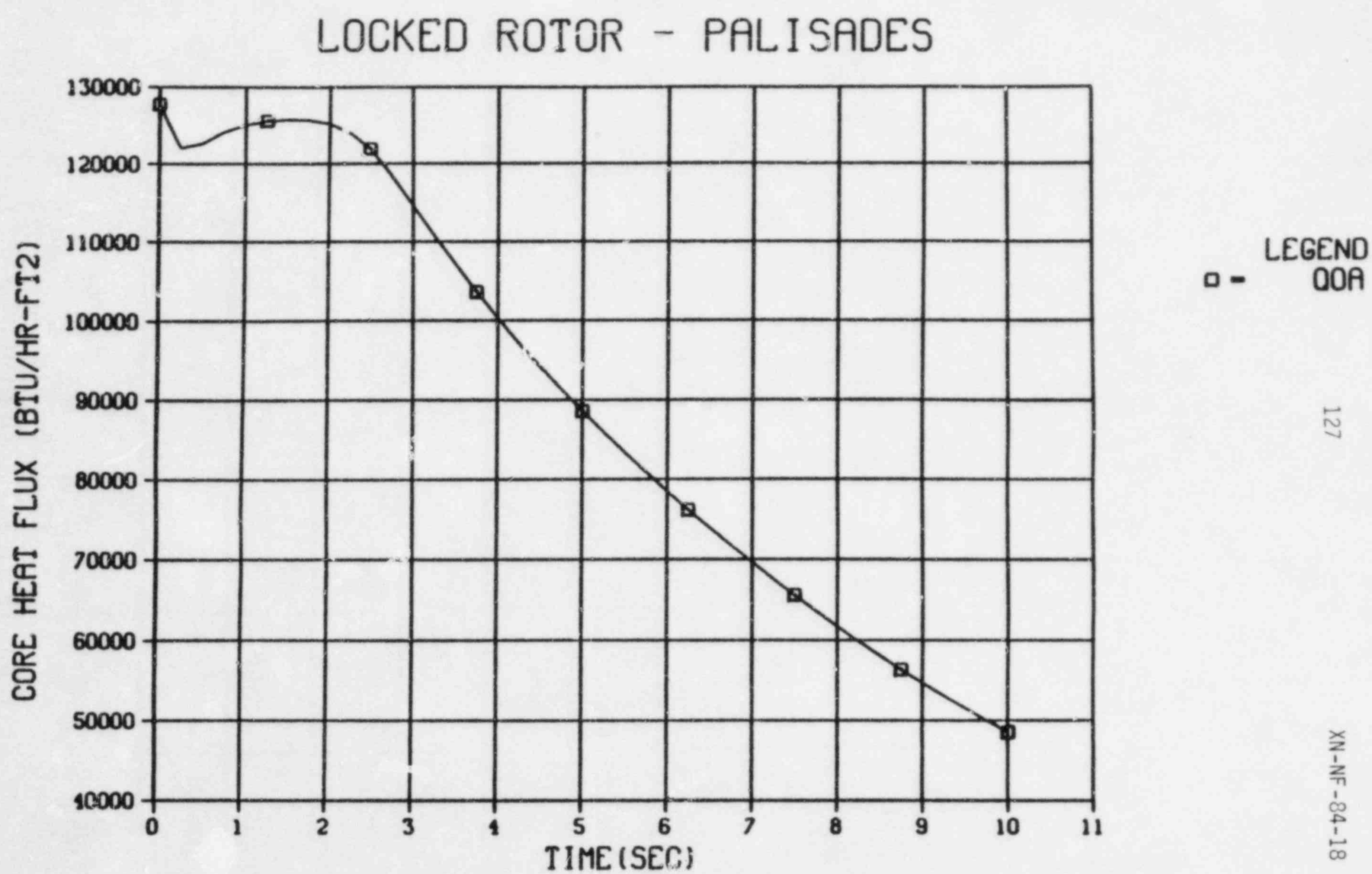

Figure 3.72 Reactor Heat Flux for the Locked Rotor

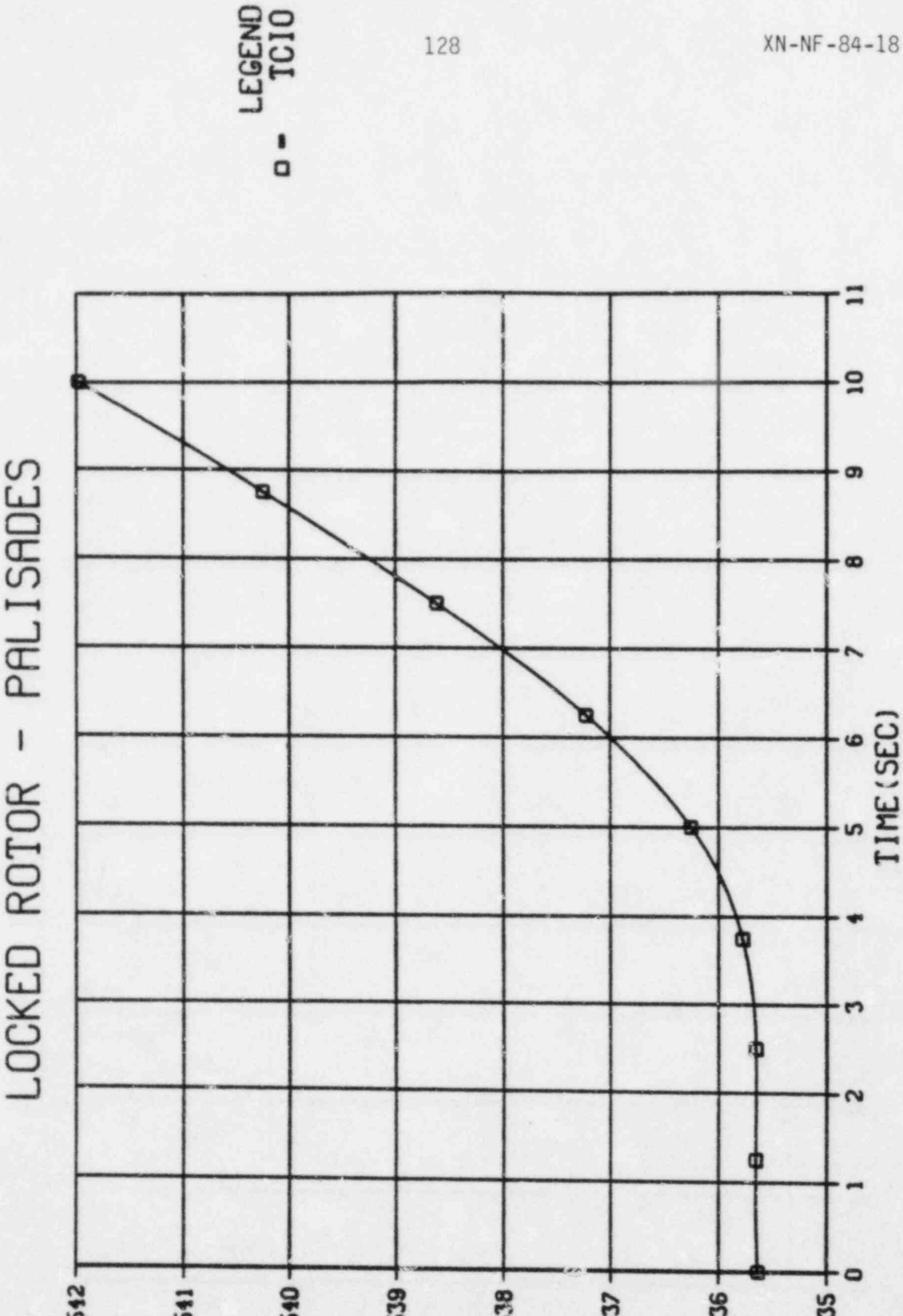

Figure 3.73 Core Inlet Temperature for the Locked Rotor

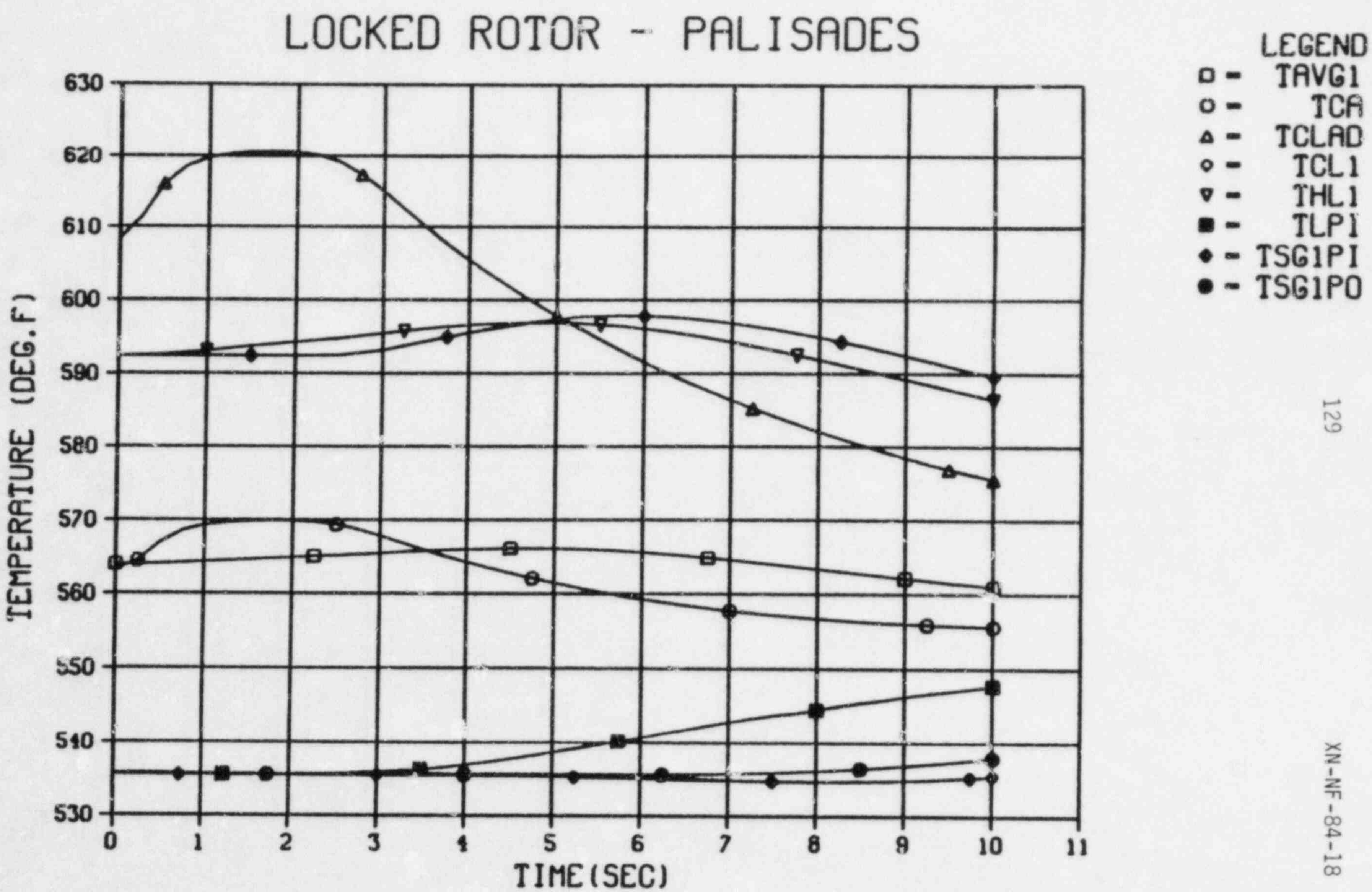

Figure 3.74 Primary Loop Temperatures for the Locked Rotor

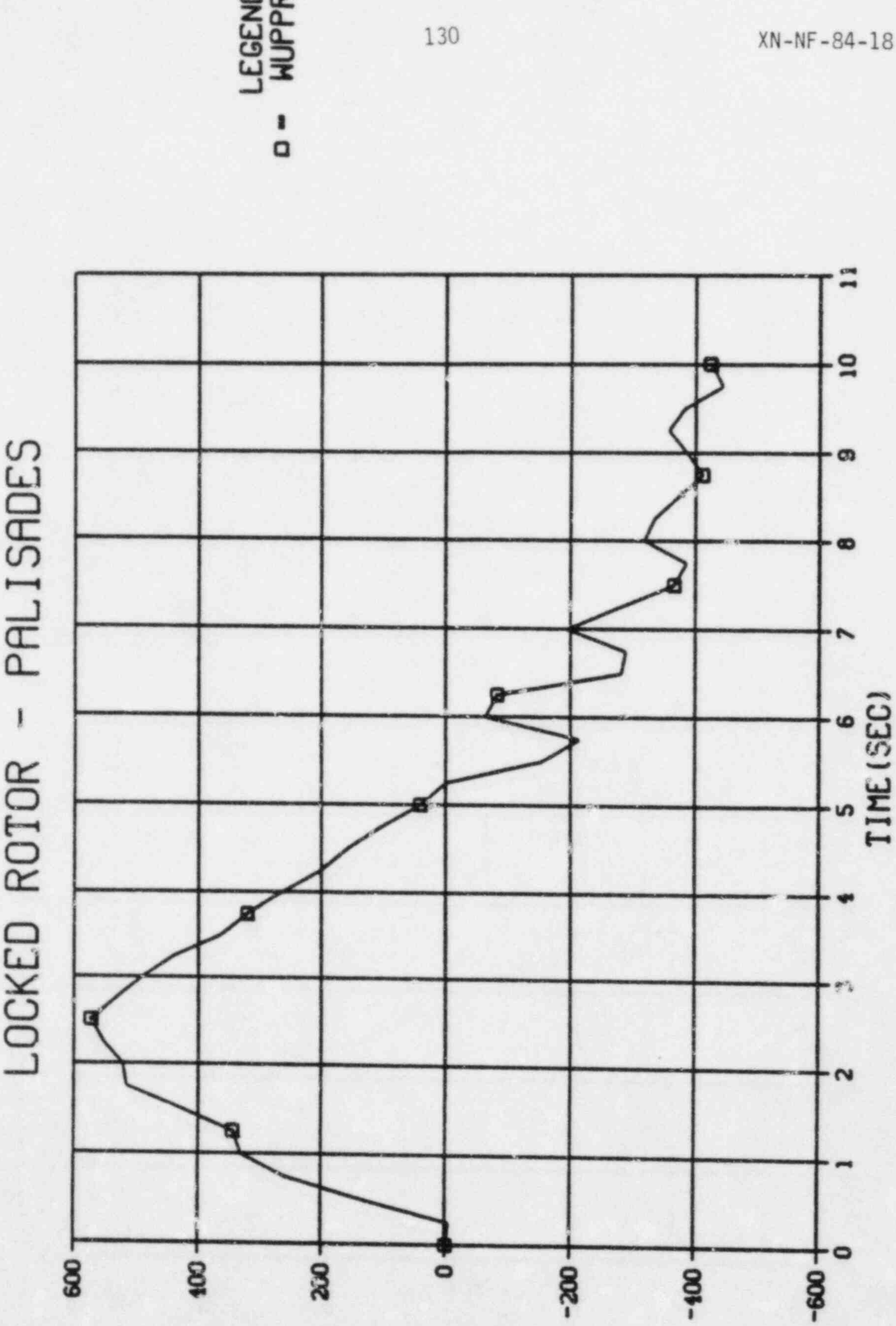

Figure 3.75 Pressurizer Surge Flow for the Locked Rotor

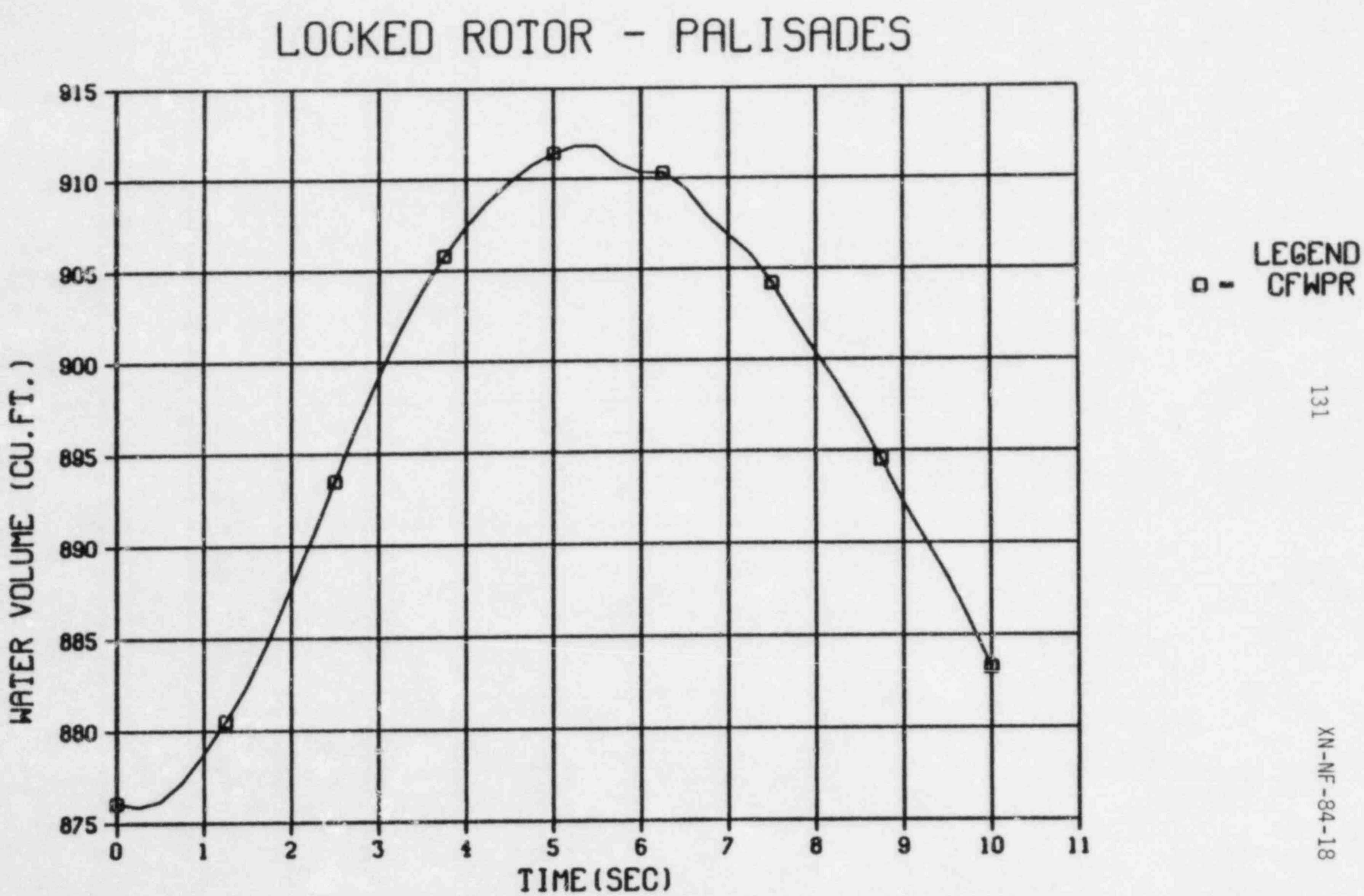

Figure 3.76 Pressurizer Water Volume for the Locked Rotor

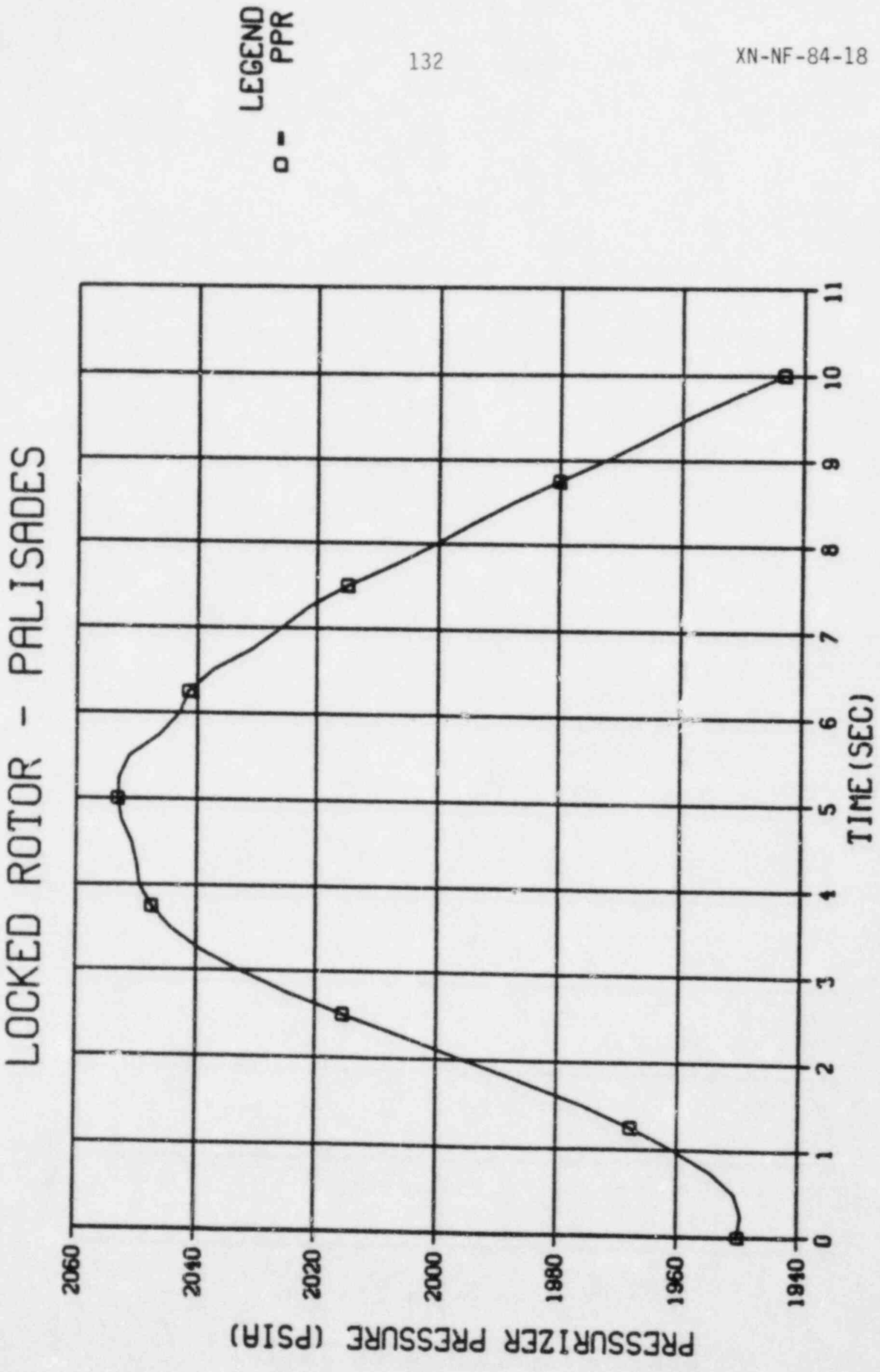

Figure 3.77 Pressurizer Pressure for the Locked Rotor

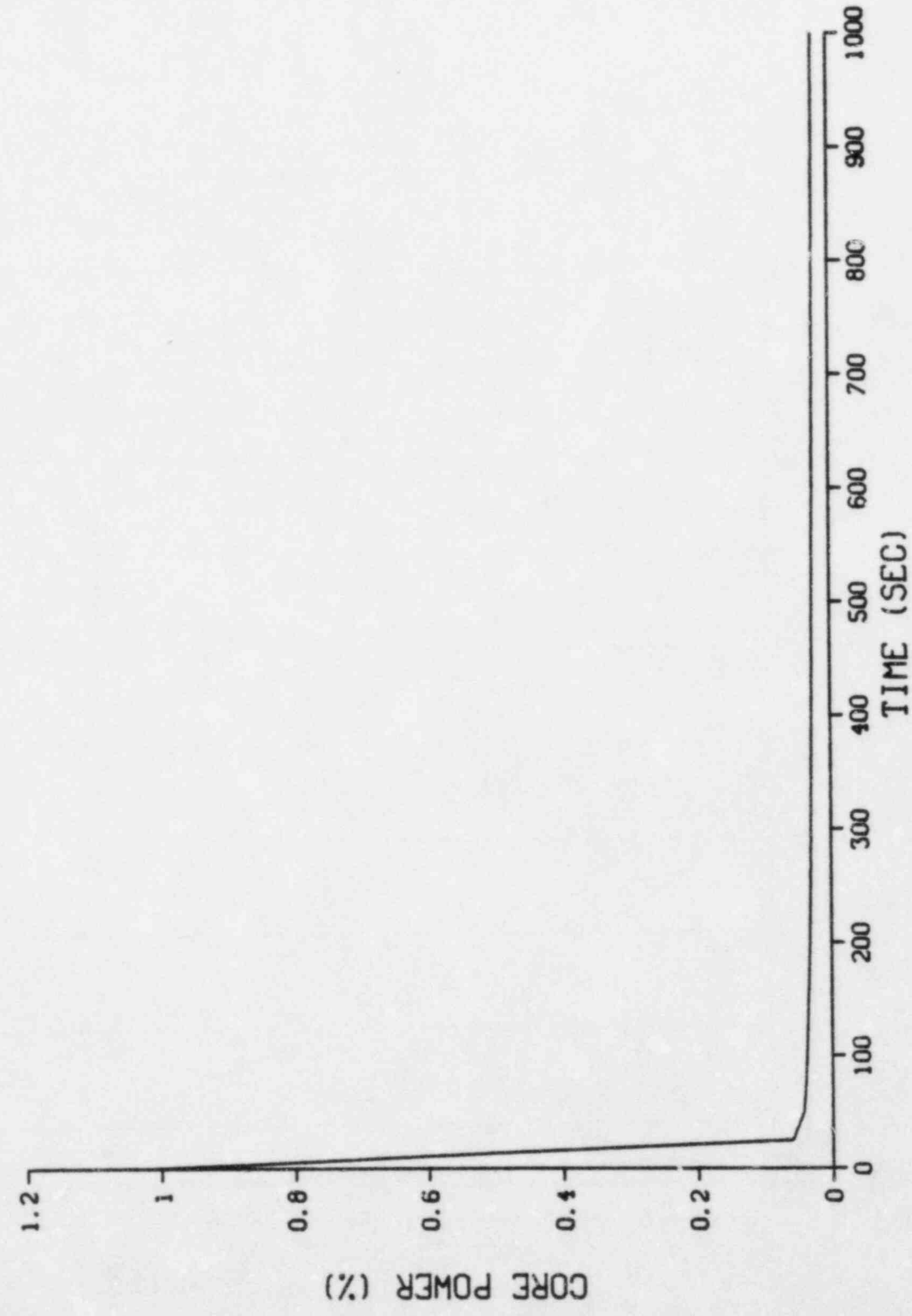

Figure 3.78 Core Power for Loss of Normal Feedwater

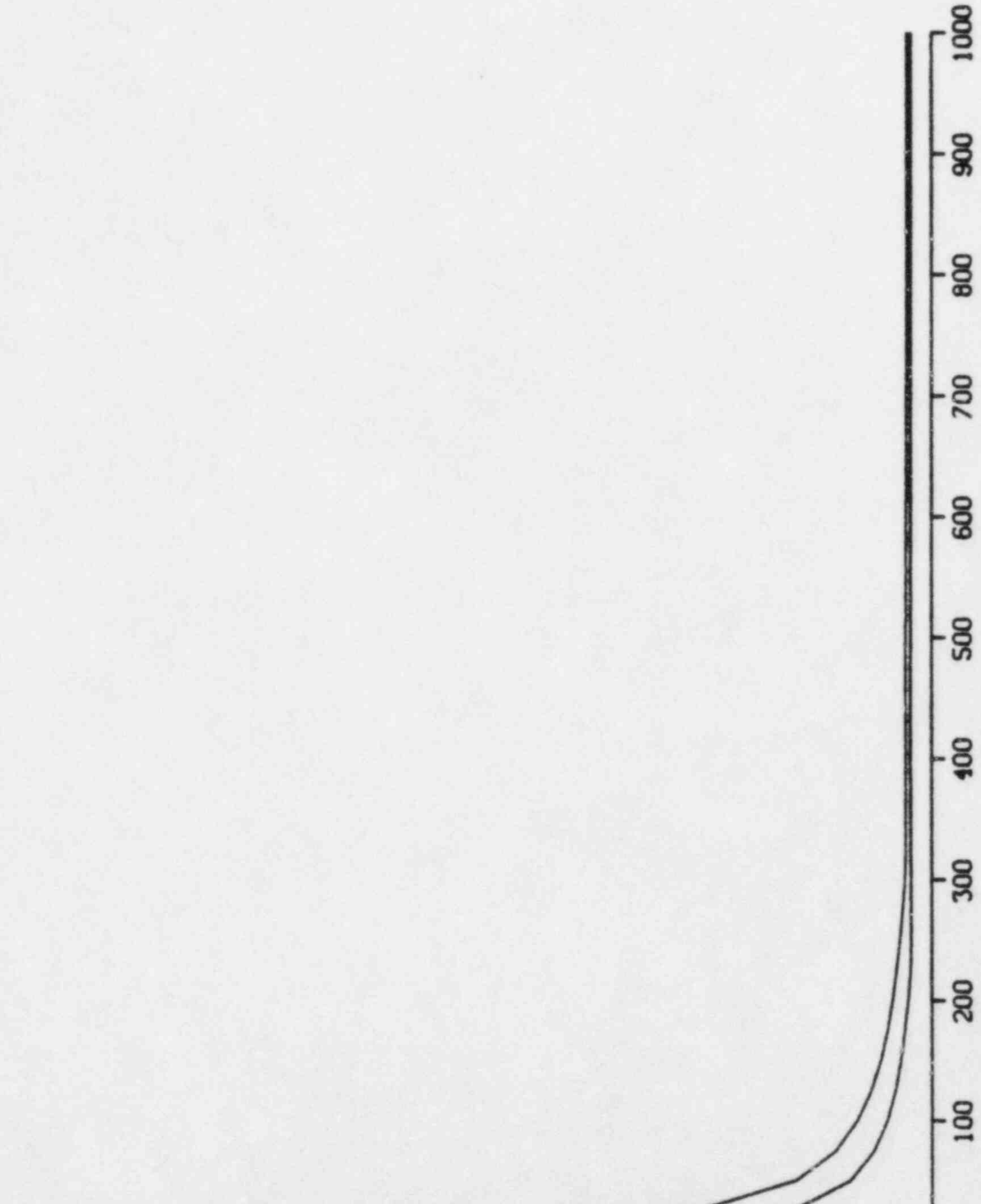

Figure 3.79 RCS Flow Rates for Loss of Normal Feedwater

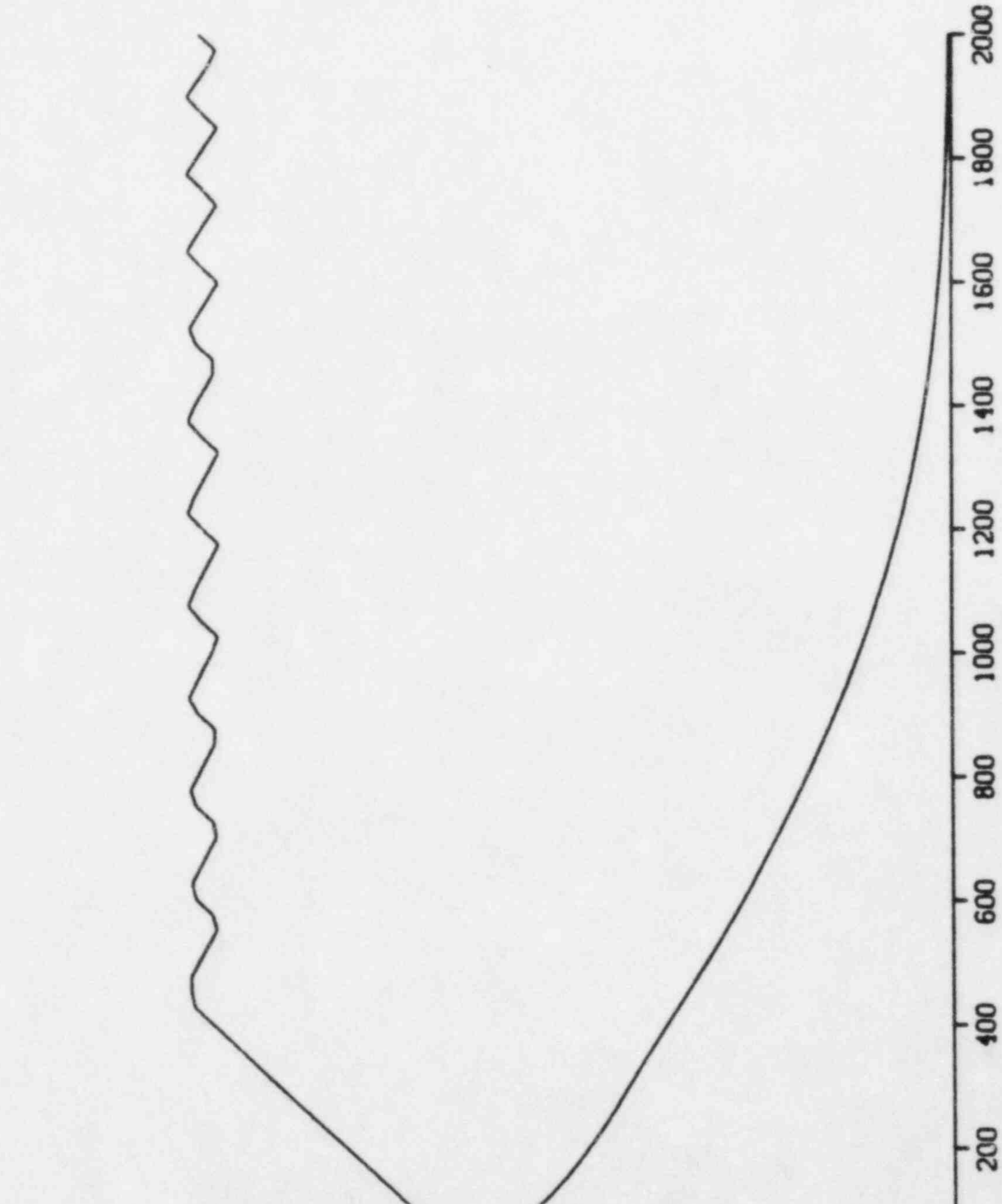

Figure 3.80 Steam Generator Liquid Levels for Loss of Normal Feedwater

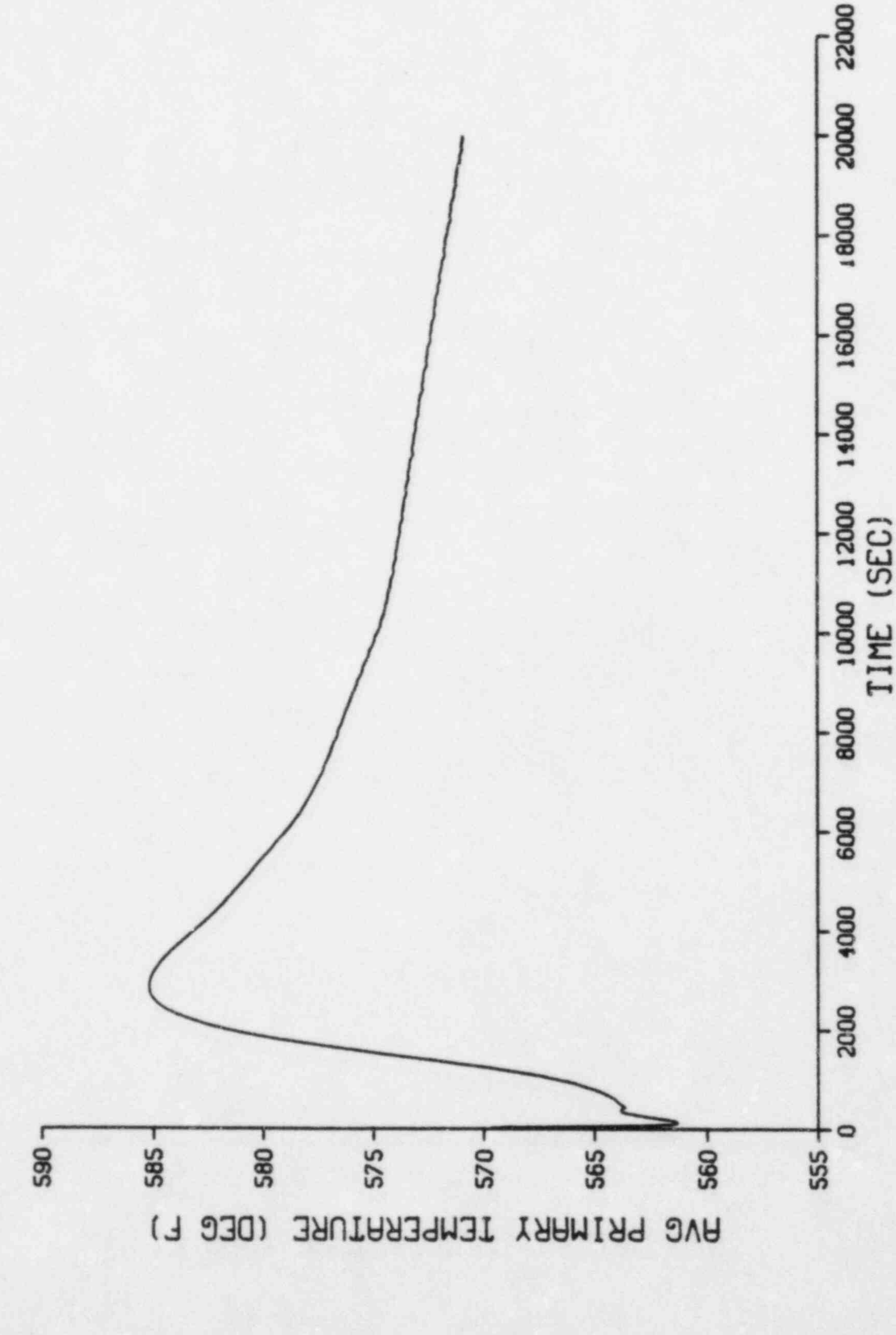

Figure 3.81 RCS Temperature for Loss of Normal Feedwater

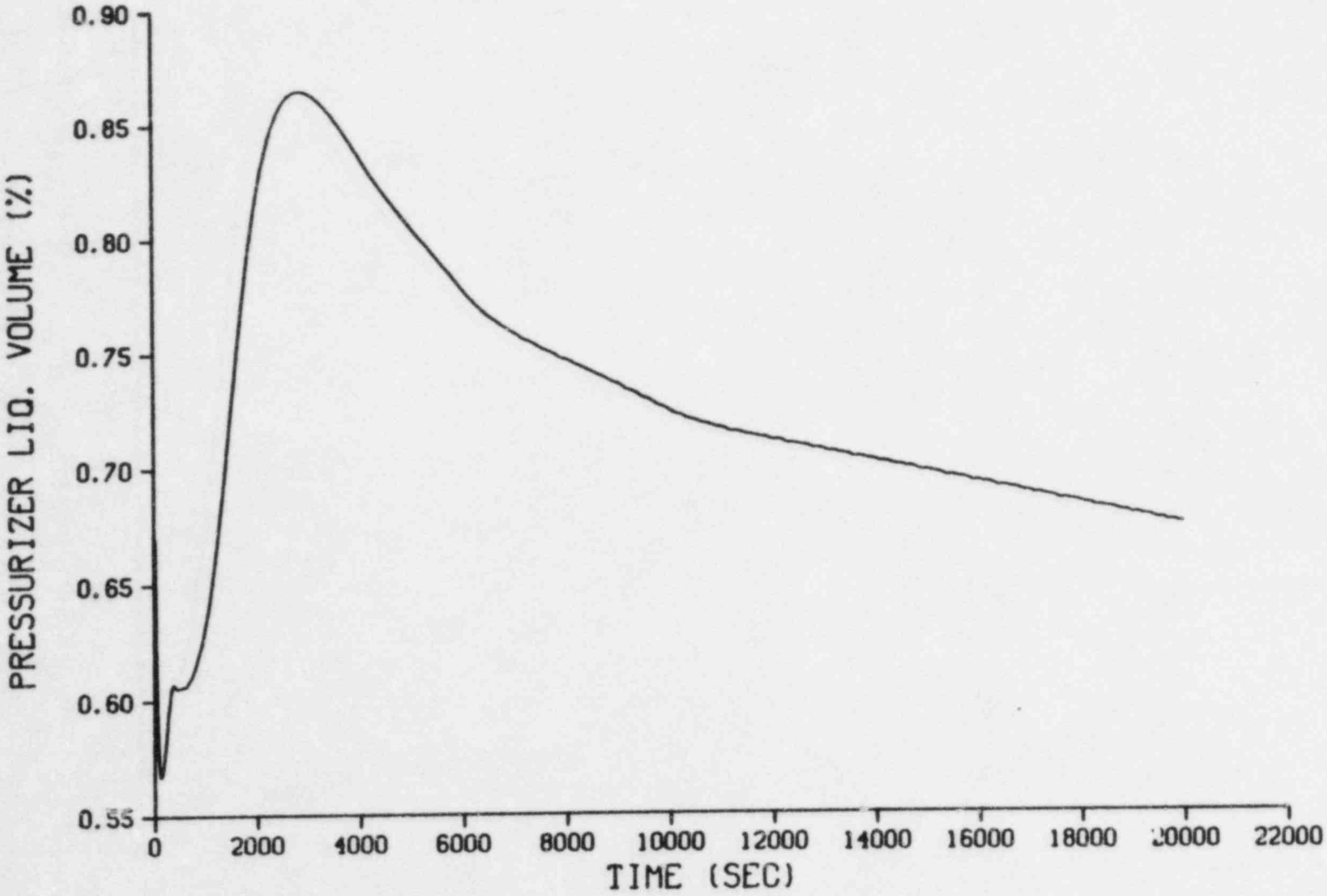

Figure 3.82 Pressurizer Liquid Level for Loss of Normal Feedwater

4.0 DISCUSSION

The ENC transient analysis performed for the Palisades nuclear power plant demonstrates adequate margin to fuel and vessel design limits for Cycle 6 under normal operation, anticipated transients, and postulated accidents. The transients analyzed in Section 3 were selected because they were shown in the prior analyses(1,2) to have less margin than the transients not analyzed.

The loss-of-load event was analyzed as an overpressurization transient and, as such, bounds events such as the loss-of-feedwater or a loss-of-heat-sink in one steam generator. The action of the pressurizer safety valve in controlling the overpressurization is sufficient to demonstrate the acceptability of the plant for overpressurization transients. The loss-of-feedwater in conjunction with a loss of A.C. power was analyzed as a long term cooldown event because of the reduced heat transfer area.

The excess-load event was analyzed as the limiting cooldown AOO. The action of the variable high power trip in terminating the transient without a significant degradation in DNBR was sufficient to bound the results of an excess-feedwater transient.

The RCS depressurization transient represents the most pressure transient in the AOO category and was used to test the TM/LP bias. As a test of the TM/LP bias, it was found to be less limiting than the CEA-withdrawal event.

The loss-of-coolant flow event is a limiting AOO for flow reduction and bounds the loss of A.C. power as a DNBR transient. Further, it provided one of the two transients which was analyzed to set the LCO for DNB.

5.0 REFERENCES

1. "Plant Transient Analysis of the Palisades Reactor for Operation at 2530 MWt", XN-NF-77-18, Exxon Nuclear Co., Inc., Richland, Washington, July 1977.

2. "Rod Withdrawal Transient Reanalysis for the Palisades Reactor", XN-NF-83-57, Exxon Nuclear Co., Inc., Richland, Washington, February 1983.

3. "Description of the Exxon Nuclear Plant Transient Simulation Model for Pressurized Water Reactors (PTSPWR)", XN-74-5(P), Rev. 2 and Rev. 2 Supplement 1, Exxon Nuclear Co., Inc., Richland, Washington, October 1983.

4. "XCOBRA-IIIC: A Computer Code to Determine the Distribution of Coolant During Steady-State and Transient Core Operation", XN-NF-75-21(P), Rev. 2, Exxon Nuclear Co., Inc., Richland, Washington, September 1982.

5. "Exxon Nuclear DNB Correlation for PWR Fuel Design", XN-NF-621(A), Rev. 1, Exxon Nuclear Co., INC., Richland, Washington, April 1982.

6. "H.B. Robinson Loss of Feedwater Transient at 1955 MWt Model Description and Results", XN-NF-82-91(P), Exxon Nuclear Co., Inc., Richland, Washington, November 1982.

7. "Palisades Cycle 6 Setpoint Document", XN-NF-84-14, Exxon Nuclear Co., Inc., Richland, Washington, March 1984.

XN-NF-84-18

Issue Date: 3/9/84

PLANT TRANSIENT ANALYSIS FOR PALISADES NUCLEAR POWER PLANT

WITH 50% STEAM GENERATOR PLUGGING

Distribution

F. T. Adams

J. C. Chandler

R. A. Copeland

J. S. Holm

W. V. Kayser

T. R. Lindquist

W. T. Nutt

G. A. Sofer

R. B. Stout (Information Only)

G. N. Ward

CPCo/H. G. Shaw (10)

Document Control (5)